

ADVANCED MRI IN CHRONIC LOW BACK
PAIN

ADVANCED STRUCTURAL AND
FUNCTIONAL MAGNETIC RESONANCE
IMAGING IN CHRONIC LOW BACK PAIN

By

GAVIN E. G. JONES, Hon. B.Sc., M.Sc.

A Thesis
Submitted to the School of Graduate Studies
in Partial Fulfillment of the Requirements
for the Degree
Doctor of Philosophy in
Biomedical Engineering

Descriptive Note

DOCTOR OF PHILOSOPHY (2012)
(Biomedical Engineering)

McMaster University
Hamilton, Ontario, Canada

TITLE: Advanced Structural and Functional Magnetic Resonance
 Imaging in Chronic Low Back Pain

AUTHOR: Gavin Eugene Guy Jones, M.Sc. (University of Toronto)

SUPERVISORS: M.D. Noseworthy, D.A. Kumbhare

NUMBER OF PAGES: xxvi, 159.

Abstract

An objective measure of muscular low back pain (LBP) symptoms eludes clinicians. The focus of this thesis is to assess effectiveness of novel magnetic resonance imaging (MRI) methods in LBP assessment. Subjects suffered from chronic LBP, being involved in automobile accidents between 9 months and 6 years prior to the study. MRI results were compared to two questionnaires, the Oswestry disability index (ODI) and visual analog score (VAS). MRI, through the L4-L5 region of the lumbar paraspinal muscles, included diffusion tensor imaging (DTI), blood oxygen level dependent (BOLD) signal fractal dimension (FD) analysis and muscle cross sectional area (CSA).

The most reliable target muscle assessed was the multifidus. Right-left asymmetry in both DTI metrics and T2-weighted (T2W) CSA were greater in the injured. Also, asymmetry measures were correlated with body mass index (BMI) but not age, height, or level of physical activity (measured via Godin activity questionnaire). The relationship between asymmetry and LBP symptoms increased for subjects with BMI below 35kg/m^2 in T2W and DTI scans.

BOLD FD did not scale with symptoms of LBP. Furthermore no notable correlation between BOLD FD and any anthropomorphic data was found. However, FD analysis showed promise following therapeutic Swedish massage, hypothesized as being related to local perfusion changes, indicating that FD is sensitive to changes in the lumbar muscle, just not LBP symptoms. Inflammation in LBP was hypothesized to alter

perfusion. However, variation in time from injury in LBP subjects likely reduced FD sensitivity.

When combining data from multiple scan types, the symptoms of LBP correlated best with the unweighted mean of DTI fractional anisotropy (FA) and T2W CSA asymmetry, and the correlation was greatest ($R^2=0.88$) when only *symptomatic (not both symptomatic and control)* subjects with BMIs from 18-25kg/m² were considered. From these results there appears to be clinical utility in characterizing the symptoms of non-acute LBP using DTI and CSA.

Acknowledgements

First, I would like to thank my co-supervisors, Drs Mike Noseworthy and Dinesh Kumbhare for their patience, advice, support, and for dragging me towards degree completion despite my efforts to the contrary. I am fortunate to have advisors who have taught me so much about both science and leadership. I hope I have the chance to apply those lessons.

I wish to thank the members of the lab and (hopefully) future collaborators Alyaa, Alireza, Sergei, Ali Fatemi, Reza, Evan, Mohammed, Saman, Ben, Oilei, Marla, Raghda, Brendan, Arv, Alex, Andrew, Peter Sheffield, Jennifer, Peter Bevan, Jeff Fortuna, Kirsten, Jeff Thompson, Graeme, Conrad, Saurabh, Paul, and Norm for all the fun times, immeasurable assistance, and many hours of discussion, some of which were even based on imaging and science.

I wish to acknowledge the contributions of my committee, Drs. Gibala, DeBruin and Harish for their insightful advice and patience as data and information accreted.

I'm grateful to my friends across the continent in Toronto, Hamilton, and San Diego, for helping when I was in need, which was often.

Above all, I want to thank my mom for her loving support over the years, and my family Veronica, Paul and Chris for their unrelenting support.

“Your beliefs become your thoughts, Your thoughts become your words, Your words become your actions, Your actions become your habits, Your habits become your values, Your values become your destiny.” – Mahatma Ghandi

“Every new beginning comes from some other beginning's end.” – Seneca (1st century AD), and ‘Closing time’ Semisonic (1998).

Table of Contents

C h a p t e r 1 .	Low Back Pain Background.....	1
1.1.	Introduction.....	1
1.2.	Low Back Pain Characteristics.....	2
1.3.	Involvement of Lumbar Musculature.....	3
1.3.1.	General Principles	4
1.3.2.	Pharmacological Intervention.....	5
1.3.3.	Functional Recovery and Exercise Regimen.....	6
C h a p t e r 2 .	Technical Background	10
2.1.	MR Diffusion Overview.....	10
2.2.	MR Diffusion for LBP.....	16
2.3.	Blood Oxygen Level Dependent (BOLD) MR	18
C h a p t e r 3 .	Hypotheses	20
C h a p t e r 4 .	Diffusion Tensor Imaging (DTI) in the Healthy Lower Back	23
4.1.	Context of Paper	23

5.3.2. Objective	45
5.3.3. Summary of Background Data	45
5.3.4. Methods	46
5.3.5. Results.....	46
5.3.6. Conclusion.....	47
5.4. Keywords.....	47
5.5. Key Points.....	47
5.5.1. Mini-Abstract.....	49
5.6. Introduction.....	50
5.7. Materials and Methods.....	52
5.7.1. Subject Population	52
5.7.2. Clinical Questionnaires	53
5.7.3. MRI Protocol	53
5.7.4. Offline Analysis	54
5.7.5. Statistical analysis	55
5.8. Results	56
5.8.1. DTI Measures.....	57
5.8.2. DTI Asymmetry index (AI).....	58
5.8.3. Intra-multifidus variability.....	60

5.8.4. Correlation.....	61
5.9. Discussion.....	63
5.10. Conclusions.....	65
5.11. References	66

**C h a p t e r 6 . Lumbar Stabilization Muscles and Low Back Pain:
Associations Between Asymmetry, Cross Sectional Area and Anthropometric**

Data 70

6.1. Context of Paper	70
6.2. Declaration Statement.....	71
6.3. Abstract	72
6.4. Keywords	73
6.5. Introduction.....	73
6.6. Methods.....	75
6.6.1. Subjects	75
6.6.2. 6.6.2 Imaging Protocol.....	76
6.6.3. Questionnaires.....	77
6.6.4. Statistical Comparisons.....	77
6.7. Results	77
6.7.1. Comparisons between LBP and control groups – CSA	79
6.7.2. Comparisons between LBP and control groups – CSA AI.....	81

6.7.3. Correlations - CSA.....	82
6.8. Discussion.....	85
6.9. Study Limitations	89
6.10. Conclusions.....	89
6.11. References	90
C h a p t e r 7 . Alterations in resting state BOLD MRI fractal dimension after Swedish massage.	93
7.1. Context of Paper	93
7.2. Declaration Statement.....	94
7.3. Abstract	95
7.4. Key Words	95
7.5. Introduction.....	96
7.6. Materials and Methods.....	98
7.6.1. Massage Therapy (MT).....	98
7.6.2. Magnetic Resonance Imaging (MRI).....	99
7.6.3. Image Analysis	100
7.7. Results	103
7.8. Discussion.....	106
7.9. Conclusion	110

7.10. References	111
C h a p t e r 8 . BOLD FD in the erector spinae in subjects with and without LBP	115
8.1. Preamble.....	115
8.2. Introduction.....	115
8.3. Materials and Methods.....	118
8.3.1. Subject population	118
8.3.2. MRI parameters and offline analysis.....	118
8.3.3. Statistical analysis	119
8.4. Results	119
8.5. Discussion.....	123
C h a p t e r 9 . Combined Measures	125
9.1. Overview	125
9.2. Combination of Data	127
9.2.1. Justification for Using only LBP Subjects in BMI Categorized Correlations Between Index and ODI.....	130
9.2.2. Comparisons Among Indices and ODI – BMI categories.....	130
C h a p t e r 10 . Future Directions.....	134
10.1. Study Limitations.....	134

10.2. Recommendations for Proposed Work.....	136
C h a p t e r 11 . References.....	138
Appendix 1 Clinical Context.....	153
Appendix 1.1 Quality Adjusted Life Years (QALYs)	154
Appendix 1.2 Stratified Primary Care.....	157

List of Figures

Figure 2.1 Depiction of the pulsed field gradient. The two equal duration (δ) and magnitude (g) gradients are separated by time (Δ). A 180 degree pulse is applied in the inter-gradient time	11
Figure 2.2 Upper left: diffusion in the absence of tissue, such as in a phantom. Diffusion is of equal magnitude in all directions. Upper centre: diffusion in a myofibril or axon, whose magnitude is much greater in one direction, the long axis of the cell. Diffusion in the other two directions is restricted. Lower depictions: Diffusion in skeletal muscle tissue, whose myofibres are all oriented in generally the same direction (although not completely parallel). The first eigenvalue (λ_1) is greatest and aligns with the muscle axis. The second and third eigenvalues (λ_2 and λ_3) are expected to be much lower in healthy tissue.....	15
Figure 4.1 ROIs superimposed on 3D-SPGR images in a 27 year old male. A) the left multifidus in the sagittal plane (red). B) the left multifidus in the axial plane. C) shows the right multifidus (green), right longissimus (yellow), iliocostalis (light orange), and quadratus lumborum (dark orange). The red ROI in C) depicts the left multifidus, longissimus and iliocostalis muscles (erector spinae + multifidus or ES+M).....	31
Figure 4.2 A) Sample T2W image in the axial plane. B) $b=0$ s/mm ² , C) λ_1 , D) λ_2 , E) λ_3 maps. All are at approximately L4 of a 27 year old male.....	32
Figure 4.3 Statistical assessment of normality was assessed for all ROIs. Sample histograms of first (λ_1 in A and D), second (λ_2 in B and E) and third (λ_3 in C and F) eigenvalues are shown. A) to C) shows data from a 22 year old right handed male's right multifidus. D) to F) are from a 27 year old right handed female's left longissimus. Data that is normally distributed, based on the Shapiro-Wilk normality test ($p>0.05$), are in A, B and D.	33

Figure 4.4 Plots of eigenvalues (λ_1 , λ_2 and λ_3) vs to body mass index (BMI). The target ROIs are the left (A-C) and right (D-F) ES+M (longissimus, iliocostalis and multifidus). The best linear fit (dashed line) and Spearman’s correlation coefficient are also shown. 35

Figure 5.1 Sample ROIs of the ES+M (erector spinae and multifidus), multifidus, iliocostalis, longissimus, and quadratus lumborum drawn on a T1W image. Only data from the multifidus with the ROI encompassing L3 to L5 are presented. 56

Figure 5.2 Asymmetry index (AI) difference in the controls and LBP groups. Student’s T test was performed to compare control and LBP data for each DTI measure. Means \pm standard deviation are plotted. 59

Figure 5.3 Asymmetry index (AI) difference in the controls and LBP groups, separated into females and males. Student’s T test was performed to compare control and LBP data for each DTI measure. Means \pm standard deviation are plotted. 59

Figure 5.4 FA variability within each multifidus, as reported by standard deviation. Note that there the standard deviation within each ROI is greater for the LBP group than the controls. 60

Figure 5.5 Sample relevant scatter plots, with Pearson’s correlation to the right. A: Plot of ODI vs FA AI shows a slight relationship. B: plot of ODI vs FA AI for only symptomatic (LBP) subjects (no controls) with BMIs under 25 kg/m². C: the relationship between BMI and FA AI, showing a slight negative correlation. 62

Figure 6.1 Plot of VAS vs. ODI scores for all subjects tested. Note that many of the asymptomatic (control) subjects scored 0 for both the VAS and ODI. The Pearson’s $R^2=0.92$ for all subjects and $R^2=0.84$ for just the LBP group. 78

Figure 6.2 Sample regions of interest (ROIs) from a 32-year-old asymptomatic (control) male. Unilateral ROIs of both the ES+M and multifidus are shown for ease of viewing. Values to the right are the CSAs measurements for each muscle. 79

Figure 6.3 Correlations plots between ODI and CSA (A), ODI and asymmetry (B), BMI and multifidus CSA, and left versus right ES+M cross sectional area. All measures were made along the top of L4. Pearson’s correlation coefficient (box in each plot) are also provided..... 83

Figure 6.4 Correlations plots between (A) ODI and cross sectional area, and (B) ODI and asymmetry index. Pearson’s correlation coefficients (R^2) are also shown..... 85

Figure 7.1 Fractal dimension maps and corresponding axial T1W images at L4 are shown from a healthy 23yr old male with no history of low back pain. A and B show maps of the fast component of FD_{RD} , C and D are slow FD_{RD} component, E and F are power spectrum FD maps (FD_{PS}), and G and H are T1W images. The FD_{PS} is clearly reduced post MT. Although the fast FD_{RD} component appears reduced in this subject neither it nor the slow FD_{RD} component were significantly different in pre compared to most MT..... 103

Figure 7.2 Plots fractal dimension (FD) power spectrum (PS) of the right and left ES+M muscle groups before massage treatment (MT). Values are means \pm standard deviation (** $p < 0.01$). 104

Figure 7.3 Plots of fast and slow components of fractal dimension (FD) relative dispersion (RD) of the right and left ES+M muscle groups before massage treatment (MT). Data are Means \pm SD, no significant effects of right/left or pre/post MT (2 way repeated measures ANOVA, background not included in ANOVA)..... 105

Figure 7.4 The ‘Koch snowflake’ where shapes have increasing complexity, self similarity and self affinity, and hence increasing FD from A to D. Plots were produced using Matlab (Mathworks, Natick, MA)..... 106

Figure 8.1 BOLD FD in subjects with and without LBP..... 119

Figure 8.2 Scatter plot of BMI vs. Mean (left and right) BOLD FD_{PS} in all subjects..... 121

Figure 8.3 Scatter plot of ODI vs. Mean (left and right) BOLD FD_{PS} in all subjects for all subjects ($R^2=0.03$) and for subjects with BMI between 18 and 25 ($R^2=0.16$)..... 122

Figure 9.1 *ODI vs. JNK Index (equally weighted mean of FA AI and CSA AI) for all subjects. $R^2=0.37$ for all subjects.* 131

Figure 9.2 ODI vs. JNK Index for LBP subjects only, with BMI between 18 and 25. $R^2=0.88$ for this group. 132

Figure 9.3 ODI vs. JNK Index for LBP subjects only, with BMI above 30 kg/m². $R^2=0.18$ for this group. 132

Figure 0.1 Cost-utility curve for the (A) low risk, (B) medium risk, and (C) high risk stratified categories. ‘Intervention’ refers to stratified care, ‘control is standard care. Reproduced from Exploring the cost-utility of stratified primary care management for low back pain compared with current best practice within risk-defined subgroups, Whitehurst et al, 2012 in press, with permission from BMJ publishing group ltd.)..... 158

List of Tables

Table 4.1 Data are mean \pm standard deviation. Eigenvalues, MD, and RD units are $\times 10^{-3}$ mm ² /sec.	36
Table 4.2 Data are mean \pm standard deviation. Eigenvalues, MD, and RD units are $\times 10^{-3}$ mm ² /sec.	36
Table 5.1 Demographic information collected, separated into male and female subjects. ODI: Oswestry Disability Index score (0-100), VAS: Visual Analog Scale (0-10), Godin: Godin questionnaire results.	52
Table 5.2 DTI parameters in control and LBP subjects. 1 way ANOVA revealed no effect of LBP/control for any measure.	57
Table 5.3 DTI metrics separated based on gender and laterality. There are no significant effects of LBP/control for any comparison (1 way ANOVA).	58
Table 6.1 The subject population. All values are listed as a mean \pm standard deviation. BMI: body mass index, ODI: Oswestry disability index, VAS: visual analog scale. Symptomatic subjects have significantly higher ODI and VAS values than controls (* $p < 0.01$).	75
Table 6.2 Muscle CSA (cm ²) for each group at the lower endplate of L4. Data are from both sexes combined, as well as parsed into that from male and females.	80
Table 6.3 Muscle CSA (cm ²) for each group at the upper endplate of L4. Data are from both sexes combined, males and females.	80
Table 6.4 CSA asymmetry index for all muscle groups and locations, with both sexes combined. Significant CSA asymmetry was noted at both upper and lower L4 in the multifidus (* $p < 0.05$). No other LBP muscles showed significant difference between healthy controls.	81
Table 6.5 CSA asymmetry index in all muscle groups and locations, when separated by gender. LBP subjects had significantly greater CSA asymmetry in the multifidus in both males and females in the	

upper L4 (* p<0.05). Additionally male LBP subjects had significantly greater CSA asymmetry in the ES+M (upper L4) muscle groups and multifidus at lower L4 (* p<0.05). 82

Table 8.1 Pearson’s correlation coefficient (R^2) for subjects (LBP and controls) for different BMI categories, and the sample sizes (n). 122

Table 9.1 Pearson’s Correlation Coefficient for each index vs ODI or VAS. 129

Table 9.2 Pearson’s correlation coefficient (R^2)for Indices #5 and #6. Only LBP subjects are used, and correlation are broken down into BMI categories. The last row are R^2 for BMIs between 18 and 30, the most reliable group, although it is not a WHO category..... 130

List of all Abbreviations and Symbols

ADC – apparent diffusion coefficient

AFNI – analysis of functional neuro-images

AI – asymmetry index

ANOVA – analysis of variance

b – ‘b value’, combination of diffusion weighting settings and gyromagnetic ratio

β - spectral index

BMI – body mass index

BOLD – blood oxygen level dependent

CLBP – chronic low back pain

CSA – cross sectional area

CSF – cerebrospinal fluid

CV – coefficient of variation

Δ - time between diffusion sensitizing gradients in pulsed field gradient protocol

δ – gradient duration in pulsed field gradient protocol

DTI – diffusion tensor imaging

DWI – diffusion weighted imaging

ε - eigenvector

EMG - electromyogram

ES – erector spinae

FA – fractional anisotropy

FD – fractal dimension

FD_{RDfast} – relative dispersion, fast component, fractal dimension

FD_{RDslow} -relative dispersion, slow component, fractal dimension

FD_{PS} – power spectrum fractal dimension

FFT – fast Fourier transform

fMRI – functional magnetic resonance imaging

FOV – field of view

FSL – FMRIB software library

g – gradient magnitude in pulse-field gradient protocol

γ - gyromagnetic ratio

Hb – haemoglobin

HR – heart rate

HRF - haemodynamic response function

I-S – inferior-superior axis

JNK – Jones, Noseworthy, Kumbhare

λ - eigenvalue

L4 – fourth lumbar vertebrae

L5 - fifth lumbar vertebrae

LBP - low back pain

M - multifidus

MD – mean diffusivity

MRI – magnetic resonance imaging

MT – massage therapy

NEX – number of excitations

NSAID – non steroidal anti inflammatory drugs

ODI – Oswestry disability index

QALY – quality-adjusted life years

QL – quadratus lumborum

RD – radial diffusivity, relative dispersion

RF - radiofrequency

R-M – Roland Morris

S – radiofrequency signal

SNR – signal to noise ratio

T1- spin- lattice relaxation

T1W – T1 weighted

T2 – transverse relaxation

T2W – T2 weighted

TE – echo time

TR – transverse relaxation time

VAS – visual analog scale

WAD – whiplash associated disorder

Declaration of Academic Achievement

In order to comply with the style requirements for thesis guidelines, the current document is in a sandwich thesis format. The study's original purpose and goals were created by Drs. Michael D. Noseworthy and Dr. Dinesh A. Kumbhare. Gavin Jones modified the study's purpose and goals, recruited patients, collected and analyzed data, and wrote the first draft for the material presented in this thesis. MATLAB programs designed by Drs. Michael D. Noseworthy and Graeme Wardlaw were modified and used by Gavin Jones.

I hereby declare that I am the sole author of this thesis. This is a true copy of the thesis, including any required revisions, as accepted by my examiners.

I understand that my thesis may be made electronically available to the public.

Chapter 1. Low Back Pain

Background

1.1. Introduction

Low back pain (LBP) affects a large majority of the western population (Fairbank *et al.* 1980; Deyo and Weinstein 2001; Davis and Kotowski 2005; Smeets *et al.* 2006; Eisenberg *et al.* 2007; Rubin 2007; Wallwork *et al.* 2009). Patients with LBP experience neuropathic pain, depression, anxiety and sleep disorders with higher frequency than those without LBP (Gore *et al.* 2012). Between 70 and 80% of adults are expected to experience at least one bout of LBP (Eisenberg *et al.* 2007) which requires a physician visit during their lifetime (Rubin 2007). Primary care physicians in the UK see approximately one LBP patient per week (Last and Hulbert 2009). The economic burden arising from chronic LBP includes treatment, loss of productivity, and government payouts. An upper estimate in the US is \$90.5 billion annually (Haldeman and Dagenais 2008), while the estimated cost in the UK is £2.10 billion annually (Chuang *et al.* 2012). Estimates from various countries from 1995 to 2002 estimate that national costs range from €8,149,000 in Sweden to \$28,170,000,000 in the US (Dagenais *et al.* 2008). Per capita costs range from \$225 to \$400 USD or equivalent. The cost per patient (not averaged over the whole population) is much greater than the per capita cost. A

retrospective study of insurance claims in the US showed that in 2008, medical costs were, on average, almost three times greater for patients with LBP than age and gender matched controls (Gore *et al.* 2012). One of the difficulties in appropriately formulating and treating LBP is that there is currently no objective measure of LBP symptoms.

1.2. Low Back Pain Characteristics

Chronic low back pain (CLBP) can be categorized several ways. (Last and Hulbert 2009) used etiology for their categories: non specific low back pain, back pain associated with radiculopathy or spinal stenosis, back pain referred from a non-spinal source, and back pain associated with another specific spinal cause.

Physical assessment by the physician includes four general methods:

- 1) Range of motion of the lumbar spine, which includes straight leg raise (Lasègue test), a sign of neural tension. A test is positive for nerve root irritation at approximately the L5 level if there is a painful response for a 30-70 degree bend (Deville *et al.* 2000). For the Lasègue test, ipsilateral pain is more sensitive (minimizing false negatives for herniation) and contralateral pain is more specific (better at ruling in herniation if positive) (Deville *et al.* 2000).
- 2) Palpation of the musculature.
- 3) Palpation of the bony structures.
- 4) Neurological examination.

The sensitivity of all of these methods of assessment is very poor for diagnosis of CLBP (Deyo et al 2001). Also, many subjects have inconclusive findings on imaging

studies (Don and Carragee 2008). False positives are a recurring problem that makes diagnosis based only on MR images difficult (Deyo et al 2001). Therefore, there is a need to develop an objective measure that correlates with the symptoms of LBP.

1.3. Involvement of Lumbar Musculature

Bergmark (1989) assessed the structure and function of the lumbar paraspinal muscles and classified the musculature into two groups: local and global. The global musculature served to bypass the lumbar architecture, and transfer loads from the thoracic spine to the pelvic area. The erector spinae (longissimus, spinalis and ilio-costalis) are among the global structures. The local structures that are attached to the lumbar facets and act on the lumbar spine directly are believed to span only a small number of vertebrae and have a limited movement to control the attached joint. The multifidus is among the local structures (Bergmark 1989), although it should be noted that the transverse abdominus, the medial fibres of quadratus lumborum, and some of the psoas fibres fit the criteria in the previous sentence (Hodges 2003). The multifidus is attached caudally to the ilia and sacrum and rostrally to several spinous processes (Macintosh and Bogduk 1991). Contraction of the lumbar multifidus results in anterior vertebral rotation and some translation of the vertebrae (Wilke *et al.* 1995). It may compress or expand intervertebral discs (Kaigle *et al.* 1995). The multifidus is implicated in LBP, and changes in cross sectional area are associated with *chronic* LBP (CLBP) regardless of the etiology but not for *acute* LBP (Deyo and Weinstein 2001; McGill 2004; Last and Hulbert 2009). Possible reasons for a correlation between the symptoms of LBP and

changes in the multifidus and erector spinae cross sectional area are through a description of the biomechanics of the paraspinal muscles of the lower back, described subsequently. The importance of the erector spinae over the multifidus is postulated elsewhere (Lee *et al.* 2011). Lee states: “*With these anatomical characteristics, the erector spinae muscle has a longer lever arm than the multifidus muscle, so most of the extensor momentum of the trunk is generated from the erector spinae muscle, rather than the multifidus muscle.*” The multifidus may be more biomechanically efficient at alleviating intervertebral stress. The erector spinae are both required to fire in unison to produce the caudal (downward) force required to alleviate pressure on the intervertebral discs, while the multifidi are medially inserted and span fewer vertebrae, so are able to produce the same downward force without coordination. Also, the multifidi insertions are mostly in the I-S direction, while some of the erector spinae fibres project obliquely. So to produce the downward force needed, a greater magnitude of force is required, whose vector will then have a downward component. The multifidus can produce forces that are closer to vertical, which is required for alleviation of pressure on the disks.

1.3.1. General Principles

Treatment of CLBP often has multiple goals, but assessment of a treatment regimen should include improvement in pain, mood, and function (Last and Hulbert 2009). Function, as is shown in chapters 1.2, 1.3, and 2.2, is closely related to gross morphological structure of the lumbar multifidus, and may be related to changes in the multifidus’ microstructure. Also, objective measures of mood and pain are difficult to

measure, since there are sometimes, at least in part, non-organic origins for the symptoms (Wong and Transfeldt 2007).

Generally, every attempt is made to ensure patients are active as soon as is possible. Extended rest may induce hypersensitivity to pain (Standaert *et al.* 2008) and may result in muscle atrophy, of the lumbar multifidus, erector spinae, psoas, and transverse abdominus, which, as described in chapter 1.4.3, are critical to lower back stabilization.

1.3.2. Pharmacological Intervention

Treatment is primarily analgesic-based. Most treatments are for short-term use, and are subject-dependent; different treatments work on different people, and are not always closely linked to etiology, severity, location or time after LBP onset. Treatment is based on an ‘analgesic ladder’ developed by the World Health Organization (WHO) for cancer treatment (MacPherson *et al.* 2004). Basically, mild pain is treated with analgesics such as aspirin, acetaminophen, non-steroidal anti-inflammatory drugs (NSAIDs) or cyclooxygenase-2 (COX-2) inhibitors. There are several classes of NSAIDs, which can be used in conjunction (Roelofs *et al.* 2008b; Roelofs *et al.* 2008a). More commonly, if one fails then another is attempted. Muscle relaxants may be useful, but it is unlikely that long term use is beneficial for patients with CLBP (Malanga and Wolff 2008). Moderate to severe pain, pain which is increasing over time, or whose symptoms don’t improve with other interventions can be treated by opioids on a short-term basis. Severe

pain is managed with combination therapy, which may include opioids, acetaminophen and/or NSAIDS.

There is some evidence that homeopathic medications, such as *Salix alba* (white willow bark, which contains salicylic acid) or *Harpagophytum procumbens* (devil's claw), may be used as an analgesic (Gagnier *et al.* 2007). Opioids can also be used sparingly, since they can lead to addiction, tolerance, hyperalgesia or allodynia (painful feeling for non-painful stimuli) (Chang *et al.* 2007). Facet blocks are another possible treatment, which are local injection of anaesthetics or corticosteroids. Epidural steroid injections are used, although they are most effective for short-term relief (Stout 2010; Benoist *et al.* 2012). Local injection of botulinum toxin (*Clostridium botulinum*) has recently increased in use, but results thus far have not conclusively shown it resolves symptoms (Waseem *et al.* 2011). There is improvement with greater coverage of the affected area. An imaging modality that can outline the affected area to both ensure adequate coverage, but allow administration to only the locally affected areas is needed.

1.3.3. Functional Recovery and Exercise Regimen

It has been postulated that there are three different (Panjabi 1992b; Panjabi 1992a) systems of spinal stability: active, passive and neural. The active system is the supporting musculoskeletal system, including paraspinal muscles and tendons. The passive system is comprised of the bony structures such as vertebrae, intervertebral discs, and ligaments. The passive system alone can buckle under loading force of minimally 90N (Hodges 2003). So the active system must be functioning properly. The neural system includes

both afferent and efferent connections, and central centers, primarily within the brainstem, but also including the cortex and spinal cord. If the passive system is damaged, such as with disc herniation or facet damage, the active and neural systems may compensate for the loss. In subjects without LBP, activation of the transverse abdominus is involved with motion, trunk loading and movement of the upper limbs, while there is increased and/or less efficient activation of the paraspinal muscles such as the erector spinae (Cresswell *et al.* 1992; Cresswell *et al.* 1994; Hodges and Richardson 1996). There is a wealth of evidence connecting decreased size of the lumbar multifidus with symptoms of LBP (Hides *et al.* 1995; Kader *et al.* 2000; Yoshihara *et al.* 2001; Yoshihara *et al.* 2003; Lee *et al.* 2006; Mengiardi *et al.* 2006; Smeets *et al.* 2006; Hyun *et al.* 2007; Kjaer *et al.* 2007; Hides *et al.* 2008; Kulig *et al.* 2009; Wallwork *et al.* 2009; Ward *et al.* 2009; Lee *et al.* 2011; Niemelainen *et al.* 2011; Beneck and Kulig 2012; Shafaq *et al.* 2012) as well as task-dependent differences in electromyogram (EMG) activity in the multifidus in subjects with CLBP (Sihvonen *et al.* 1997). Exercise programs which encourage hypertrophy of the lumbar paraspinal muscles recover multifidus mass (Hides *et al.* 1996). Core stabilization exercises are beneficial for acute occurrences (O'Sullivan *et al.* 1997) or the first episode of LBP (Hides *et al.* 2001). Core stability exercises generally fall into two categories: i) those that restore strength and endurance to the musculature and ii) those that increase postural control (Hodges 2003; McGill 2004). The strength rationale would suggest that the 'local' musculature under Bergmark's classification should be targeted, and that under Panjabi's classification, the active and neural components should be improved. In subjects with CLBP, there is a larger deficit

for changes in loads when the challenge is from an external force (e.g., from a box dropped into the hands) than from an internal force (e.g. swinging arms during gait) (Panjabi 1992a). The information from internal forces is from efference copies as well as proprioceptive input, whereas external challenges are from proprioceptive input alone. There is evidence in the simpler motor control system of the extraocular muscles of the eye that internal movements initiated by efference copies provide quicker and more accurate information (Broussard *et al.* 1999; Roy and Cullen 2002). The improvement of control [ii] in Hodges' classification above] may improve the response to external changes.

To enhance control, muscle retraining is necessary. Movements are performed as parts of a greater movement, called segmentation (Cowan *et al.* 2002). This will allow the therapist to identify specific deficits in parts of a movement, which must be targeted. Task simplification is the other aspect of increasing control, and consists of changing postural loads (movement in a supported position) or reduced speed of movement. Motor learning occurs in three phases: cognitive, associative, and autonomous (Mannion *et al.* 2001). Cognitive movements involve reproducing the precise movements with appropriate feedback either visually or from the therapist. The associative phase involves increased repetitions and holding time with the critical parts of the movement. During the autonomous phase, the task should become automatic, and only limited conscious control is needed, and is tested often under distracted conditions to ensure appropriate control is achieved (Jull *et al.* 2002). These training regimens should also consider the differing initial positions of the lumbar spine.

The strength training, part of Hodges category ‘i’, is aimed at reducing the stress on the spinal column during movement, and stasis. Swiss ball programs and stability exercises (McGill 2002) are used to enhance core stabilization. The primary aspects include movement of extremities while balancing on unstable surfaces to exacerbate the torsional requirements. Although both closed and open chain exercises are used, close chained exercises are emphasized (where the hand or foot is immobile on a surface) (O'Sullivan *et al.* 1997).

Exercises that improve both i) and ii) above, are required. However, the local system's deficits are critical. Local musculature is ideal for controlling intervertebral motion, where global musculature is ideal for orientation (Bergmark 1989).

There are other forms of treatment, which, under certain circumstances, may alleviate the symptoms of CLBP. They include spinal manipulation, yoga for therapeutic reasons (Viniyoga), lumbar supports, transcutaneous nerve stimulation, massage, and acupuncture (Chou *et al.* 2007a; Chou *et al.* 2007b; Williams *et al.* 2007; Furlan *et al.* 2009).

Chapter 2. Technical Background

2.1. MR Diffusion Overview

Diffusion is based on the random, multidirectional movement of particles or molecules, first described with pollen grains in 1827 by Robert Brown (hence the term Brownian motion). Magnetic resonance imaging (MRI) is the only *in vivo* imaging modality that can acquire diffusion sensitized information. Although MRI can acquire information from atomic spins of many different isotopes, most often they are sensitive to the probing of water molecule diffusion as MRI signal, based on the signal from hydrogen.

Diffusion MRI is routinely done by encoding water diffusivity in 3 orthogonal directions. By default (in an axially acquired acquisition), these are called diffusion along X (left-right), Y (anterior-posterior), and Z (inferior-superior), or D_X , D_Y , and D_Z . This approach is called diffusion weighted imaging (DWI) and is minimally quantitative, giving only mean diffusion weighting, $(D_X+D_Y+D_Z)/3$, and apparent diffusion coefficient (ADC):

$$S = S_0 e^{-b \cdot ADC} \quad (2.1)$$

where S is the signal at a specific diffusion weighting (b-value; described below), S_0 is signal without diffusion weighting, ADC is the apparent diffusion coefficient (in units mm^2/s) and b (in units s/mm^2) is the prescribed diffusion weighting (see equation 2.2 for the b-value components).

Diffusion can be encoded in several ways, most commonly using the ‘pulse field gradient’ (Stejskal and Tanner 1965; Callaghan and Soderman 1983; Le Bihan *et al.* 2001), where a spin echo experiment (i.e. 90° radiofrequency (RF) pulse, followed by time $\tau/2$ and then a 180° RF pulse) is modified to include two diffusion encoding gradients of equal direction and magnitude applied equatorially on either side of the refocusing RF pulse, as shown pictorially in figure 2.1.

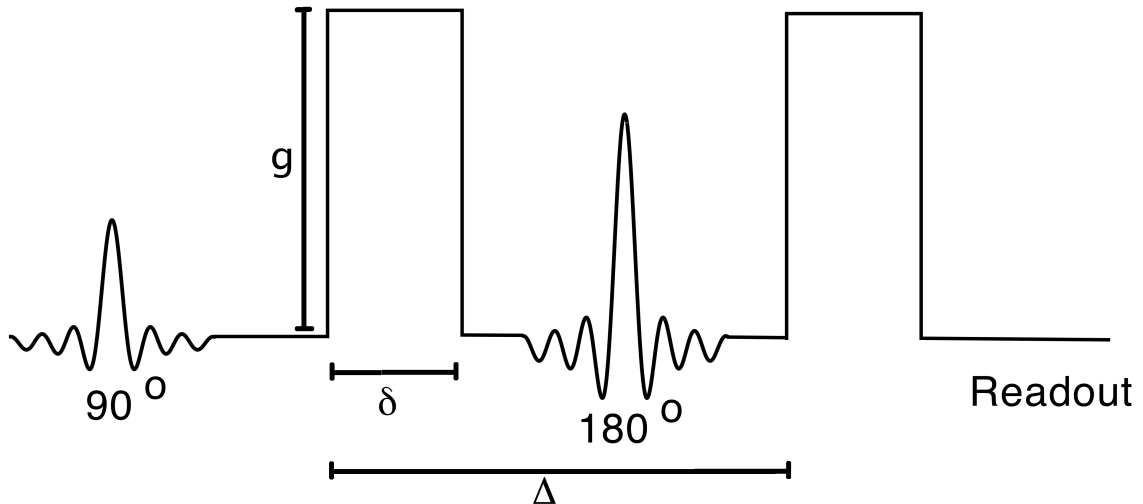


Figure 2.1 Depiction of the pulsed field gradient. The two equal duration (δ) and magnitude (g) gradients are separated by time (Δ). A 180 degree pulse is applied in the inter-gradient time

Diffusion weighted images show reduced signal intensity where [water] spins are more mobile. This is due to the reduced echo intensity that results from unequal gradient-

induced phase shifts that results when spins have diffused over time, Δ . Diffusion weighting can be increased by increasing the gradient duration (δ), magnitude (g) or time between diffusion sensitizing gradients, Δ . They are interrelated with the b value:

$$b = \gamma^2 \delta^2 g^2 \left(\Delta - \frac{\delta}{3} \right) \quad (2.2)$$

The symbol γ is the gyromagnetic ratio (42.576 MHz T⁻¹ for hydrogen ¹H). An extension of DWI is diffusion tensor imaging (DTI), which applies the tensor encoding of diffusion weighted images resulting in a rotationally invariant diffusion matrix. Rotational invariance indicates insensitivity to the angle of fibers within the magnet's Cartesian framework and hence provides robust quantitation of water diffusion characteristics. Diffusion tensors are encoded using at least six diffusion directions, which are typically geometrically optimized. Data is then 'distilled' from multiple directions into a 3×3 matrix whose diagonal components are diffusion magnitudes. This can be visualized as an ellipse, where the magnitudes along the three greatest directions are the eigenvalues ($\lambda_1, \lambda_2, \lambda_3$), whose directions are given by their eigenvectors ($\epsilon_1, \epsilon_2, \epsilon_3$). The lower right drawing in figure 2.2 shows a description of the diffusion ellipsoid and associated eigenvalues. Data from the eigenvalues are typically presented, along with the re-formulated data such as mean diffusivity (MD), fractional anisotropy (FA), and radial diffusivity (RD), which are:

$$MD = \frac{\lambda_1 + \lambda_2 + \lambda_3}{3} \quad (2.3)$$

$$FA = \sqrt{\frac{3 \times [(MD - \lambda_1)^2 + (MD - \lambda_2)^2 + (MD - \lambda_3)^2]}{2 \times (\lambda_1^2 + \lambda_2^2 + \lambda_3^2)}} \quad (2.4)$$

$$RD = \frac{\lambda_2 + \lambda_3}{2} \quad (2.5)$$

FA scales between 0 and 1, with 0 being a perfect sphere, where all λ s are equal, and 1 is a hypothetical cylinder of infinite length. FA is often used as a measure of abnormal tissue structure. In tissues with elongated cell structure, as in neurons, axonal membrane rupture will result in decreased barriers to diffusion and the second and third eigenvalues increase. So, a change in FA might arise from increases in λ_2 and λ_3 , *or* a decrease in λ_1 . For this reason, RD is used since changes in its value are independent of λ_1 . Conversely, it is theoretically possible that λ_1 may increase if intracellular components are damaged, and the level of damage is not sufficient for cell membrane rupture. Diffusion *in vivo* is also altered by membrane permeability, the relative size of free and bound water pools, the interaction and size of associated macromolecules, tissue viscosity, and local temperature (Andre and Bammer 2010). Diffusion MRI is an important imaging modality since it reveals changes in detailed microstructural anatomy, which no other imaging modality is able to do. It has been invaluable in several applications, including the early evaluation of cerebrovascular disease, muscle pathology and cancer, and in the assessment of brain functional connectivity in health and disease (Price 2007; Madden *et al.* 2009; Sosnovik *et al.* 2009; Vadakkumpadan *et al.* 2010; Gerstner and Sorensen 2011; Jang 2011; O'Donnell and Westin 2011; Madden *et al.* 2012).

Of importance in biological systems is the fact that living tissues have hydrophobic lipid bilayers (constituents of cell and organelle membranes), which restrict the random translation of water molecules at both sub and supra-cellular scales. The ideal tissue micro-structure for diffusion MRI is one in which the cells are elongated and thin, such as with neural tissue. Also, the sarcomere structure of skeletal muscle is ideal, since, not only are the cells elongated, but also have similar orientation within a voxel, as depicted in figure 2.2. Of course, this is a simplistic description; intracellular structures such as the mesh-like sarcoplasmic reticulum and t-tubules also provide intracellular barriers to diffusion, and thus may reduce λ_1 . The sarcoplasmic reticulum may reduce any or all three eigenvalues, and damage to the sarcoplasmic reticulum may be reflected by increased diffusion in any or all eigenvalues. Neurons typically have less uniform direction in the cerebral cortex, given the typical voxel size for diffusion tensor imaging (DTI) of approximately 8 mm^3 . This is the lower size limit for reasonable scan times.

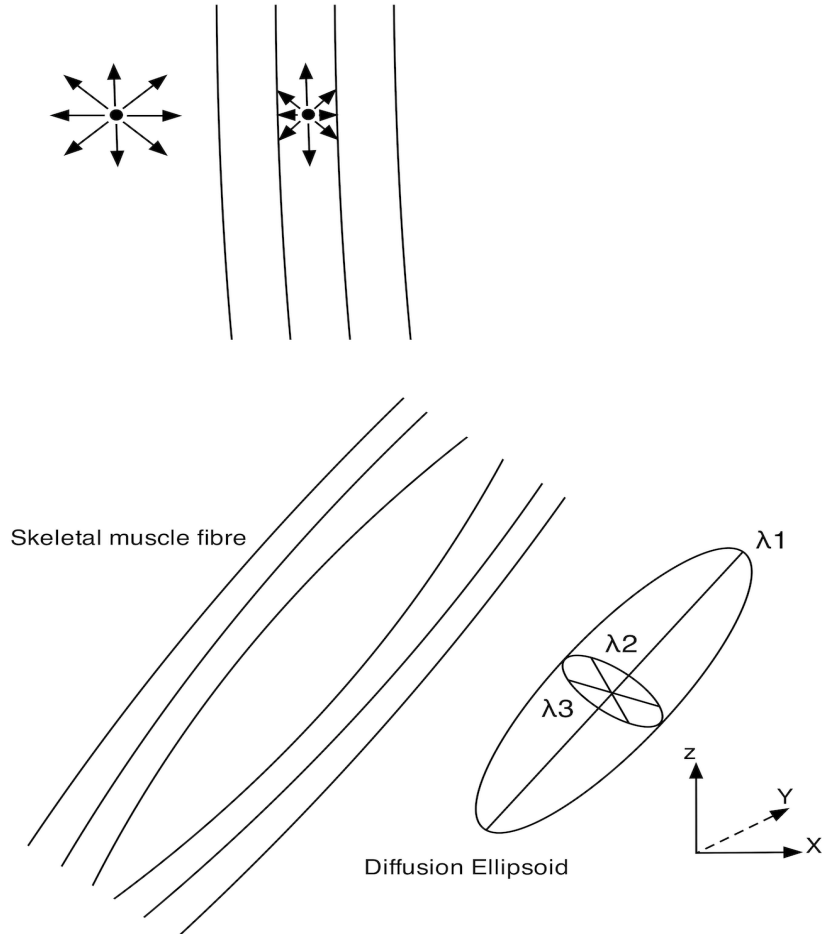


Figure 2.2 Upper left: diffusion in the absence of tissue, such as in a phantom. Diffusion is of equal magnitude in all directions. Upper centre: diffusion in a myofibril or axon, whose magnitude is much greater in one direction, the long axis of the cell. Diffusion in the other two directions is restricted. Lower depictions: Diffusion in skeletal muscle tissue, whose myofibres are all oriented in generally the same direction (although not completely parallel). The first eigenvalue (λ_1) is greatest and aligns with the muscle axis. The second and third eigenvalues (λ_2 and λ_3) are expected to be much lower in healthy tissue.

2.2. MR Diffusion for LBP

MRI of the lower back is well studied, however, most data is only from the spinal cord and some associated anatomy such as the dorsal root ganglion. At time of thesis submission, there are no other diffusion MRI studies of the lumbar paraspinal muscles, the multifidus, quadratus lumborum and erector spinae. The paragraphs below describe the uses and limitations of diffusion MRI in the spinal cord, and later, why DTI in the lower back musculature is relevant and is less technically challenging than spinal cord DTI.

For pathology associated with low back pain, diffusion-MRI research is being evaluated as a potential means of clinical assessment. However, many diffusion studies in the lumbar area focus directly on the spine, in an attempt to confirm etiology. Eguchi used diffusion MRI to identify the location of endplate abnormalities (Eguchi *et al.* 2011b) or nerve root entrapment (Eguchi *et al.* 2011a). DTI is also used to specifically study intervertebral discs (Zhang *et al.* 2012) and other aspects of the lumbar spinal cord (Adhikari *et al.* 2011; Balbi *et al.* 2011; Mohamed *et al.* 2011; Pease and Miller 2011; Barakat *et al.* 2012; Mulcahey *et al.* 2012). There are, however, challenges with DTI in the spinal cord, which are not as prominent in muscular DTI. There are inhomogeneities in areas around the vertebral column (Barakat *et al.* 2012), which are due to the presence of differing bone densities of the spinous, auricular and transverse processes, pedicle, and other bony structures (Bammer and Fazekas 2003). The target structures in the spinal cord are typically very small, necessitating high resolution. If imaging of any nerve-

related pathology is required, partial voluming becomes an issue. Also, narrowing of the spinal canal through disc herniation or spondylolisthesis would further shrink the target structure. Finally, artifacts due to bulk motion, such as cerebrospinal fluid (CSF) pulsation, swallowing in the cervical regions, and/or respiratory motion interferes with image acquisition and ultimately quality.

Diffusion in the lumbar musculature, specifically the lumbar erector spinae and multifidus, minimizes these difficulties. The tissue to be imaged is homogeneous, the movement artifacts from breathing, heart rate and swallowing are minimized, and the difficulties in bone density differences are minimized, since the multifidus and erector spinae are farther away from the bony structures than the intervertebral discs and nerve roots. Further, DTI in the muscle (but not lumbar paraspinal muscles) is well studied relative to spinal column. A standard body surface coil can be used, since the tissue is very superficial. Skeletal muscle is an ideal target tissue since myofibres are organized in a regular, repeated structure, and the intracellular architecture (composed of actin and myosin filaments, parallel to the muscle axis and membranous T-tubules perpendicular to the muscle axis) also has the same orientation and similar structure. These structures form a barrier to water diffusion. The DTI metric FA has shown high sensitivity to muscle injury from eccentric (muscle contraction during lengthening) contractions, more so than T2-weighted imaging, and the differences in FA were not based only on local oedema (McMillan *et al.* 2011). DTI metrics in skeletal muscle are more variable if the SNR is below 25, and data with SNR below 20 should not be used (Damon 2008).

2.3. Blood Oxygen Level Dependent (BOLD) MR

Blood oxygen level dependent (BOLD) MR uses the different susceptibilities of oxygenated and deoxygenated haemoglobin (Hb) of red blood cells to infer the metabolic status of the tissue supplied by the vessels. Changes in the BOLD signal can originate from changes in any phenomena that alter local blood oxygenation, such as perfusion, blood volume, heart rate, local metabolism, and vasodilation. Defined first in the brain by Ogawa *et al.* (1990), BOLD signal forms the basis behind functional MRI (fMRI). Often, especially for brain, BOLD signal change is driven by a defined paradigm and data are fitted to a haemodynamic response function (HRF) model that puts blood flow, blood volume oxy:deoxyHb ratio and metabolism into one signal. Resting state BOLD analysis is appealing in that no models are needed and, therefore no model-associated assumptions or constraints are required. One such approach is to determine the fractal dimension of the BOLD signal. In short, the fractal dimension (FD) is a measure of the signal temporal complexity. Noisy signals, with little sinusoidal modulation from blood flow, are complex signals and a higher fractal dimension reflects this. Sinusoidal signals, such as those with greater blood flow contribution within a voxel, have less complexity and lower FD values. The FD scales between 1.0 and 1.5, where higher values are more complex signals. Fractal dimension can be calculated by several methods. One, the power spectrum method, requires conversion into the frequency domain using a fast Fourier transform (FFT) and assumes a relationship where β (the spectral index) is determined by:

$$|A|^2 = \frac{1}{f^\beta} \quad (2.6)$$

Where A is the amplitude of the BOLD ($T2^*$) signal at a particular frequency, f . The fractal dimension (FD_{PS}) is then calculated as:

$$FD_{PS} = 2 - \frac{(\beta + 1)}{2} \quad (2.7)$$

Alternatively, FD may be calculated using the relative dispersion method (FD_{RD}). Relative dispersion is a synonym for coefficient of variation (CV), which is simply a sample's standard deviation divided by mean. FD_{RD} is then calculated using:

$$RD(m) = RD(m_{ref}) \times \left(\frac{m}{m_{ref}} \right)^{1-FD_{RD}} \quad (2.8)$$

Where m is the scale and m_{ref} is set to 1. Biological tissues often have two FD_{RD} components, called simply the slow and fast components of the FD_{RD} , where $FD_{RD-slow}$ is calculated with $4 < m < 64$ seconds, and $FD_{RD-fast}$ is with $0.25 < m < 2.00$ seconds.

Chapter 3. Hypotheses

As described in Chapter 1.1 and 1.2, LBP and CLBP in particular, are difficult to diagnose with clinical observation and with standard imaging including conventional MRI sequences. There is a need for accurate diagnoses. It is clear that there are levels of treatment both pharmacologically (based on the analgesic ladder described in the previous section) and there are different stages of recovery exercises (section 1.4). It has been shown that stratified care (Whitehurst et al 2012), whose endpoint may be forgoing the lower ‘rungs’ of the ladder for more severe cases, or not undergoing the more initial stages of exercises for the less severe cases, may improve symptoms and lower cost. As such, it is critical to describe the forms of treatment adequately as in sections 1.4.2 and 1.4.3. Physicians are able to diagnose abnormalities in the spinal column, and this area is typically scanned in clinical lower back MRI. However, 70% of symptoms are related to the musculature (Deyo et al 2001), and are not the central focus of clinical MRI. This is one possible reason why current conventional scans show limited correlation with LBP symptoms. This study, whose central focus is the paraspinal musculature, may help close a gap in MR diagnosis.

Decisions involving governmental or insurance company assistance require accuracy, and the current gold standards (such as the Lasègue test described in chapter 1, or questionnaires) all have subjective elements. An objective accurate, precise measure is

needed. Further, stratified care, placing LBP patients into one of three categories, may improve symptoms at lower cost compared to current best practices (Hill *et al.* 2010; Hill *et al.* 2011; Whitehurst *et al.* 2012). It is critical to accurately evaluate LBP symptoms to ensure that patients are placed in the appropriate stream. The MRI scans described below may assist in that placement.

Current clinical MRI paradigms cannot distinguish between new and old injury (as described in chapter 1). Using DTI in the spinal cord (as shown in chapter 2.2), there is some utility, but there must be some pre-scan knowledge of the location (in the I-S direction) of injury, and scans are not of use for some forms of lower back dysfunction, such as stenosis (cannot separate old from new injury). Scans of the skeletal paraspinal muscles avoid these pitfalls; they are altered in subjects regardless of etiology and location for injuries originating the lumbar and thoracic regions, as shown in chapter 1.3.

MRI scans and analyses were performed on subjects with and without the symptoms of CLBP to test the hypothesis:

- 1) Can advanced MRI scans differentiate between subjects with CLBP and healthy control subjects;
- 2) Do the advanced MRI scans correlate with the symptoms of CLBP; and
- 3) Correlations between CLBP and MRI metrics will increase when taking cofactors such as age, gender, weight, height, BMI, and/or level of physical activity into consideration.

The proposed advanced MRI scans, analyses, and resultant MRI metrics are: DTI measures (λ_1 , λ_2 , λ_3 , FA, MD, RD), blood oxygen level dependent (BOLD) signal fractal dimension (FD) and T2 weighted (T2W) muscle cross sectional area (CSA). Data from these three scans will be compared in subjects with CLBP and controls. Further, data from BOLD FD, DTI and T2W CSA will be correlated with questionnaires that measure the symptoms of LBP. Finally, data will be correlated with other anthropomorphic factors such as age, gender, weight, height, BMI, and/or level of physical activity (which will be estimated with the Godin leisure time exercise questionnaire) to determine any mitigating influence.

Chapter 4 . Diffusion Tensor Imaging (DTI) in the Healthy Lower Back

Gavin E.G. Jones, M.Sc., Dinesh A. Kumbhare, M.Sc., M.D., FRCPC, Srinivasan Harish MBBS, FRCPC, and Michael D. Noseworthy, PhD, P.Eng.

4.1. Context of Paper

DTI in skeletal muscle has been explored in the lower extremities and the forearm, but this is the first study in the lumbar musculature, and only the second to study the multifidus. The first is in the cervical multifidus and uses diffusion weighted imaging (Elliott *et al.* 2010), and is not relevant for lower back dysfunction. The following submitted publication determines the reliability of DTI parameters, compares them to those acquired in other body parts, such as the soleus and gastrocnemius of the calf, and determines whether DTI metrics are affected by any demographic characteristics in a healthy population. Determining these factors is a necessary first step in evaluating DTI's efficacy in measuring the lumbar musculature in subjects with pathology such as CLBP.

4.2. Declaration Statement

Gavin Jones as principle author wrote the article, performed all analysis and inserted data images/tables as appropriate. MRI scanning protocols were designed by

Michael D. Noseworthy (MDN). Experimental design was done by MDN and Dinesh A. Kumbhare (DAK). Srinivasan Harish (SH) assessed scans for clinical anomalies. MDN, DAK, and SH provided guidance and advice, in proofreading and editing prior to submission. The manuscript was submitted for publication to the Journal of Computer Assisted Tomography (JCAT) on July 6, 2012.

4.3. Abstract

Objectives: To characterize diffusion tensor imaging (DTI) tensor eigenvalues (λ_1 , λ_2 , λ_3), fractional anisotropy (FA), mean diffusivity (MD), and radial diffusivity (RD) in healthy lumbar musculature.

Methods: Seventeen healthy subjects (10 men, 7 women, 28 ± 7 yrs) were scanned using a 3.0T MRI. Axial DTI was performed using 15 diffusion directions ($b=400 \text{mm}^2/\text{s}$) at the L4 level. Oswestry low back pain and Godin physical activity questionnaires were administered to rule out underlying lower back problems.

Results: Skeletal muscle DTI metrics were similar to those previously published. All measurements showed low coefficient of variation, except for quadratus lumborum. Laterality was not significant. Significant gender differences were observed in the quadratus lumborum ($p < 0.05$). Significant correlations were found between subjects' weight and BMI with FA and λ_1 of the multifidus muscles.

Conclusion: DTI metrics in paraspinal muscles can be reliably measured and are influenced by BMI and weight, but not age or physical activity.

4.4. Keywords

Magnetic resonance imaging (MRI), diffusion tensor imaging (DTI), skeletal muscle, lumbar spine

4.5. Introduction

Diffusion tensor imaging (DTI) is a well recognized method used for assessment of anisotropic tissues such as brain, muscle, and myocardium. It was first used for imaging skeletal muscle fifteen years ago¹. Since then, DTI of skeletal muscle has become more widely used²⁻⁵, with a dominant focus on the lower extremity^{3, 5-9}.

DTI results are influenced by the anisotropic diffusivity of water. It is hypothesized that diffusion along the long axis of the myofibre is greater than that perpendicular to it (due to membranous barriers, including the sarcolemma and perimysium). The regular repeated structure of myofibrils is another reason for the proposed reliability of DTI in skeletal muscle¹⁰. The first eigenvector (ϵ_1) of the DTI matrix is believed to align with the direction of the myofibre. Furthermore, increased second and/or third eigenvalues (λ_2, λ_3), or decreased fractional anisotropy (FA), are thought to indicate structural abnormality¹⁰.

The lumbar multifidus muscle is implicated in mechanical low back pain¹¹. Fatty infiltration of the lumbar multifidus (LM) is correlated to leg pain, when other anatomic structures appear normal. However a causal relationship has not been conclusively

proven in this regard¹¹. Patients with degenerative disc disease have lower cross sectional area (CSA) of the paraspinal muscles as well as the quadratus lumborum¹². This suggests that structural abnormalities in the lumbar stabilization muscles may be implicated in low back pain (LBP). It is recognized that anatomical abnormalities seen on routine MRI of the lumbar spine do not necessarily correlate to the functional disability of the patient¹³. Also, conventional MRI techniques do not assess the functional contribution of the paraspinal muscles in the natural course of mechanical LBP. Hence, a new imaging approach would be helpful for the evaluation of LBP. DTI may reveal abnormalities in the muscles that are not visible using conventional MRI techniques used for LBP evaluation. Also, the reliable characterization of DTI metrics in the uninjured/asymptomatic paraspinal musculature is an essential initial step to allow assessment of any pathological state. Hence, the purposes of this study were to 1) quantify tensor eigenvalues ($\lambda_1, \lambda_2, \lambda_3$), mean diffusivity (MD), fractional anisotropy (FA) and radial diffusivity (RD) of muscles of the lower back (longissimus, iliocostalis, multifidus and quadratus lumborum) at the level of L4 in asymptomatic healthy volunteers; and 2) to determine whether those measures are correlated to anthropometric (height, weight, age, gender, BMI) information. Once healthy lumbar skeletal muscles can be reliably characterized it is hoped this study will provide the foundation for comparing LBP patients.

4.6. Methods

4.6.1. 4.6.1 Subjects

Ten men and seven women (mean age of 28 ± 6 years) with no symptoms of low back pain (LBP) in the 6 years preceding the study were recruited. Subjects were not permitted to perform strenuous exercise, drink alcohol or caffeine in the six hours before scanning. Informed consent was obtained from each volunteer. Full approval from our institution's Research Ethics Board was obtained prior to the start of the study.

4.6.2. Magnetic Resonance Imaging

All MRI scans were performed using a GE Signa HD 3T MRI scanner and 12-channel neck/spine array RF coil (GE Healthcare, Milwaukee WI). Subjects were scanned in a supine position with the isocenter approximately at the L4 level. Following a 3-plane localizer scan, the following sequences were done: 3D fast IR prepped SPGR (axial acquisition, TE in phase, TI=450, flip angle=120, 512x224 over 20cm FOV, 2mm thick, 0mm skip, 120 slices); Sagittal T2-weighted FRFSE (ETL=23, TE/TR=150/3800ms, 448x224 matrix, 4 averages (NEX), rbw=41.67kHz, 28cm FOV, 4mm thick, 1mm space); axial and sagittal T1-weighted FSE (ETL=3, TE=minimum, TR=575, 28cm FOV, 4mm thick, 1mm space, 416x256, 3NEX, rbw=41.67kHz); and Axial T2-weighted FRFSE (TE/TR=150/4625ms, ETL=23, FOV=20, thickness=5mm, 0mm skip, 448x224, NEX=3, rbw=41.67kHz). None of our subjects showed any signs of gross pathology.

To ensure accurate quantification, DTI data were collected in 4 separate scans, each with the same prescan values (shim values, centre frequency, and transmit/receive gain values) and geometric prescription. In effect the scans were done with 4 averages (NEX). However, each acquisition was corrected for motion and eddy currents prior to being summed and subsequently the tensor was processed on the resultant summed dataset. Each DTI scan was done with one $b=0s/mm^2$ image and 15 optimized diffusion encoding gradient directions, with a b-value of $400s/mm^2$ (TE/TR=62/10000ms, acquisition and reconstruction matrix size = 64x64, 20 slices covering L3 to L5 in the I-S direction, 5.0mm thick. 0mm skip, FOV=40cm). The total scan time for all 4 NEX was 12 minutes.

4.6.3. Questionnaires

Standard English Oswestry Low Back Disability Questionnaire¹⁴ and Godin Leisure-Time Exercise Questionnaires were given to subjects immediately after the MRI. The Oswestry questionnaire has 10 questions revealing the effect of LBP on everyday activities. The answers range from 0 (least severe) to 5 (most severe), resulting in an Oswestry Disability Index (ODI) from 0-100%, with 100 being the most severe. Information is generally interpreted as: 0-20%: minimal disability; 21-40%: moderate disability; 41-60%: severe disability; 61-80%: crippled; 81-100%: subjects are either bed-bound or exaggerating their symptoms. The ODI was measured to ensure that subjects had no symptoms of LBP, which may influence our results. Since multifidus and erector spinae (which include the iliocostalis and longissimus) are altered in subjects with LBP¹⁵⁻²⁰, the muscle microstructure, which may influence DTI measures, may also be

affected. Collecting and ensuring a low ODI score for each of our asymptomatic subjects is an important quality control measure to ensure that LBP symptoms do not contaminate our results. The Godin questionnaire is a measure of the person's activity level.

4.6.4. Data Analysis

DTI measurements were made of the bilateral multifidus, longissimus, iliocostalis, and quadratus lumborum, although regions of interest (ROIs) were separated into right and left muscles. Tensor analyses was performed using FSL 4.1 (FMRIB Analysis Group; <http://www.fmrib.ox.ac.uk/fsl/>). Registration of each NEX was performed by registering each $b=0\text{s/mm}^2$ image to the chronologically first $b=0\text{s/mm}^2$ image (i.e. from NEX=1). Eddy current correction was performed after image registration. Singular value decomposition was used to create the 3x3 diffusion tensor, from which the three eigenvalues ($\lambda_1, \lambda_2, \lambda_3$) and eigenvectors ($\epsilon_1, \epsilon_2, \epsilon_3$) were calculated. Fractional anisotropy (FA), a parameter widely reported as a measure of the elliptical nature of the tensor, was calculated using:

$$FA = \sqrt{\frac{3}{2}} \cdot \sqrt{\frac{(\lambda_1 - \bar{\lambda})^2 + (\lambda_2 - \bar{\lambda})^2 + (\lambda_3 - \bar{\lambda})^2}{\lambda_1^2 + \lambda_2^2 + \lambda_3^2}}$$

Where mean diffusivity (MD) or $\bar{\lambda}$ was calculated with:

$$\bar{\lambda} = \frac{\lambda_1 + \lambda_2 + \lambda_3}{3}$$

Radial Diffusivity (RD) was calculated by:

$$RD = \frac{\lambda_2 + \lambda_3}{2}$$

Individual muscle diffusion analysis was done by drawing regions of interest (ROIs) over the axial T1-weighted images using AFNI (National Institute of Mental Health, NIMH). The ROIs were then resampled to the lower resolution of the DTI data. Care was taken to ensure that no other tissue was included other than the target muscle, even if some of the outer limits of the target muscle were not included, to minimize partial voluming. In the axial plane, ROIs were chosen to encompass the lumbar multifidus, iliocostalis, longissimus, or all three muscles (erector spinae + multifidus or ES+M), as well as the quadratus lumborum. **Figure 4.1** shows several sample ROIs in both axial and sagittal planes of a 27-year-old man.

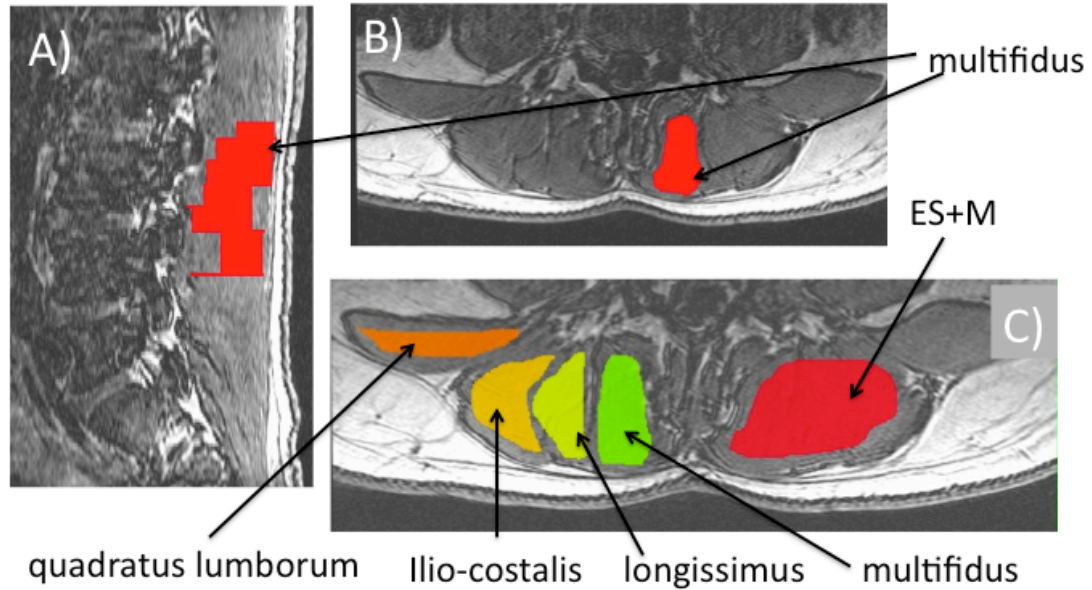


Figure 4.1 ROIs superimposed on 3D-SPGR images in a 27 year old male. A) the left multifidus in the sagittal plane (red). B) the left multifidus in the axial plane. C) shows the right multifidus (green), right longissimus (yellow), iliocostalis (light orange), and quadratus lumborum (dark orange). The red ROI in C) depicts the left multifidus, longissimus and iliocostalis muscles (erector spinae + multifidus or ES+M).

4.6.5. Statistical Evaluation

Analyses were performed using SPSS 17.0 (IBM). DTI results (FA, mean diffusivity MD, λ_1 , λ_2 , λ_3 , RD) were examined using 2-way ANOVA, with laterality (left-right) and gender as factors. If ANOVA significance was achieved, Fisher's Least Squares Differences post-hoc test was performed.

To determine whether the subject data (age, height, weight), or results from questionnaires were correlated with DTI results, Spearman's correlations coefficient were

calculated (ρ). A correlation was determined to be significant if a 95% level threshold was achieved ($p < 0.05$).

4.7. Results

None of the subjects had any lumbar stenoses, disc abnormality or other pathology, as judged using routine MR imaging. Furthermore, the results of the Oswestry questionnaires indicated that subjects did not suffer from LBP; the mean \pm SD for ODI was $0.0 \pm 0.0\%$. Crombach's alpha was 0.98 for the 10 questions asked.

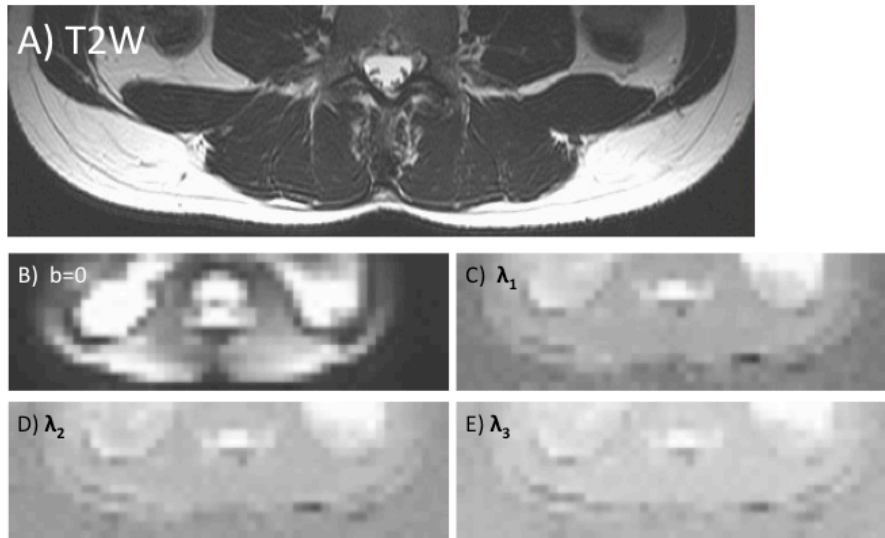


Figure 4.2 A) Sample T2W image in the axial plane. B) $b=0$ s/mm², C) λ_1 , D) λ_2 , E) λ_3 maps. All are at approximately L4 of a 27 year old male.

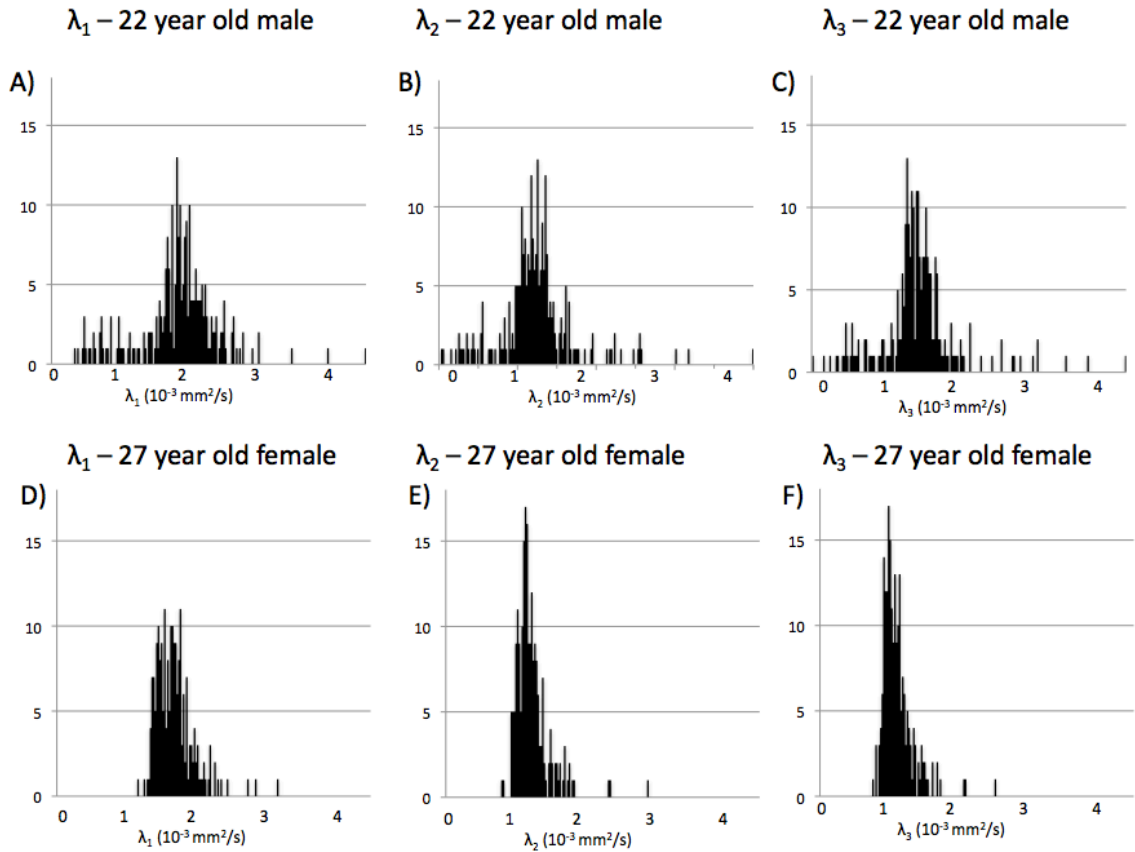


Figure 4.3 Statistical assessment of normality was assessed for all ROIs. Sample histograms of first (λ_1 in A and D), second (λ_2 in B and E) and third (λ_3 in C and F) eigenvalues are shown. A) to C) shows data from a 22 year old right handed male’s right multifidus. D) to F) are from a 27 year old right handed female’s left longissimus. Data that is normally distributed, based on the Shapiro-Wilk normality test ($p > 0.05$), are in A, B and D.

A sample T2W image, an image with no diffusion weighted gradients (i.e. $b=0\text{s/mm}^2$) and eigenvalue maps are presented (fig 4.2). Eigenvalue histograms from the multifidus of a 22-year-old male’s right multifidus muscle (fig 4.3A-C) are compared to that of a 27 year old female’s left longissimus (fig 4.3D-F) to show variability in ROI distributions. Very few voxels had λ_1 greater than $3.0 \times 10^{-3} \text{ mm}^2/\text{sec}$, indicating inclusion of larger blood vessels within selected ROIs was minimal². All data passed a Shapiro-Wilk normality test ($p > 0.05$) with data distributions appearing similar to Froeling *et al.*².

DTI measures were highly correlated between each other. For example, the FA values from left and right ES+M showed a Spearman's correlation of $\rho=0.97$. Furthermore, right MD was positively correlated with λ_1 ($\rho=0.89$) and λ_2 ($\rho=0.92$). Since both λ_1 and λ_2 are used to calculate MD, these correlations are expected. Most correlations of DTI metrics with anthropometric data (e.g. age, weight, height, Godin score and BMI) were often low, based on Spearman's correlation coefficient (i.e. $-0.15 < \rho < +0.15$). However, higher correlation values were noted between right ES+M FA and weight ($\rho=0.38$), right ES+M FA and height ($\rho=0.38$), right ES+M λ_1 and age ($\rho=0.34$), and Godin score and both right ES+M MD and λ_1 ($\rho=0.37$ and 0.36 , respectively). As an example, **Fig. 4.4** shows scatter plots of the eigenvalues for left and right ES+M target muscle group vs. BMI, as well as their associated correlation coefficients. All eigenvalues negatively correlated with BMI, with λ_1 being the most correlated (**fig 4.4**).

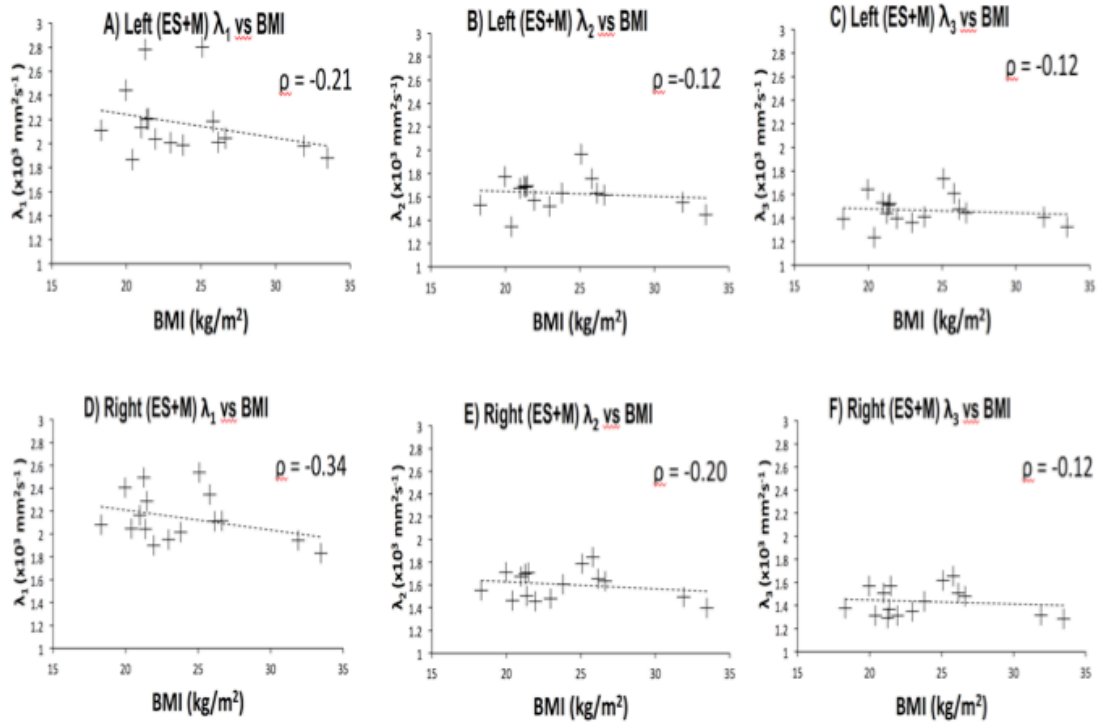


Figure 4.4 Plots of eigenvalues (λ_1 , λ_2 and λ_3) vs to body mass index (BMI). The target ROIs are the left (A-C) and right (D-F) ES+M (longissimus, iliocostalis and multifidus). The best linear fit (dashed line) and Spearman's correlation coefficient are also shown.

Values for FA, RD, MD, and eigenvalues are shown in tables 4.1 and 4.2. Two way ANOVAs, for each muscle, were performed with laterality (left vs. right) and gender as factors. The only significant effect was gender, specifically for the quadratus lumborum muscle ($p < 0.05$).

Multifidus

Left							Right						
	FA	MD	λ_1	λ_2	λ_3	RD	FA	MD	λ_1	λ_2	λ_3	RD	
FEMALES	0.21±0.03	1.72±0.11	2.12±0.14	1.60±0.14	1.42±0.08	1.51±0.09	0.21±0.02	1.79±0.15	2.19±0.18	1.67±0.14	1.49±0.15	1.58±0.14	
MALES	0.20±0.03	1.68±0.10	2.05±0.16	1.57±0.09	1.40±0.06	1.49±0.07	0.21±0.03	1.61±0.13	2.00±0.16	1.53±0.09	1.35±0.10	1.43±0.09	
TOTAL	0.20±0.03	1.69±0.10	2.08±0.16	1.58±0.09	1.41±0.06	1.50±0.07	0.21±0.03	1.69±0.16	2.08±0.19	1.59±0.13	1.40±0.14	1.50±0.13	

Longissimus

Left							Right						
	FA	MD	λ_1	λ_2	λ_3	RD	FA	MD	λ_1	λ_2	λ_3	RD	
FEMALES	0.23±0.03	1.74±0.16	2.17±0.18	1.54±0.15	1.43±0.14	1.49±0.14	0.22±0.02	1.74±0.06	2.13±0.14	1.59±0.16	1.42±0.13	1.51±0.14	
MALES	0.21±0.04	1.68±0.16	2.07±0.25	1.56±0.15	1.41±0.11	1.47±0.13	0.19±0.02	1.51±0.17	1.85±0.22	1.40±0.16	1.30±0.14	1.35±0.15	
TOTAL	0.21±0.03	1.70±0.16	2.11±0.22	1.55±0.15	1.42±0.12	1.48±0.13	0.21±0.02	1.72±0.17	2.11±0.21	1.59±0.16	1.43±0.14	1.51±0.14	

Ilio-costalis

Left							Right						
	FA	MD	λ_1	λ_2	λ_3	RD	FA	MD	λ_1	λ_2	λ_3	RD	
FEMALES	0.21±0.03	1.78±0.18	2.21±0.21	1.66±0.18	1.50±0.18	1.57±0.15	0.23±0.03	1.66±0.16	2.09±0.20	1.49±0.13	1.36±0.15	1.57±0.13	
MALES	0.19±0.04	1.75±0.13	2.13±0.23	1.64±0.10	1.49±0.08	1.55±0.15	0.21±0.03	1.62±0.23	2.02±0.28	1.48±0.21	1.35±0.20	1.15±0.15	
TOTAL	0.20±0.04	1.76±0.15	2.16±0.22	1.65±0.13	1.49±0.12	1.56±0.14	0.22±0.03	1.64±0.20	2.05±0.25	1.48±0.18	1.36±0.18	1.56±0.14	

Table 4.1 Data are mean ± standard deviation. Eigenvalues, MD, and RD units are $\times 10^{-3} \text{ mm}^2/\text{sec}$.

3 Muscles (Multifidus, Longissimus, Ilio-costalis)

Left							Right						
	FA	MD	λ_1	λ_2	λ_3	RD	FA	MD	λ_1	λ_2	λ_3	RD	
FEMALES	0.23±0.06	1.78±0.17	2.26±0.29	1.62±0.14	1.47±0.13	1.55±0.13	0.24±0.04	1.76±0.11	2.24±0.17	1.62±0.10	1.43±0.12	1.53±0.10	
MALES	0.19±0.03	1.76±0.19	2.14±0.29	1.65±0.16	1.47±0.13	1.57±0.14	0.20±0.02	1.71±0.18	2.10±0.24	1.60±0.16	1.44±0.14	1.52±0.15	
TOTAL	0.21±0.05	1.77±0.17	2.20±0.28	1.64±0.15	1.48±0.13	1.56±0.13	0.22±0.04	1.74±0.15	2.17±0.21	1.61±0.13	1.44±0.13	1.52±0.13	

Quadratus Lumborum

Left							Right						
	FA	MD	λ_1	λ_2	λ_3	RD	FA	MD	λ_1	λ_2	λ_3	RD	
FEMALES	0.34±0.10	1.55±0.49	2.05±0.51	1.47±0.49	1.12±0.47	1.30±0.48	0.32±0.07	1.60±0.32	2.17±0.44	1.44±0.20	1.20±0.29	1.32±0.29	
MALES	0.24±0.04	1.80±0.29	2.26±0.29	1.70±0.35	1.44±0.25	1.57±0.30	0.27±0.04	1.70±0.16	2.22±0.20	1.55±0.18	1.35±0.14	1.45±0.16	
TOTAL	0.29±0.09	1.67±0.40	2.15±0.41	1.57±0.42	1.28±0.40	1.43±0.40	0.29±0.06	1.66±0.25	2.19±0.33	1.49±0.24	1.28±0.23	1.39±0.24	

Table 4.2 Data are mean ± standard deviation. Eigenvalues, MD, and RD units are $\times 10^{-3} \text{ mm}^2/\text{sec}$.

For most of the target muscles the CV was 15-23% for FA and approximately 10% for the eigenvalues. MD and RD were also approximately 10% of the mean. We did note much higher FA values for quadratus lumborum. Also, FA values from females' left and right quadratus lumborum had SD as 29% and 21%, respectively. Some subjects

had a much thinner quadratus lumborum and the ROI consisted of a lower number of voxels, which could have contributed to higher SD than for other muscle ROIs.

4.8. Discussion

In this study we characterized DTI metrics and their variability, and how they relate to anthropometric data in the lower back muscles of healthy adults. FA and eigenvalues are similar to those found in other studies on different muscle groups^{2, 4, 8, 21-23} but with higher eigenvalues than those reported by Van Donkelaar *et al.*²⁴, and slightly lower than those found in the quadriceps muscles⁴. Furthermore, we show similar coefficient of variation as those shown in other studies^{2, 5-8, 25}. No other studies, to the best of our knowledge, also evaluated laterality, gender, and height/weight as possible influences on DTI metrics. We did not find left/right asymmetry in any of the lumbar muscles analyzed. Laterality may or may not be of importance in certain populations. For example healthy professional cricketers are expected to have asymmetric lumbar hypertrophy²⁶. There was no significant difference among DTI metrics in the multifidus, longissimus, quadratus lumborum and iliocostalis, or ES+M ROIs. The ES+M may have included more fatty tissue than other muscle ROIs, although this fact didn't affect our measures. However, this is an important observation for future studies of pathology such as low back pain, since increased fatty infiltration in injured erector spinae muscles has previously been observed^{27, 28}

The correlations between Godin and the left multifidus λ_1 , λ_2 , λ_3 , and RD were very low, implying that eigenvalues measured in the lower back musculature are not

affected by the subject's level of physical activity. Also, no significant correlation between any DTI metric and age, height, or gender was found. Our age range was fairly narrow. However, the range for our subjects was between 19 and 47 years. Elsewhere, a lack of age dependence was found for DTI tractography of calf muscles²⁹. Thus a larger age range in our study would not likely have resulted in any different conclusion with respect to DTI metrics.

The observations described above would indicate that, in future DTI studies in the lumbar musculature at the L4 level, it would be best if data were separated into groups based on BMI. DTI metrics are not related to other subject characteristics, such as gender, age, height and physical fitness, and such data may be grouped together.

Based on a literature survey, DTI is thought to be useful in assessing dysfunction associated with muscular structural abnormalities^{13, 27, 30, 31, 32, 33, 34}. However, there have been no lower back DTI studies. It is well understood there is a strong connection between LBP symptoms and lower back musculature abnormalities. For example, data from conventional MRI has shown that lumbar multifidus muscle of LBP subjects may have different CSAs during active contraction²⁶. Furthermore, these muscles show increased fatty infiltration²⁸. Subjects with various forms of LBP have been shown to have altered multifidi and erector spinae^{13, 27, 30, 31}. Specifically, electromyography (EMG) of the multifidus is different between subjects with LBP, compared to healthy controls, during active movement³²⁻³⁶. In the lumbar erector spinae and multifidus, EMG and MRI results are related, where increased EMG activity is correlated with increases in muscle T2 relaxation³⁷. There is other evidence implicating the erector spinae and

multifidus in LBP, based on CSA of the lumbar multifidus^{32, 38-44}. To the best of our knowledge, our work is the second report using diffusion weighted MRI in the multifidus⁴⁵, and the only study using DTI to assess both the lumbar multifidus and erector spinae muscles. It should be noted, however, that routine spinal MRI studies often fail to correlate with symptoms¹³. In these studies frequently an older stenosis or other injury is attributed to the current symptoms.

In this current study, we have demonstrated that measurement of DTI metrics in the multifidus and erector spinae are repeatable and agree with previously published results for other skeletal muscles. BMI and weight scale with FA, but DTI measures did not correlate with other subject factors such as age, height, and level of physical activity. Furthermore, gender was not a significant factor. Our protocol can be done in a reasonable time on most clinical scanners.

4.9. References

1. Bassler PJ, Mattiello J, LeBihan D. MR diffusion tensor spectroscopy and imaging. *Biophys J*. 1994;66:259-267.
2. Froeling M, Oudeman J, van den Berg S, et al. Reproducibility of diffusion tensor imaging in human forearm muscles at 3.0 T in a clinical setting. *Magn Reson Med*. 2010;64:1182-1190.
3. Heemskerk AM, Sinha TK, Wilson KJ, et al. Quantitative assessment of DTI-based muscle fiber tracking and optimal tracking parameters. *Magn Reson Med*. 2009;61:467-472.
4. Kan JH, Heemskerk AM, Ding Z, et al. DTI-based muscle fiber tracking of the quadriceps mechanism in lateral patellar dislocation. *J Magn Reson Imaging*. 2009;29:663-670.
5. Sinha S, Sinha U. Reproducibility analysis of diffusion tensor indices and fiber architecture of human calf muscles in vivo at 1.5 Tesla in neutral and plantarflexed ankle positions at rest. *J Magn Reson Imaging*. 2011;34:107-119.
6. Galban CJ, Maderwald S, Uffmann K, et al. Diffusive sensitivity to muscle architecture: a magnetic resonance diffusion tensor imaging study of the human calf. *Eur J Appl Physiol*. 2004;93:253-262.
7. Heemskerk AM, Strijkers GJ, Vilanova A, et al. Determination of mouse skeletal muscle architecture using three-dimensional diffusion tensor imaging. *Magn Reson Med*. 2005;53:1333-1340.
8. Zaraiskaya T, Kumbhare D, Noseworthy MD. Diffusion tensor imaging in evaluation of human skeletal muscle injury. *J Magn Reson Imaging*. 2006;24:402-408.
9. Lansdown DA, Ding Z, Wadington M, et al. Quantitative diffusion tensor MRI-based fiber tracking of human skeletal muscle. *J Appl Physiol*. 2007;103:673-681.
10. Noseworthy MD, Davis AD, Elzibak AH. Advanced MR imaging techniques for skeletal muscle evaluation. *Semin Musculoskelet Radiol*. 2010;14:257-268.
11. Kader DF, Wardlaw D, Smith FW. Correlation between the MRI changes in the lumbar multifidus muscles and leg pain. *Clin Radiol*. 2000;55:145-149.

12. Ploumis A, Michailidis N, Christodoulou P, et al. Ipsilateral atrophy of paraspinal and psoas muscle in unilateral back pain patients with monosegmental degenerative disc disease. *Br J Radiol.*84:709-713.
13. Deyo RA, Weinstein JN. Low back pain. *N Engl J Med.* 2001;344:363-370.
14. Fairbank JC, Couper J, Davies JB, et al. The Oswestry low back pain disability questionnaire. *Physiotherapy.* 1980;66:271-273.
15. Hides J, Gilmore C, Stanton W, et al. Multifidus size and symmetry among chronic LBP and healthy asymptomatic subjects. *Man Ther.* 2008;13:43-49.
16. Hides JA, Stokes MJ, Saide M, et al. Evidence of lumbar multifidus muscle wasting ipsilateral to symptoms in patients with acute/subacute low back pain. *Spine (Phila Pa 1976).* 1994;19:165-172.
17. Hyun JK, Lee JY, Lee SJ, et al. Asymmetric atrophy of multifidus muscle in patients with unilateral lumbosacral radiculopathy. *Spine (Phila Pa 1976).* 2007;32:E598-602.
18. Lee HI, Song J, Lee HS, et al. Association between Cross-sectional Areas of Lumbar Muscles on Magnetic Resonance Imaging and Chronicity of Low Back Pain. *Ann Rehabil Med.* 2011;35:852-859.
19. Niemelainen R, Briand MM, Battie MC. Substantial asymmetry in paraspinal muscle cross-sectional area in healthy adults questions its value as a marker of low back pain and pathology. *Spine (Phila Pa 1976).* 2011;36:2152-2157.
20. Beneck GJ, Kulig K. Multifidus atrophy is localized and bilateral in active persons with chronic unilateral low back pain. *Arch Phys Med Rehabil.* 2012;93:300-306.
21. Budzik JF, Le Thuc V, Demondion X, et al. In vivo MR tractography of thigh muscles using diffusion imaging: initial results. *Eur Radiol.* 2007;17:3079-3085.
22. Saupé N, White LM, Stainsby J, et al. Diffusion tensor imaging and fiber tractography of skeletal muscle: optimization of B value for imaging at 1.5 T. *AJR Am J Roentgenol.* 2009;192:W282-290.
23. Saupé N, White LM, Sussman MS, et al. Diffusion tensor magnetic resonance imaging of the human calf: comparison between 1.5 T and 3.0 T-preliminary results. *Invest Radiol.* 2008;43:612-618.

24. Van Donkelaar CC, Kretzers LJ, Bovendeerd PH, et al. Diffusion tensor imaging in biomechanical studies of skeletal muscle function. *J Anat.* 1999;194 (Pt 1):79-88.
25. Karampinos DC, King KF, Sutton BP, et al. Myofiber ellipticity as an explanation for transverse asymmetry of skeletal muscle diffusion MRI in vivo signal. *Ann Biomed Eng.* 2009;37:2532-2546.
26. Hides J, Stanton W, Freke M, et al. MRI study of the size, symmetry and function of the trunk muscles among elite cricketers with and without low back pain. *Br J Sports Med.* 2008;42:809-813.
27. Freeman MD, Woodham MA, Woodham AW. The role of the lumbar multifidus in chronic low back pain: a review. *PM R.* 2010;2:142-146; quiz 141 p following 167.
28. Kjaer P, Bendix T, Sorensen JS, et al. Are MRI-defined fat infiltrations in the multifidus muscles associated with low back pain? *BMC Med.* 2007;5:2.
29. Okamoto Y, Kunimatsu A, Kono T, et al. Gender differences in MR muscle tractography. *Magn Reson Med Sci.* 2010;9:111-118.
30. Deyo RA, Cherkin DC, Weinstein J, et al. Involving patients in clinical decisions: impact of an interactive video program on use of back surgery. *Med Care.* 2000;38:959-969.
31. Deyo RA, Mirza SK, Martin BI, et al. Trends, major medical complications, and charges associated with surgery for lumbar spinal stenosis in older adults. *JAMA.* 2010;303:1259-1265.
32. Dehner C, Schmelz A, Volker HU, et al. Intramuscular pressure, tissue oxygenation, and muscle fatigue of the multifidus during isometric extension in elite rowers with low back pain. *J Sport Rehabil.* 2009;18:572-581.
33. Tunnell J. Needle EMG Response of Lumbar Multifidus to Manipulation in the Presence of Clinical Instability. *J Man Manip Ther.* 2009;17:E19-24.
34. Ekstrom RA, Osborn RW, Hauer PL. Surface electromyographic analysis of the low back muscles during rehabilitation exercises. *J Orthop Sports Phys Ther.* 2008;38:736-745.
35. MacDonald D, Moseley GL, Hodges PW. People with recurrent low back pain respond differently to trunk loading despite remission from symptoms. *Spine (Phila Pa 1976).* 2010;35:818-824.

36. Mayer JM, Graves JE, Clark BC, et al. The use of magnetic resonance imaging to evaluate lumbar muscle activity during trunk extension exercise at varying intensities. *Spine (Phila Pa 1976)*. 2005;30:2556-2563.
37. Dickx N, D'Hooge R, Cagnie B, et al. Magnetic resonance imaging and electromyography to measure lumbar back muscle activity. *Spine (Phila Pa 1976)*. 2010;35:E836-842.
38. Hides J, Fan T, Stanton W, et al. Psoas and quadratus lumborum muscle asymmetry among elite Australian Football League players. *Br J Sports Med*. 2010;44:563-567.
39. Hides JA, Stanton WR, McMahon S, et al. Effect of stabilization training on multifidus muscle cross-sectional area among young elite cricketers with low back pain. *J Orthop Sports Phys Ther*. 2008;38:101-108.
40. Belavy DL, Armbrecht G, Richardson CA, et al. Muscle atrophy and changes in spinal morphology: is the lumbar spine vulnerable after prolonged bed-rest? *Spine (Phila Pa 1976)*. 2011;36:137-145.
41. Cole MH, Grimshaw PN. Trunk muscle onset and cessation in golfers with and without low back pain. *J Biomech*. 2008;41:2829-2833.
42. Kalichman L, Hodges P, Li L, et al. Changes in paraspinal muscles and their association with low back pain and spinal degeneration: CT study. *Eur Spine J*. 2010;19:1136-1144.
43. Silfies SP, Mehta R, Smith SS, et al. Differences in feedforward trunk muscle activity in subgroups of patients with mechanical low back pain. *Arch Phys Med Rehabil*. 2009;90:1159-1169.
44. Franca FR, Burke TN, Hanada ES, et al. Segmental stabilization and muscular strengthening in chronic low back pain: a comparative study. *Clinics (Sao Paulo)*. 2010;65:1013-1017.
45. Elliott J, Pedler A, Beattie P, et al. Diffusion-weighted magnetic resonance imaging for the healthy cervical multifidus: a potential method for studying neck muscle physiology following spinal trauma. *J Orthop Sports Phys Ther*. 2010;40:722-728.

Chapter 5. Lumbar Multifidus DTI and Chronic Low Back Pain (CLBP)

Gavin E.G. Jones, M.Sc., Dinesh A. Kumbhare, M.Sc., M.D., FRCPC, Srinivasan Harish MBBS, FRCPC, and Michael D. Noseworthy, PhD, P.Eng.

5.1. Context of Paper

DTI measures in subjects with LBP and uninjured controls are compared. DTI metrics are also correlated with both demographic information and the symptoms of LBP, as measured by standard questionnaires. The relationship between BMI and DTI FA AI is re-established (originally uncovered in chapter 4.3) and the relationship between LBP symptoms and DTI FA AI is shown for certain BMI categories, confirming both the relationship between DTI FA AI and BMI, and showing that DTI FA AI is an appropriate measure only for subjects with a certain BMI range. Determining the efficacy of DTI measures to correlate with LBP symptoms and characterizing the limits of those correlations may provide valuable information in the study of CBLP, and may provide a tool to objectively measure injury.

5.2. Declaration Statement

This chapter is a manuscript in preparation for submission to SPINE, and the final draft will be submitted in subsequent months. As such it meets the formatting requirements for SPINE. The concept and hypothesis for this paper was developed by

Dinesh A. Kumbhare (DAK), Michael D. Noseworthy (MDN) and Gavin EG Jones (GEGJ). MR scanning of patients was done by MRI technologists in the Imaging Research Centre (IRC) at St. Joseph's Healthcare, according to technical suggestions provided by MDN and GEGJ. All image and statistical analysis was performed by GEGJ who also wrote the entire first draft of the manuscript. Guidance, advice, proofreading and editing were provided by MDN, DAK and Srinivasan Harish (SH).

5.3. Abstract

5.3.1. Study Design

This is a cross sectional observational study.

5.3.2. Objective

To determine whether diffusion tensor imaging (DTI) of the lumbar multifidus can explain the symptoms of low back pain (LBP) and whether DTI measures are correlated with subject demographics.

5.3.3. Summary of Background Data

The lumbar multifidus is implicated in chronic low back pain. DTI is becoming widely used to study skeletal muscle.

5.3.4. Methods

Twenty six asymptomatic (controls) and 28 symptomatic (LBP) subjects underwent DTI scans on a 3.0T GE Signa MRI with b value of 400s/mm^2 in 15 optimized directions, with NEX=4 and TR/TE=10,000/62ms. Before MRI, subjects completed Oswestry, visual analog scale (VAS), and Godin questionnaires. Eigenvalues ($\lambda_1, \lambda_2, \lambda_3$), fractional anisotropy (FA), mean diffusivity (MD) and radial diffusivity (RD) are presented in subjects with and without the symptoms of LBP. Asymmetry index (AI) was also calculated: $(x_{\text{left}} - x_{\text{right}}) / (x_{\text{left}} + x_{\text{right}})$, where 'x' is any DTI measure (FA, MD, RD, $\lambda_1, \lambda_2, \lambda_3$). Also, DTI measures were correlated with the severity of LBP symptoms as measured by the Oswestry disability index (ODI) and VAS, as well as subject demographics; age, height, weight, and body mass index (BMI). Statistical comparisons were made with ANOVA and Pearson's correlation coefficient.

5.3.5. Results

Evaluating standard measures (FA, $\lambda_1, \lambda_2, \lambda_3$, MD and RD), between control and LBP groups were not significantly different. However, DTI measures were more asymmetric in the LBP group, and significantly greater for FA AI and λ_1 AI. This is due to a greater difference in the females' asymmetry than males. Also, there is greater FA variability with the multifidus' of the LBP group than controls. FA AI correlated with the ODI ($R^2=0.32$) but also weight ($R^2=-0.38$) and BMI $R^2=-0.37$). DTI metrics did not correlate strongly with other demographics.

5.3.6. Conclusion

DTI can differentiate the symptoms of LBP, but measures such as AI and within-multifidus variability should be used, and data should be compared to subjects with similar BMIs.

5.4. Keywords

Diffusion Tensor Imaging, Magnetic Resonance Imaging, Chronic Low Back Pain, Multifidus

5.5. Key Points

- This study evaluated the efficacy of DTI of the lumbar (L4) multifidus to 1) differentiate between a population with and without the symptoms of low back pain (LBP) and 2) correlate DTI measures with the severity of LBP or the subject's age, height, weight, BMI, or level of physical activity using 3.0T MRI.
- Standard DTI measures did not resolve the symptoms of LBP, but the LBP or symptomatic group showed more asymmetric fractional anisotropy (FA) and first eigenvalues (λ_1), which is a more pronounced difference in females than males.
- FA asymmetry correlates with the symptoms of LBP but also with the subject's weight and BMI.
- FA variability within each subject's multifidus, as measured by standard deviation, is greater in the symptomatic group than controls.

- DTI of the lumbar multifidus is a useful technique to objectively measure the symptoms of LBP but non-standard measures such as left/right asymmetry or within-multifidus variability are required, and subject's weight or BMI should be taken into account when such comparisons are made.

5.5.1. Mini-Abstract

Diffusion Tensor Imaging (DTI) can resolve the symptoms of low back pain (LBP) by comparing the left /right asymmetry of the lumbar multifidus' fractional anisotropy (FA). The FA asymmetry is related to both the symptoms of LBP and body mass index (BMI). For BMI below 30.00kg/m^2 , the relationship between FA asymmetry and LBP increases.

5.6. Introduction

It is estimated that 60-80% of the population will have low back pain (LBP) sometime through their life, and that up to 86% of that population experiences more than one bout of LBP^{1,2}.

Diffusion magnetic resonance imaging (MRI) has shown utility in evaluating spinal injuries, however these studies focus on abnormalities within the spinal cord³⁻⁸. Quantifying the results from diffusion tensor imaging (DTI) in the lumbar multifidus muscle may be useful because

DTI is sensitive to micro-structural changes as a result of skeletal muscle strain injury, even at early points when local oedema may influence the results⁹.

The lumbar stabilization muscles, especially the multifidus, are ideal targets since they are altered in subjects with low back pain^{10,11}.

Bergmark et al (1980) postulated that global musculature (the erector spinae) served to transfer loads from the thoracic spine to the pelvis, while local musculature (the multifidus) acts directly on the lumbar spine¹². Studies of the lumbar multifidus in target regions from L4 to S1 have shown that there is decreased volume with unilateral chronic LBP¹³ and more asymmetric cross sectional area (CSA) in the LBP-injured population, compared to controls^{10,14-20}. Improvement in the symptoms of chronic LBP can occur with an exercise-related regimen which involves stimulation of the lumbar core muscles including the multifidus^{21,22}. Exercises that specifically target the lumbar multifidus are

believed to improve symptoms of chronic LBP²³⁻²⁵. Thus, the multifidus is an ideal target for DTI.

DTI uses a pulsed-field gradient in which a lack of coherence and a reduction in signal is related to water's diffusion in one direction. Diffusion in at least six directions are required. Using singular volume deconvolution, a 3X3 matrix of either diffusion directions ($\epsilon_1, \epsilon_2, \epsilon_3$) or magnitudes or eigenvalues ($\lambda_1, \lambda_2, \lambda_3$) is created. These eigenvalues are 3 components of an ellipse. Theoretically, in skeletal muscle, which is a regular repeated structure whose cells are elongated, the λ_1 is aligned with the long axis of the muscle. Diffusion in that direction is maximal, while diffusion is restricted by sarcolemmal membranes in the other two directions. If there is damaged tissue within a voxel, the diffusion ellipse should be more spherical than in intact tissue.

The purpose of this study was to test the efficacy of DTI in differentiating subjects' symptoms of LBP, by comparing the DTI metrics in the multifidus of controls and symptomatic (LBP) subjects. Further, we sought to determine whether the DTI metrics are correlated with the severity of LBP symptoms and whether they are correlated to any other subject demographic information (age, gender, weight, height, BMI and/or differences in physical activity).

5.7. Materials and Methods

5.7.1. Subject Population

The St. Joseph’s Healthcare Research Ethics Board approved all procedures. Fifty-three subjects were used for this study. See table 5.1 for a summary of the two groups’ demographic information and the results of each questionnaire.

	N	Wt(kg)	Height (m)	Age(yrs)	BMI(kg/m ²)	ODI SCORE	VAS	Godin
CONTROL:						*	*	
Females	12	63.4±15.7	1.63±0.11	37±14	24±7	0.5±0.9	0.2±0.3	25.3±23.2
Males	14	83.7±16.2	1.76±0.07	39±14	27±4	1.9±4.1	0.1±0.2	45.6±32.3
Both (M+F)	26	75.0±18.7	1.70±0.11	38±14	26±6	1.3±3.2	0.1±0.3	36.9±30.1
LBP:								
Females	17	74.9±23.5	1.63±0.07	45±13	28±10	48.6±23.5	5.8±3.0	18.2±18.1
Males	11	83.2±14.4	1.72±0.10	45±11	28±8	40.8±20.7	6.7±2.5	29.9±37.4
Both (M+F)	28	78.2±20.5	1.67±0.09	45±12	28±8	45.8±25.2	6.1±2.7	22.4±26.5

* p<0.05 comparing LBP and controls (M+F combined)

Table 5.1 Demographic information collected, separated into male and female subjects. ODI: Oswestry Disability Index score (0-100), VAS: Visual Analog Scale (0-10), Godin: Godin questionnaire results.

Subjects with LBP symptoms were recruited from one of the author’s (DK) practice. When possible, control subjects were recruited who were gender matched and had similar ages, within 5 years. There were no significant differences between the LBP and control groups when subject weight, height, age, body mass index (BMI) and Godin score (a measure of physical activity) were compared (Student’s T test, p>0.05), while Oswestry disability index (ODI) and visual analog score (VAS) scores were significantly different (Student’s T test, p<0.05). For the non-significant comparisons only the Godin approached significance (Student’s T test, p=0.13).

5.7.2. Clinical Questionnaires

To measure low back pain, the widely used standard English Oswestry questionnaire was administered^{26,27}. The ODI scales between 0 and 100% where lower scores indicate less severe symptoms. The Oswestry questionnaire is believed to be preferable when the subject's symptoms are more severe, while a competing questionnaire, the Roland-Morris is better at detecting moderate disability²⁶. The Oswestry questionnaire was used since our subjects had a mean ODI of 48, which the Oswestry questionnaire categorizes as 'Severe Disability'. Subjects were also asked to complete a VAS questionnaire. This continuous measure where 0 is no low back pain and 10 is unbearable pain. Finally, subjects completed the Godin Leisure time questionnaire, which is a measure of their physical activity, which starts at 0 and has no upper limit.

5.7.3. MRI Protocol

MRI was performed on a Signa 3.0T horizontal bore magnet (General Electric Healthcare, Milwaukee, WI). A standard twelve channel body coil was used, using the lower elements (8-12) with the subject in the supine position.

Subjects had axial 3d SPGR, T1 FSE, axial T2W, sagittal T1W, and 4 separate DTI scans.

DTI scans used a diffusion weighting b value of 400 mm/s in 15 optimized directions, with TR/TE of 10,000/62msec, matrix size of 64X64, phase direction A/P, 40 cm FOV, 5 mm thickness and 20 slices. Four separate scans were performed, each with

the same prescan values and geometric prescription. They were summed offline (see below for specifics) so that the DTI NEX is 4.

Axial T1FSE used TR/TE of 450/8 msec, matrix size 256X192, phase direction R/L, NEX was 3, FOV was 40.0 cm, with a slice thickness of 5.0 mm and 20 slices. Axial T2W images were also acquired with TR/TE=5366/149ms, flip angle 90°, slice thickness 4 mm, 20 slices covering at least L3-L5, matrix size 512X512, FOV 28 cm.

5.7.4. Offline Analysis

Data was analyzed using freeware AFNI (National Institute of Mental Health, NIMH) and FSL 4.1 (FMRIB Analysis Group). First, the $b=0\text{s/mm}^2$ images for each of the three DTI NEX were registered to the chronological first set's $b=0\text{s/mm}^2$ image. Then B_0 correction was performed. Next, eddy current correction was performed in FSL. After that, the 4 NEX were summed. Then singular value decomposition was used to create the 3X3 tensor, whose magnitude eigenvalues ($\lambda_1, \lambda_2, \lambda_3$) are reported.

Eigenvalues were also re-formulated so that mean diffusivity (MD), radial diffusivity (RD) and fractional anisotropy (FA) are calculated:

$$MD = \frac{\lambda_1 + \lambda_2 + \lambda_3}{3} \quad (1)$$

$$RD = \frac{\lambda_2 + \lambda_3}{2} \quad (2)$$

$$FA = \sqrt{\frac{3 \times [(MD - \lambda_1)^2 + (MD - \lambda_2)^2 + (MD - \lambda_3)^2]}{2 \times (\lambda_1^2 + \lambda_2^2 + \lambda_3^2)}} \quad (3)$$

To illustrate the normalized difference between a left and right measure, asymmetry index (AI), was calculated:

$$AI = \frac{|x_{left} - x_{right}|}{x_{left} + x_{right}} \times 100 \quad (4)$$

where x_{left} and x_{right} are the left and right multifidus' values for any DTI measure. x_{left} may be the left multifidus' FA, MD, RD λ_1 , λ_2 , or λ_3 .

Regions of interest (ROIs) were hand drawn on the higher resolution axial T1W image, registered, down-sampled, and a mask was created to fit the DTI data. There are no units for AI.

5.7.5. Statistical analysis

Data was analyzed using SPSS 17.0. The Shapiro-Wilk test was used to test for normality. Data, which contribute to means, are distributed normally, so parametric statistics are used.

To compare the symptomatic and control group, 2-way randomized ANOVA was used, with disability (LBP pain symptoms) and laterality (left-right) as the factors for each DTI metric (data which are compiled in table 5.3 and figures 5.2 and 5.3). One-way ANOVA was also used (data in figure 5.4).

Pearson's correlation coefficient was used to compare the questionnaire results or any demographic information with the magnitude of a DTI metric (from figure 5.5).

Student's T test was calculated to compare control and LBP group's demographic information or questionnaire indices (from table 5.1).

5.8. Results

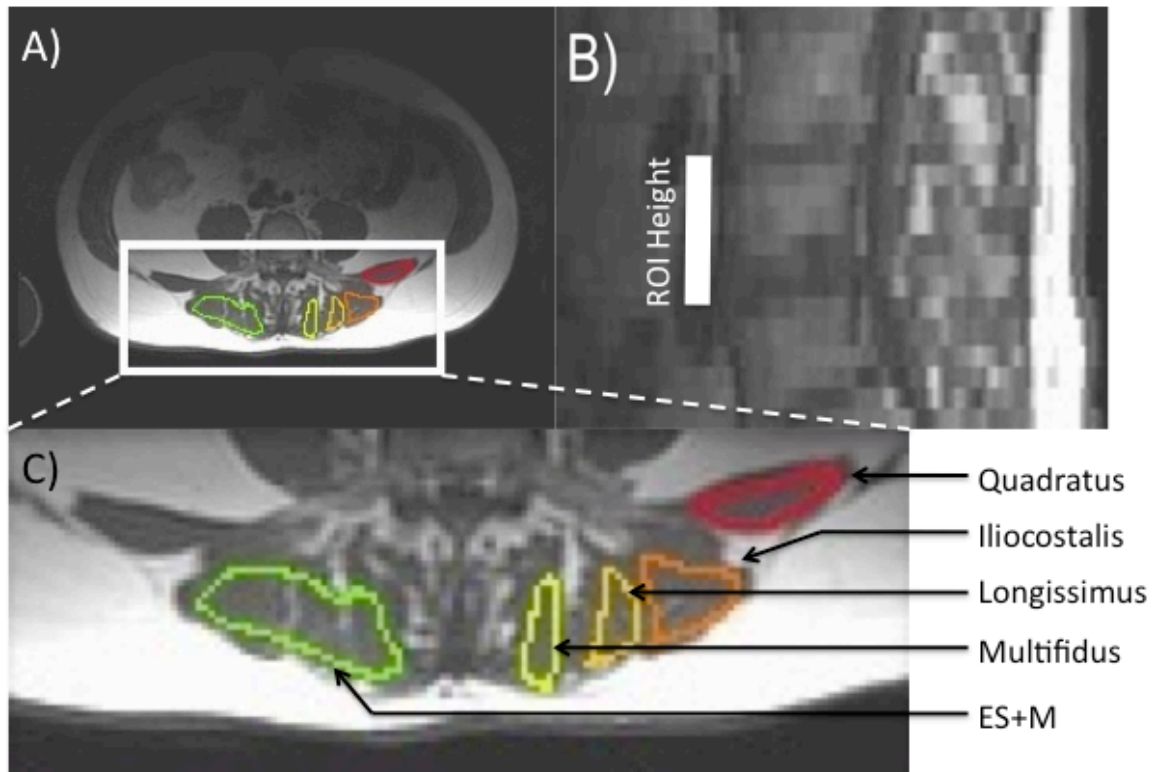


Figure 5.1 Sample ROIs of the ES+M (erector spinae and multifidus), multifidus, iliocostalis, longissimus, and quadratus lumborum drawn on a T1W image. Only data from the multifidus with the ROI encompassing L3 to L5 are presented.

Figure 5.1 shows a sample set of ROIs drawn on the T1W image. Fat was not included in the ROI. All of the ROIs shown in the image were collected, but only data from the multifidus are presented since its structure is ideal for lower back stability but not necessarily movement^{28,29}.

5.8.1. DTI Measures

Male, Female, Right, Left combined		
	Controls LBP	
FA	0.21±0.03	0.22±0.04
MD	1.67±0.15	1.65±0.17
λ_1	2.07±0.18	2.05±0.25
λ_2	1.56±0.15	1.55±0.18
λ_3	1.38±0.104	1.35±0.15
RD	1.46±0.14	1.45±0.16

Table 5.2 DTI parameters in control and LBP subjects. 1 way ANOVA revealed no effect of LBP/control for any measure.

Table 5.2 shows the mean values for all DTI results with males, females, left and right are all combined. There is no significant difference between the symptomatic (LBP) and asymptomatic (control) groups for any DTI measurement (1 way ANOVA comparing the control/LBP groups). There is virtually no difference in FA, RD, and MD.

A) Female, Left Multifidus

	Controls	LBP
FA	0.22±0.04	0.23±0.04
MD	1.65±0.15	1.69±0.17
λ_1	2.08±0.17	2.12±0.22
λ_2	1.53±0.17	1.59±0.20
λ_3	1.35±0.16	1.37±0.16
RD	1.44±0.17	1.48±0.17

B) Female, Right Multifidus

	Controls	LBP
FA	0.22±0.04	0.22±0.04
MD	1.69±0.17	1.66±0.22
λ_1	2.11±0.22	2.07±0.31
λ_2	1.57±0.19	1.56±0.24
λ_3	1.39±0.19	1.35±0.18
RD	1.48±0.19	1.45±0.20

C) Male, Left Multifidus

	Controls	LBP
FA	0.21±0.03	0.22±0.04
MD	1.69±0.12	1.64±0.11
λ_1	2.07±0.18	2.02±0.18
λ_2	1.59±0.11	1.53±0.09
λ_3	1.41±0.08	1.36±0.09
RD	1.46±0.14	1.44±0.09

D) Male, Right Multifidus

	Controls	LBP
FA	0.21±0.03	0.21±0.05
MD	1.63±0.13	1.60±0.17
λ_1	2.02±0.15	2.22±0.27
λ_2	1.56±0.10	1.50±0.14
λ_3	1.36±0.10	1.32±0.14
RD	1.46±0.10	1.41±0.14

Table 5.3 DTI metrics separated based on gender and laterality. There are no significant effects of LBP/control for any comparison (1 way ANOVA).

Mean data, which are parsed into right and left, and male and female, is shown in table 5.3. Using two way ANOVA with laterality and LBP disability (either LBP or control) as the factors, there was no main effect of LBP for either the male or female data (2 separate comparisons, one for each gender).

5.8.2. DTI Asymmetry index (AI)

When all data is combined and plotted in figure 5.2, the LBP group had greater asymmetry, which reached significance for FA and λ_1 . AI was separated into male and female data, which is shown in figure 5.3.

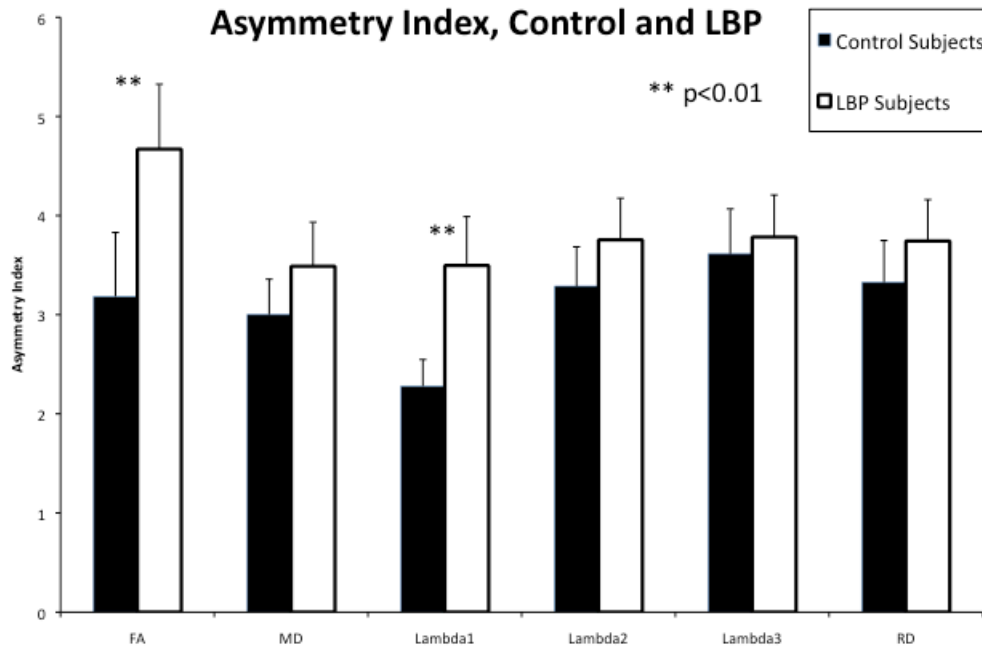


Figure 5.2 Asymmetry index (AI) difference in the controls and LBP groups. Student’s T test was performed to compare control and LBP data for each DTI measure. Means \pm standard deviation are plotted.

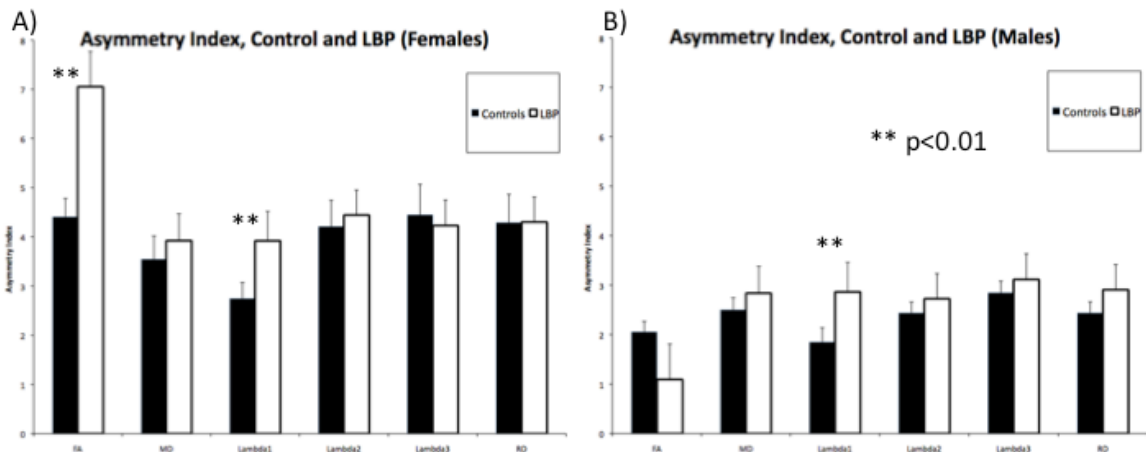


Figure 5.3 Asymmetry index (AI) difference in the controls and LBP groups, separated into females and males. Student’s T test was performed to compare control and LBP data for each DTI measure. Means \pm standard deviation are plotted.

In females, the differences are more pronounced. There are significant differences in FA and λ_1 AI, while in males there are only significant differences in λ_1 . In fact, the FA AI

changes in males are in the opposite direction as expected, where the controls are more asymmetric. In calculating the mean FA AI, all of the males low values less than 0.5 with one exception.

5.8.3. Intra-multifidus variability

The amount of FA variability in each subject's multifidus is presented as the standard deviation (SD) for each multifidus. Each subject's multifidus has one SD value (for all voxels contributing to that ROI). Data from the FA SD are plotted in figure 5.4.

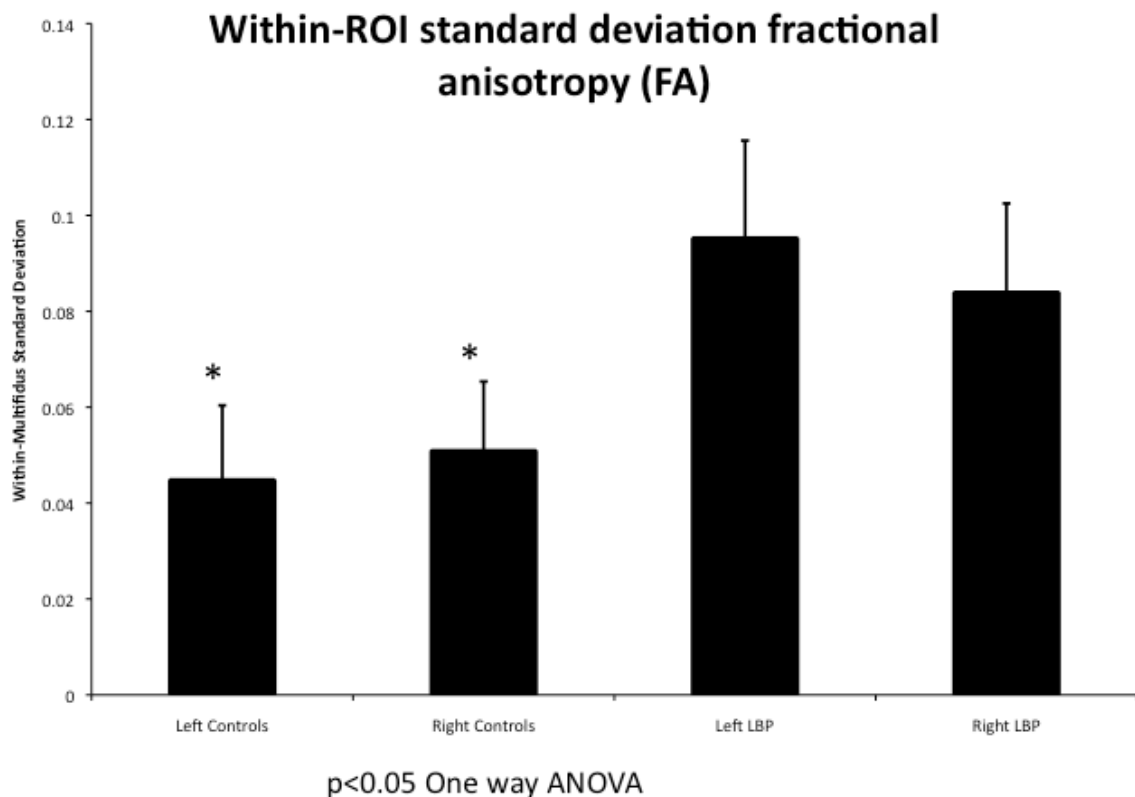


Figure 5.4 FA variability within each multifidus, as reported by standard deviation. Note that there the standard deviation within each ROI is greater for the LBP group than the controls.

The other measures (λ_1 , λ_2 , λ_3 , MD, RD) showed no significant LBP/control effect. The standard deviation is significantly greater (Student's T-test, $p < 0.05$) in the multifidus of our symptomatic population than controls.

For measure of within-ROI standard deviation, there are high correlation coefficients between metrics we would expect, such as right λ_1 SD and left λ_1 SD ($R^2=0.68$) and right MD SD and left MD SD ($R^2=0.83$). This indicates that the phenomena underlying within-ROI variability exist within the subject, and are not simply random differences in variability.

5.8.4. Correlation

Pearson's correlation coefficients were calculated between factors for both groups combined, and relevant, but not all, data are presented.

There is a strong correlation between the VAS and ODI results ($R^2=0.93$), indicating that the scores from both questionnaires effectively measure the similar phenomena, likely the symptoms of LBP. Also, many of the DTI parameters show high correlations with other DTI parameters (not graphed). This is expected. For example, the correlations between the right multifidus' RD and either λ_2 or λ_3 are very high (R^2 are 0.98 and 0.97, respectively) simply indicating an accurate calculation.

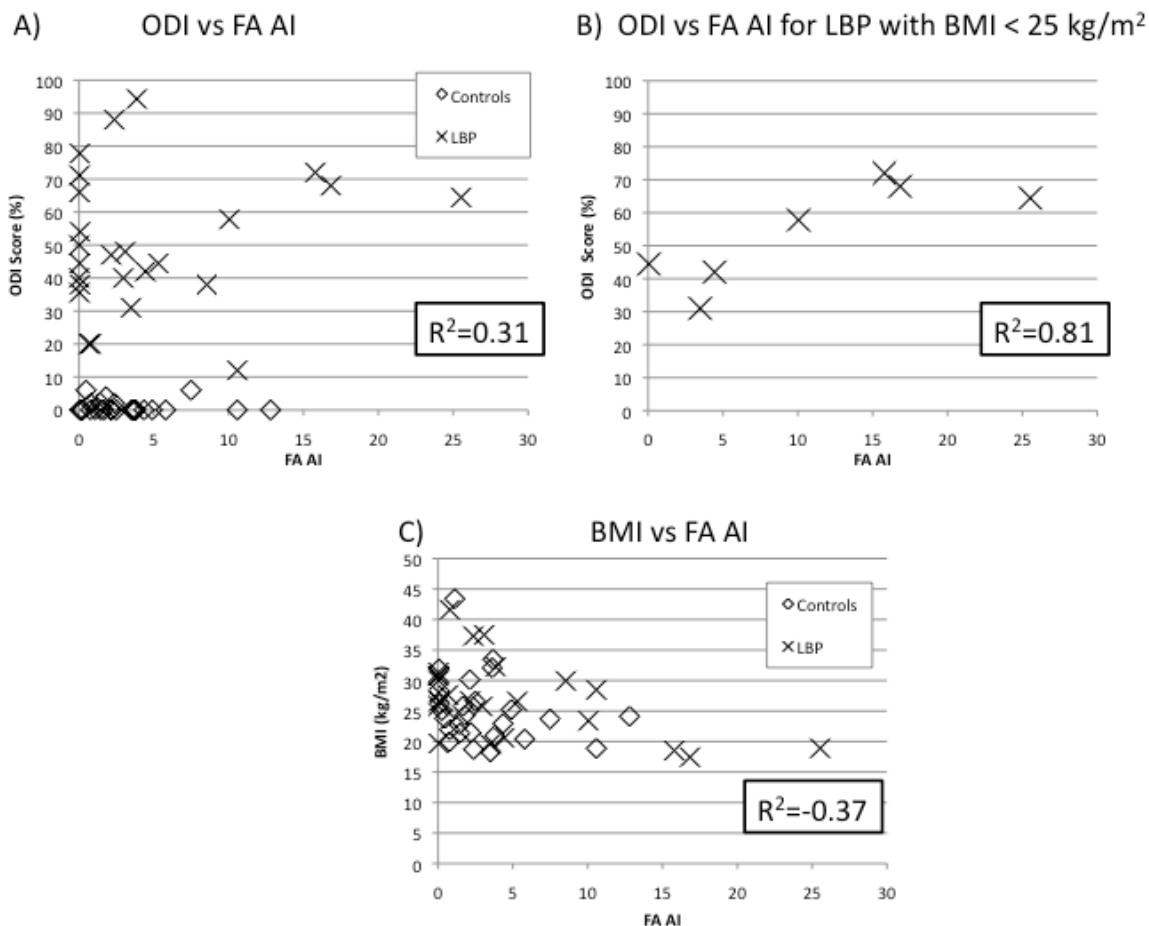


Figure 5.5 Sample relevant scatter plots, with Pearson’s correlation to the right. A: Plot of ODI vs FA AI shows a slight relationship. B: plot of ODI vs FA AI for only symptomatic (LBP) subjects (no controls) with BMIs under 25 kg/m². C: the relationship between BMI and FA AI, showing a slight negative correlation.

The data from figures 5.5A-C show some most relevant correlations for DTI’s efficacy in predicting LBP symptoms. The correlation between FA AI and VAS is $R^2=0.31$ and FA AI and ODI is $R^2=0.32$ (plotted in figure 5.5A). These are 0.34 and 0.35, respectively, when only the LBP group is considered. The greatest correlation between FA AI and demographic information was between FA AI and weight ($R^2=-0.38$), although FA AI and BMI also had a high correlation ($R^2=-0.37$), as seen in figure 5.5C. It is unlikely that the relationship is due only to the postulate that people with LBP

symptoms are less active due to their injuries, and likely have a higher BMI/weight. In the *control group only*, there are correlations between FA AI and either weight ($R^2=-0.26$) or BMI ($R^2=-0.22$). Also, the relationship between FA AI and ODI is positive, while there is a negative correlation between FA AI and BMI. This would indicate that the correlations between FA AI and weight ($R^2=-0.38$) and BMI ($R^2=-0.37$) are at least in part due to LBP symptoms independent of inactivity. When differences in BMI are taken into account, the correlation between FA AI and ODI scores increases from $R^2=0.32$ to $R^2=0.81$ for the group with BMI between 16.00 and 24.99 ($n=9$, figure 5.5B) and to $R^2=0.59$ for the ‘pre-obese’ group, for symptomatic (LBP) subjects with BMIs between 25 and 29.99. There are also low correlation between FA AI and ODI score for subjects with BMIs between 30.00 and 34.99 ($R^2=0.05$).

Surprisingly, the correlation between BMI and Godin score was very low ($R^2=-0.18$) which may indicate the limitation of one or both measures. The Godin scores showed high negative correlation with both the VAS ($R^2=-0.43$) and ODI ($R^2=-0.47$) scores, since it’s probable that subjects in the LBP group were more likely to be sedentary.

5.9. Discussion

FA AI was significantly greater for the LBP group. FA AI also scales with severity of symptoms of LBP. Other studies have shown an increase in multifidus CSA asymmetry^{14,15,19,30,31}, altered EMG activity of the erector spinae as well as the multifidus during gait, and increased muscle stiffness³² in LBP subjects compared to controls³³.

Interestingly, Hides did not find that there was a correlation between the severity of LBP and degree of multifidus asymmetry with ultrasound imaging³⁰. It is possible that MR DTI is more sensitive to such changes. We found a correlation between FA AI and ODI score, which increases with increasing LBP symptoms. There was also a relationship between FA AI and BMI or subject weight, but a negative correlation. Since the correlations are in opposite directions, the FA AI-ODI relationship is based on the LBP phenomenon, not simply that symptomatic subjects have higher BMI and that there is a FA AI-BMI relationship. The correlation between FA AI and ODI increases for BMIs under 30.00, thus minimizing the effect of BMI. The connection between FA AI and ODI is greatly reduced for subjects with BMIs above 30. Also, we found that the reliability of FA AI is greater in females than males, and that the changes in FA are due to λ_1 and not λ_2 and λ_3 , which is expected if there is sarcolemmal damage. It is possible that the damaged tissue may not be extreme, such as with sarcolemma damage, but intracellular components may be affected. With mild damage to muscle, such as with delayed onset muscle soreness (DOMS), there may be intracellular structural damage such as z-line streaming³⁴ which would be consistent with increases in λ_1 . Z-line streaming is a disruption of the sarcomere found after eccentric exercise where the myosin-dense z disk intermingles with the I-band, and is a measure of disruption of the intracellular contractile structure³⁵. There may other mild intracellular effects, such as a slight change in mitochondrial density or possibly slight damage to the t-tubular system, whose directions are perpendicular to the sarcomere, and would affect λ_1 .

We found that standard presentation of DTI metrics did not resolve the symptoms of LBP but FA AI and intra-multifidus were both greater in the LBP group than controls. A hypothetical cause for this may be incomplete fibre damage to the multifidus in symptomatic (LBP) subjects, where some voxels are affected, but many are normal and do not have altered FA values. Typically multifidus ROIs have approximately 70 voxels. If only a few were damaged, they might not greatly affect the mean FA value, but will slightly increase the SD values, thus an increased SD for affected multifidi in the LBP group.

DTI has previously shown to reveal altered skeletal muscle conditions; DTI of skeletal muscle has previously shown to be sensitive to masseter muscle position³⁶, tibialis anterior muscle length³⁷, calf muscle contraction^{38,39} and patellar dislocation⁴⁰.

5.10. Conclusions

This is the first study of the efficacy of MR DTI in the lumbar multifidus in subjects with and without LBP. Standard presentation of the data does not differentiate between the LBP and control groups; however both FA AI and within-multifidus SD are greater in the symptomatic group than controls. Greater FA AI is primarily due to asymmetry in λ_1 in females. FA AI correlates with ODI scores (a measure of LBP disability) but also BMI. When groups are broken down into BMI categories, 3 of the 4 BMI categories show much higher correlations between FA AI and ODI scores,

indicating that DTI of the lower back may be promising, but only if the mitigating factor of weight/BMI is accounted for.

5.11. References

1. Suni J, Rinne M, Natri A, et al. Control of the lumbar neutral zone decreases low back pain and improves self-evaluated work ability: a 12-month randomized controlled study. *Spine (Phila Pa 1976)* 2006;31:E611-20.
2. Aure OF, Nilsen JH, Vasseljen O. Manual therapy and exercise therapy in patients with chronic low back pain: a randomized, controlled trial with 1-year follow-up. *Spine (Phila Pa 1976)* 2003;28:525-31; discussion 31-2.
3. Mulcahey M, Samdani A, Gaughan J, et al. Diffusion Tensor Imaging in Pediatric Spinal Cord Injury: Preliminary Examination of Reliability and Clinical Correlation. *Spine (Phila Pa 1976)* 2011.
4. Kerkovsky M, Bednarik J, Dusek L, et al. Magnetic resonance diffusion tensor imaging in patients with cervical spondylotic spinal cord compression: correlations between clinical and electrophysiological findings. *Spine (Phila Pa 1976)* 2012;37:48-56.
5. Fujikawa A, Tsuchiya K, Takeuchi S, et al. Diffusion-weighted MR imaging in acute spinal cord ischemia. *Eur Radiol* 2004;14:2076-8.
6. Ai F, Ai T, Li X, et al. Value of diffusion-weighted magnetic resonance imaging in early diagnosis of ankylosing spondylitis. *Rheumatol Int* 2012.
7. Eguchi Y, Ohtori S, Yamashita M, et al. Diffusion magnetic resonance imaging to differentiate degenerative from infectious endplate abnormalities in the lumbar spine. *Spine (Phila Pa 1976)* 2011;36:E198-202.
8. Byun WM, Jang HW, Kim SW, et al. Diffusion-weighted magnetic resonance imaging of sacral insufficiency fractures: comparison with metastases of the sacrum. *Spine (Phila Pa 1976)* 2007;32:E820-4.
9. McMillan AB, Shi D, Pratt SJ, et al. Diffusion tensor MRI to assess damage in healthy and dystrophic skeletal muscle after lengthening contractions. *J Biomed Biotechnol* 2011;2011:970726.

10. Kim WH, Lee SH, Lee DY. Changes in the cross-sectional area of multifidus and psoas in unilateral sciatica caused by lumbar disc herniation. *J Korean Neurosurg Soc* 2011;50:201-4.
11. Lee SW, Chan CK, Lam TS, et al. Relationship between low back pain and lumbar multifidus size at different postures. *Spine (Phila Pa 1976)* 2006;31:2258-62.
12. Bergmark A. Stability of the lumbar spine. A study in mechanical engineering. *Acta Orthop Scand Suppl* 1989;230:1-54.
13. Beneck GJ, Kulig K. Multifidus atrophy is localized and bilateral in active persons with chronic unilateral low back pain. *Arch Phys Med Rehabil* 2012;93:300-6.
14. Hides J, Gilmore C, Stanton W, et al. Multifidus size and symmetry among chronic LBP and healthy asymptomatic subjects. *Man Ther* 2008;13:43-9.
15. Hyun JK, Lee JY, Lee SJ, et al. Asymmetric atrophy of multifidus muscle in patients with unilateral lumbosacral radiculopathy. *Spine (Phila Pa 1976)* 2007;32:E598-602.
16. Lee HI, Song J, Lee HS, et al. Association between Cross-sectional Areas of Lumbar Muscles on Magnetic Resonance Imaging and Chronicity of Low Back Pain. *Ann Rehabil Med* 2011;35:852-9.
17. Lescher S, Bender B, Eifler R, et al. Isometric non-machine-based prevention training program: effects on the cross-sectional area of the paravertebral muscles on magnetic resonance imaging. *Clin Neuroradiol* 2011;21:217-22.
18. Niemelainen R, Briand MM, Battie MC. Substantial asymmetry in paraspinal muscle cross-sectional area in healthy adults questions its value as a marker of low back pain and pathology. *Spine (Phila Pa 1976)* 2011;36:2152-7.
19. Shafaq N, Suzuki A, Matsumura A, et al. Asymmetric Degeneration of Paravertebral Muscles in Patients with Degenerative Lumbar Scoliosis. *Spine (Phila Pa 1976)* 2012.
20. Wallwork TL, Stanton WR, Freke M, et al. The effect of chronic low back pain on size and contraction of the lumbar multifidus muscle. *Man Ther* 2009;14:496-500.
21. Hansen FR, Bendix T, Skov P, et al. Intensive, dynamic back-muscle exercises, conventional physiotherapy, or placebo-control treatment of low-back pain. A randomized, observer-blind trial. *Spine (Phila Pa 1976)* 1993;18:98-108.
22. Kankaanpaa M, Taimela S, Airaksinen O, et al. The efficacy of active rehabilitation in chronic low back pain. Effect on pain intensity, self-experienced disability, and lumbar fatigability. *Spine (Phila Pa 1976)* 1999;24:1034-42.

23. Danneels LA, Cools AM, Vanderstraeten GG, et al. The effects of three different training modalities on the cross-sectional area of the paravertebral muscles. *Scand J Med Sci Sports* 2001;11:335-41.
24. Danneels LA, Vanderstraeten GG, Cambier DC, et al. Effects of three different training modalities on the cross sectional area of the lumbar multifidus muscle in patients with chronic low back pain. *Br J Sports Med* 2001;35:186-91.
25. Smeets RJ, Wade D, Hidding A, et al. The association of physical deconditioning and chronic low back pain: a hypothesis-oriented systematic review. *Disabil Rehabil* 2006;28:673-93.
26. Fairbank JC, Couper J, Davies JB, et al. The Oswestry low back pain disability questionnaire. *Physiotherapy* 1980;66:271-3.
27. Fairbank JC, Pynsent PB. The Oswestry Disability Index. *Spine (Phila Pa 1976)* 2000;25:2940-52; discussion 52.
28. Freeman MD, Woodham MA, Woodham AW. The role of the lumbar multifidus in chronic low back pain: a review. *PM R* 2010;2:142-6; quiz 1 p following 67.
29. Ward SR, Tomiya A, Regev GJ, et al. Passive mechanical properties of the lumbar multifidus muscle support its role as a stabilizer. *J Biomech* 2009;42:1384-9.
30. Hides JA, Stokes MJ, Saide M, et al. Evidence of lumbar multifidus muscle wasting ipsilateral to symptoms in patients with acute/subacute low back pain. *Spine (Phila Pa 1976)* 1994;19:165-72.
31. Hides JA, Stanton WR, McMahon S, et al. Effect of stabilization training on multifidus muscle cross-sectional area among young elite cricketers with low back pain. *J Orthop Sports Phys Ther* 2008;38:101-8.
32. Jones SL, Henry SM, Raasch CC, et al. Individuals with non-specific low back pain use a trunk stiffening strategy to maintain upright posture. *J Electromyogr Kinesiol* 2012;22:13-20.
33. Hanada EY, Johnson M, Hubley-Kozey C. A comparison of trunk muscle activation amplitudes during gait in older adults with and without chronic low back pain. *PM R* 2011;3:920-8.
34. Yu JG, Carlsson L, Thornell LE. Evidence for myofibril remodeling as opposed to myofibril damage in human muscles with DOMS: an ultrastructural and immunoelectron microscopic study. *Histochem Cell Biol* 2004;121:219-27.
35. Davies KE, Nowak KJ. Molecular mechanisms of muscular dystrophies: old and new players. *Nat Rev Mol Cell Biol* 2006;7:762-73.

36. Shiraishi T, Chikui T, Inadomi D, et al. Evaluation of diffusion parameters and T2 values of the masseter muscle during jaw opening, clenching, and rest. *Acta Radiol* 2012;53:81-6.
37. Englund EK, Elder CP, Xu Q, et al. Combined diffusion and strain tensor MRI reveals a heterogeneous, planar pattern of strain development during isometric muscle contraction. *Am J Physiol Regul Integr Comp Physiol* 2011;300:R1079-90.
38. Schwenzer NF, Steidle G, Martirosian P, et al. Diffusion tensor imaging of the human calf muscle: distinct changes in fractional anisotropy and mean diffusion due to passive muscle shortening and stretching. *NMR Biomed* 2009;22:1047-53.
39. Okamoto Y, Kunimatsu A, Kono T, et al. Changes in MR diffusion properties during active muscle contraction in the calf. *Magn Reson Med Sci* 2010;9:1-8.
40. Kan JH, Heemskerk AM, Ding Z, et al. DTI-based muscle fiber tracking of the quadriceps mechanism in lateral patellar dislocation. *J Magn Reson Imaging* 2009;29:663-70.

Chapter 6 . Lumbar Stabilization Muscles and Low Back Pain: Associations Between Asymmetry, Cross Sectional Area and Anthropometric Data

Gavin E.G. Jones, M.Sc., Dinesh A. Kumbhare, M.Sc., M.D., FRCPC, Srinivasan Harish MBBS, FRCPC, and Michael D. Noseworthy, PhD, P.Eng.

6.1. Context of Paper

The CSA of the multifidus in subjects with CLBP is well studied. The novel analyses in this manuscript include:

1. Male and female data are separated, and LBP and the efficacy of CSA on CLBP are shown for both genders, separated.
2. Several different muscle groups are studied: the multifidus, erector spinae, psoas, and quadratus lumborum.
3. The correlation between CSA and the subjects' demographic characteristics are studied in the injured and control subjects combined, and in controls alone,

to ensure there is no interaction between demographic characteristics and LBP symptoms.

4. The CSA data is correlated with the results of questionnaires which are indicators of the symptoms of LBP, in addition to comparing between control and LBP groups.

The relationships studied above are shown in two critical locations, at the upper and lower endplate of L4, an analogous publication compared control and LBP populations at the top of L3 and the bottom of L5 (Lee *et al.* 2011) but very few other studies used multiple locations in the inferior/superior (I-S) direction.

6.2. Declaration Statement

The concept and hypothesis for this paper was developed by Gavin EG Jones (GEGJ). MR scanning of patients was done by MRI technologists in the Imaging Research Centre (IRC) at St. Joseph's Healthcare, according to technical suggestions provided by MDN. All image and statistical analysis was performed by GEGJ who also wrote the entire first draft of the manuscript. Guidance, advice, proofreading and editing were provided by MDN, and Dinesh A. Kumbhare (DAK) and Srinivasan Harish (SH). The manuscript was submitted to The Archives of Physical Medicine and Rehabilitation on July 17 2012.

6.3. Abstract

Objective: To determine the relationship between lumbar spinal muscle cross sectional area (CSA) and their left/right asymmetry, with low back pain (LBP) severity, level of physical activity, gender, age, weight height and BMI.

Design: CSA and CSA asymmetry of the multifidus, erector spinae and multifidus muscle group (ES+M), quadratus lumborum (QL), and psoas at the upper and lower L4 endplate were evaluated on axial T2-weighted MR images acquired using a 3.0T MRI scanner.

Setting: Subjects were from the general community, scanned using a research dedicated MRI system at a university teaching hospital.

Participants: Subjects with chronic low back pain, LBP (n=26), and age and gender matched asymptomatic controls (n=25).

Interventions: Not applicable.

Results: CSA showed gender based differences in the QL and psoas ($p < 0.05$) but not ES+M or multifidus. When males and females were combined, only the QL at the lower L4 endplate showed a main effect of LBP ($p < 0.05$). CSA left-right asymmetry was significantly different for many comparisons of the multifidus muscle, and only one other target muscle group (male ES+M at the upper L4 endplate). Correlation between CSA asymmetry and (a) symptoms of LBP in multifidus was 0.35 (Pearson's R^2); and (b) 0.63

with BMI. When BMI in LBP patients was narrowed to include only slightly overweight ($25.00 \leq \text{BMI} < 30.00$) the correlation for multifidus CSA asymmetry increased to $R^2=0.66$.

Conclusions: CSA asymmetry significantly correlates in subjects with LBP, and the correlation increases when the range for BMI is minimized to include only overweight subjects. The most sensitive muscle to CSA change in chronic LBP is the multifidus, since its changes most positively correlate with LBP symptoms, and is not affected by gender.

6.4. Keywords

magnetic resonance imaging (MRI); cross sectional area (CSA); morphology, low back pain

6.5. Introduction

Low back pain (LBP) is pervasive through many societies¹⁻⁴. As many as 80% of adults will experience low back pain during their lifetime⁵. Societal costs can be substantial. Cost per capita per year (not per patient) range from €209 in Sweden to \$474 in Australia^{6,7}. In the United States, direct costs alone are estimated to have been \$90 million in 1998⁸ and 100 million in 2008⁹. Diagnosis is made more difficult by old injuries, which can be interpreted as the cause of symptoms¹⁰. More accurate diagnosis may reduce costs.

Initially, for most subjects experiencing the symptoms of LBP, the cause of the symptoms cannot be defined, and are said to have non-specific LBP (NSLBP)¹¹. Of those

diagnosed, disk herniation is common, and is associated with both gross morphological and functional deficits in the paraspinal muscles¹².

The muscles associated with LBP are the erector spinae (lumbar iliocostalis and longissimus), multifidus, and psoas¹³⁻¹⁵. MRI findings have shown that atrophy of the multifidus is associated with symptoms of LBP¹⁶. Decreased muscle cross sectional area (CSA) and fatty infiltration¹⁷ are related to the symptoms of LBP¹⁸⁻²⁷. Multifidus CSA was also found to be more asymmetric in subjects with the symptoms of LBP¹⁸. It is estimated that <10% difference between right and left CSA values at the L5 region “could be related to previous episodes of LBP”. However, a 10% CSA difference was also found in control subjects²⁸. Changes in tonic activity have also been observed; task-related EMG activity is related to multifidus atrophy²⁹ and LBP³⁰.

Evaluation of the LBP literature shows the symptomatic patients are routinely considered one homogenous group. Many LBP populations are heterogenous, as measured by questionnaires such as the Visual Analog Scale (VAS) and the Oswestry Low Back Pain Disability Questionnaire.

The goals of our study were to determine lumbar muscle (lumbar multifidus, erector spinae and multifidus (ES+M), quadratus lumborum (QL), and psoas) CSA in subjects with and without LBP, and to determine whether measurement location (upper and lower endplate of L4), or gender, specific effects exist. Also, the study was designed to determine the relationship between CSA and a number of factors, including severity of pain, subject age, height, weight and BMI.

6.6. Methods

6.6.1. Subjects

In a study approved by our research ethics review board in accordance to the Helsinki Declaration, 51 subjects (25 healthy controls and 26 subjects with LBP symptoms) were recruited to participate (see **table 6.1** for subject data). Every attempt was made to recruit controls with similar age (± 5 years), and BMI ($\pm 3\text{kg/m}^2$) values and gender to those of the LBP subjects.

		N	Wt(kg)	Height (m)	Age(yr)	BMI(kg/m ²)	ODI (0-100)	VAS (0-10)	Godin
Control:	Females	12	54±14	1.62±0.12	37±14	24±7	1±1	0.1±0.4	23±22
	Males	13	69±13	1.75±0.07	37±14	26±4	1±2	0.0±0.1	51±33
	Both (M+F)	25	62±15	1.69±0.11	37±14	25±6	1±2**	0.1±0.2**	38±31
LBP:	Females	15	63±17	1.64±0.06	43±12	27±7	51±22	5.8±2.9	17±16
	Males	11	72±12	1.72±0.09	45±11	28±3	45±20	5.8±2.8	19±28
	Both (M+F)	26	67±16	1.68±0.08	44±12	27±6	49±22	5.8±2.8	18±21

Means±SD **p<0.01

Table 6.1 The subject population. All values are listed as a mean ± standard deviation. BMI: body mass index, ODI: Oswestry disability index, VAS: visual analog scale. Symptomatic subjects have significantly higher ODI and VAS values than controls (* p<0.01).

Almost all symptomatic (LBP) subjects had either radiculopathic or non-specific LBP (NSLBP). Subjects in the LBP group had been involved in an automobile accident, which ranged from 9 months to 6 years prior to MR imaging. Although the LBP group had symptoms greater than some other studies^{31,32} the symptoms were not life-altering or excessive. All subjects were ambulatory. No subjects were previously characterized as having whiplash associated disorder (WAD) grade 3 or 4; all were grade 2 or lower.

6.6.2. 6.6.2 Imaging Protocol

All subjects were imaged supine with legs slightly raised to improve comfort. Images were acquired using a GE Signa HD 3.0Tesla MRI scanner and 12 channel-phased array receive coil (General Electric Healthcare, Milwaukee, WI).

Following patient positioning, with isocentre set approximately at L4, a routine clinical spine imaging protocol was followed. This included; axial T2-weighted (T2W; TR/TE=5366/149ms, slice thickness 4mm, 0mm gap, 20 slices covering at least L3-L5, matrix=512 ×512, FOV=28cm); sagittal T2W FRFSE (TR/TE=5000/149ms, slice thickness 4 mm, 1mm slice gap, NEX=2, 14 slices, matrix=512×512, FOV=40cm); sagittal T1W (TR/TE=566/10ms, slice thickness 4 mm, 0mm gap, matrix=512×512, FOV=28cm); and axial T1W (TR/TE=450/9ms, slice thickness 4 mm, 14 slices covering at least L3 to L5, matrix=512×512, FOV=40cm). The T1W images were used strictly for diagnosing additional abnormalities but not to calculate CSA. Axial T2W images were used to draw regions of interest (ROIs) on left and right multifidus, erector spinae and multifidus (ES+M), psoas, and quadratus lumborum. ROI analysis was done using Osirix (<http://www.osirix-viewer.com/>). ROIs were drawn around each muscle epimysium, at the top and bottom endplate of L4. No attempt to exclude fat from ROIs was performed as it was decided that this decision would add too much subjectivity to the analysis.

Asymmetry Index (AI) was calculated as the normalized difference between left and right CSA values:

$$AI = \frac{|CSA_{left} - CSA_{right}|}{CSA_{left} + CSA_{right}} \quad (6.1)$$

6.6.3. Questionnaires

All subjects filled out a standard English Oswestry low back disability (version 2.0), visual analog scale (VAS) for pain, and a Godin activity questionnaire. The Oswestry Disability Index (ODI) was calculated in the standard manner³³.

6.6.4. Statistical Comparisons

To compare anthropomorphic data between the LBP and control groups, one tailed Student's t-test was used. To compare between the LBP and control groups, ANOVA was used. If one-way ANOVA was used, LBP/control was the factor, and if two way ANOVA was used, laterality (left/right) was the other factor. Correlation comparisons were made with Pearson's correlation coefficient (R^2).

6.7. Results

A high correlation (Pearson's $R^2=0.92$) between VAS and ODI was noted (**fig 6.1**). There are many points at the origin because all controls scored 0 for both the VAS and ODI. When only the LBP group was considered (crosses in **fig 6.1**), and the data at the origin are not considered, Pearson's R^2 is 0.84. We believe this high correlation indicates that measures are internally reliable, and an accurate measure of LBP.

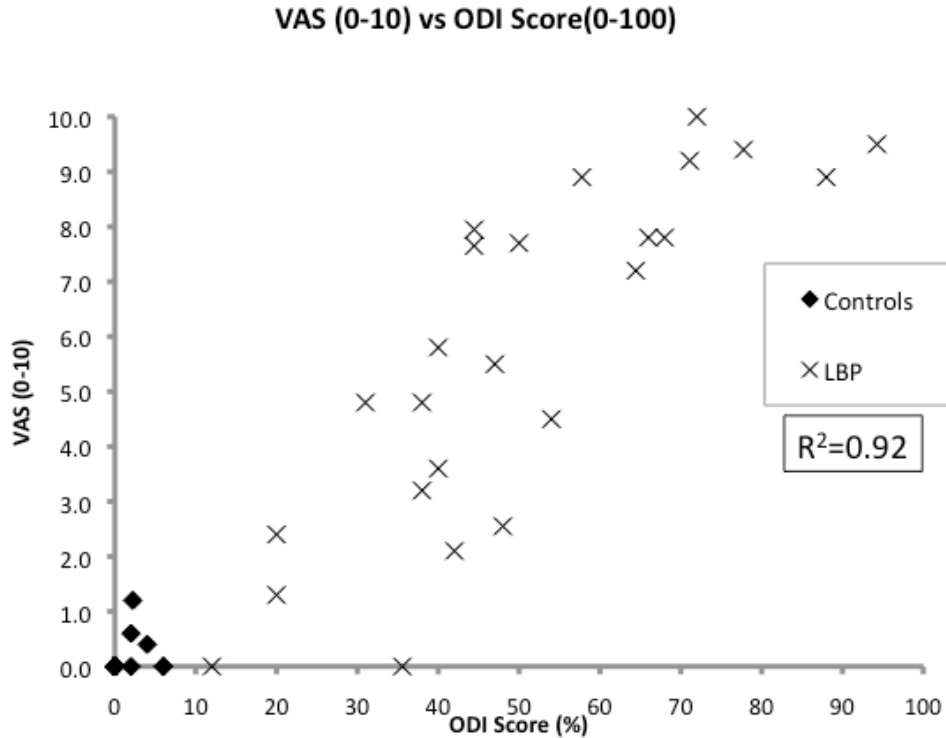


Figure 6.1 Plot of VAS vs. ODI scores for all subjects tested. Note that many of the asymptomatic (control) subjects scored 0 for both the VAS and ODI. The Pearson's $R^2=0.92$ for all subjects and $R^2=0.84$ for just the LBP group.

There are significantly greater ODI and VAS scores in the symptomatic (LBP) group than controls (two tailed Student's t-test, $p<0.01$, **table 6.1**). There were no other significant differences for any demographic values comparing the control and LBP groups (**table 6.1**). Two-way ANOVA revealed main gender effects for both weight and height ($p<0.01$), but there was no gender-related age or BMI effect, so that males were not of different ages or BMI than females. There were no significant LBP/gender interactions for either weight or height. As expected, the ODI and VAS scores were significantly greater than in controls ($p<0.01$).

6.7.1. Comparisons between LBP and control groups – CSA

Sample ROIs from a 32-year-old control male are shown (**fig 6.2**). Axial slice (**figs 6.2B and 6.2D**) locations were prescribed on sagittal images (**figs 6.2A and 6.2C**).

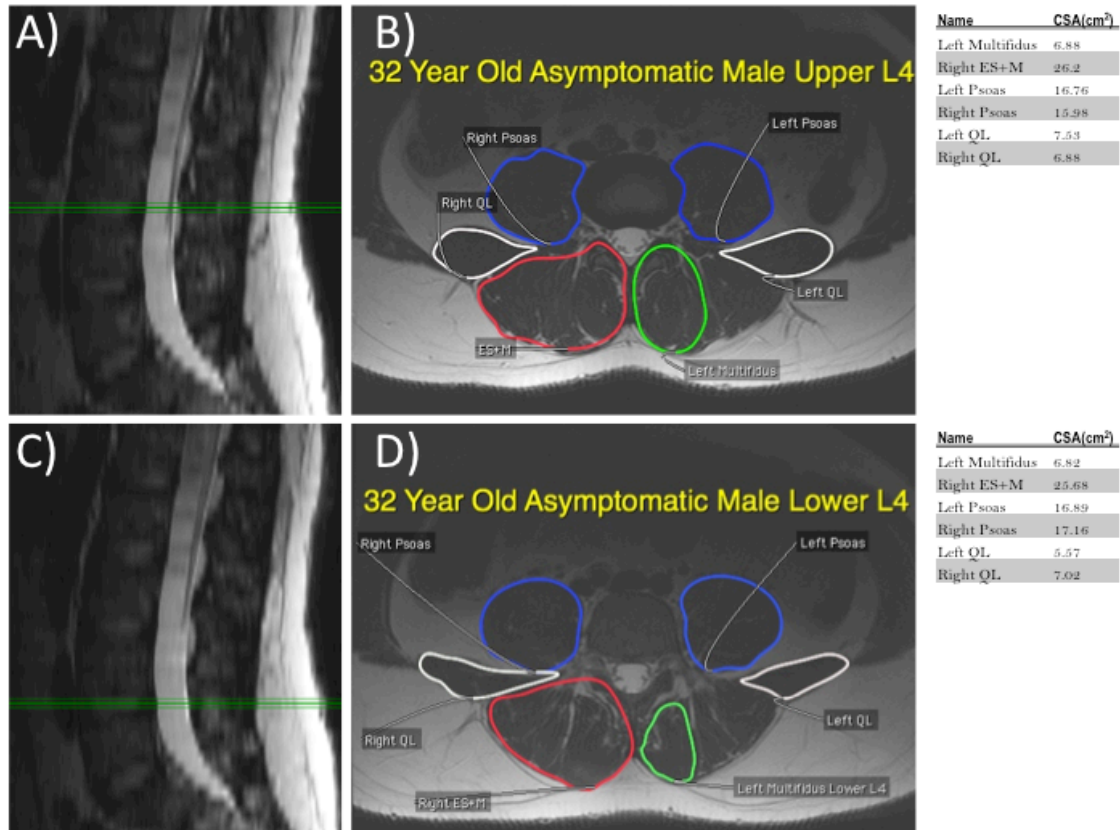


Figure 6.2 Sample regions of interest (ROIs) from a 32-year-old asymptomatic (control) male. Unilateral ROIs of both the ES+M and multifidus are shown for ease of viewing. Values to the right are the CSAs measurements for each muscle.

For many comparisons, there was no significant effect of LBP on CSA, when compared to healthy controls. However, some notable exceptions include: female left ($p < 0.01$) and right ($p < 0.05$) ES+M at the upper L4 endplate (**table 6.2**) and female right QL at the lower L4 level ($p < 0.05$, **table 6.3**).

Muscle CSA (cm²), Lower L4 Endplate

		Both Genders		Males		Females	
		Controls	LBP	Controls	LBP	Controls	LBP
Left	Multifidus	6.84±1.86	5.71±2.22	7.28±2.32	6.63±2.35	6.52±1.43	4.72±1.63
	ES+M	21.38±4.03	17.11±4.36	22.36±5.26	18.85±4.69	20.49±2.77	15.23±3.17
	QL	4.48±1.87	4.40±1.59	5.23±1.61	4.35±2.04	3.49±0.99	4.58±1.90
	Psoas	11.74±4.18	11.72±3.73	14.93±2.93	15.17±2.63	8.28±1.91	9.17±1.93
Right	Multifidus	7.08±1.99	5.69±1.77	7.35±1.92	6.19±1.80	6.88±2.07	4.93±1.55
	ES+M	21.48±4.79	16.74±4.31	22.42±5.09	18.32±4.87	20.78±3.65	15.02±2.91
	QL	4.53±1.25	4.43±1.59	5.37±0.99	4.40±2.04	4.46±1.24	3.63±0.79
	Psoas	12.15±4.28	11.55±3.41	15.32±3.23	14.55±1.87	9.35±2.45	8.72±1.98

Table 6.2 Muscle CSA (cm²) for each group at the lower endplate of L4. Data are from both sexes combined, as well as parsed into that from male and females.

Muscle CSA (cm²), Upper L4 Endplate

		Both Genders		Males		Females	
		Controls	LBP	Controls	LBP	Controls	LBP
Left	Multifidus	6.24±1.83	5.60±2.13	6.54±1.67	6.37±2.39	6.02±1.97	4.77±1.47
	ES+M	21.40±5.12	19.01±5.16	23.42±6.07	21.98±5.01	19.91±3.86	15.93±3.16
	QL	4.55±1.91	3.92±1.80	5.17±1.77	5.92±1.54	3.01±1.19	3.06±0.62
	Psoas	10.20±4.09	9.70±3.15	13.33±2.95	11.88±2.86	8.10±2.33	6.81±1.73
Right	Multifidus	5.86±1.52	5.40±1.89	5.98±1.21	6.07±2.19	5.77±1.75	4.68±1.20
	ES+M	21.47±5.26	19.12±4.78	23.69±5.67	21.55±4.61	19.85±4.44	16.49±3.47
	QL	4.82±1.84	4.39±1.71	6.19±1.46	5.41±1.77	3.73±1.19	3.23±0.62
	Psoas	10.58±4.29	9.24±3.17	13.82±3.15	11.54±2.56	7.55±2.44	7.07±1.91

Table 6.3 Muscle CSA (cm²) for each group at the upper endplate of L4. Data are from both sexes combined, males and females.

There were several others, which approached significance (for example, female left upper L4 multifidus p=0.08, comparing controls with LBP, **table 6.3**). So, for many

of comparisons, more significant differences between LBP subjects and healthy controls was noted for females relative to males. No propensity between upper and lower L4 location was noted in significant comparisons between LBP and controls; i.e. this was split roughly evenly between both locations.

In trying to determine whether there were any gender-based differences, only the control group was used for statistical comparison, so that effects of LBP symptoms would not contaminate gender-only effects. One-way ANOVA in the control group revealed that in the upper and lower endplate of L4, the right and left psoas, and left QL muscles demonstrated significant gender effects ($p < 0.05$).

6.7.2. Comparisons between LBP and control groups – CSA AI

CSA Asymmetry Index, M+F			
Muscle		Group	
		Controls	LBP
Upper L4	Multifidus	4.8±3.8*	10.4±8.5
	ES+M	4.0±3.4	5.0±3.7
	QL	8.8±5.1	11.7±8.4
	Psoas	4.6±3.6	5.4±3.8
<hr/>			
Muscle		Group	
		Controls	LBP
Lower L4	Multifidus	6.1±4.3*	11.0±5.3
	ES+M	4.2±4.1	5.9±3.2
	QL	9.9±7.0	15.0±8.9
	Psoas	4.6±3.4	5.2±3.6

* $p < 0.05$

Table 6.4 CSA asymmetry index for all muscle groups and locations, with both sexes combined. Significant CSA asymmetry was noted at both upper and lower L4 in the multifidus (* $p < 0.05$). No other LBP muscles showed significant difference between healthy controls.

		CSA Asymmetry Index			
		Females		Males	
	Muscle	Controls	LBP	Controls	LBP
Upper L4	Multifidus	4.2±3.8*	10.7±8.4	5.2±4.2*	11.0±5.5
	ES+M	5.0±4.2	4.9±3.9	3.1±2.4*	6.3±3.9
	QL	8.7±7.1	13.6±9.4	8.8±5.4	16.0±10.0
	Psoas	6.5±4.1	5.4±4.4	2.7±1.8	3.4±2.2
Lower L4	Multifidus	6.0±5.0	11.0±6.9	6.2±4.9*	10.0±6.7
	ES+M	5.4±5.2	5.6±2.9	3.0±2.7	5.3±3.7
	QL	9.9±8.4	14.2±9.8	9.9±5.9	9.0±6.5
	Psoas	5.6±3.7	6.6±3.9	3.7±2.8	5.5±2.9

* P<0.05

Table 6.5 CSA asymmetry index in all muscle groups and locations, when separated by gender. LBP subjects had significantly greater CSA asymmetry in the multifidus in both males and females in the upper L4 (* p<0.05). Additionally male LBP subjects had significantly greater CSA asymmetry in the ES+M (upper L4) muscle groups and multifidus at lower L4 (* p<0.05).

CSA AI values are shown in **tables 6.4** and **6.5**. The LBP's multifidus was significantly more asymmetric in the lower L4 region of the multifidus (p<0.05, one way ANOVA) when data from both sexes were used. There were no significant differences between the control and LBP groups for any other muscle group or location when both sexes were combined (**table 6.4**). For data parsed into sexes (**table 6.5**), there were several significant effects (p<0.05, one way ANOVA) of LBP, in the upper L4 region's multifidus for both males and females, and the male's ES+M ROI.

6.7.3. Correlations - CSA

Among comparisons between muscle CSA and either ODI or VAS, one of the most significant correlations was between ODI and right multifidus at the top endplate of L4

($R^2=-0.39$) and left multifidus at the same location ($R^2=-0.35$) (**fig 6.3A**). The multifidus AI at the top of L4 correlated with ODI score with $R^2=0.38$ (**fig 6.3B**).

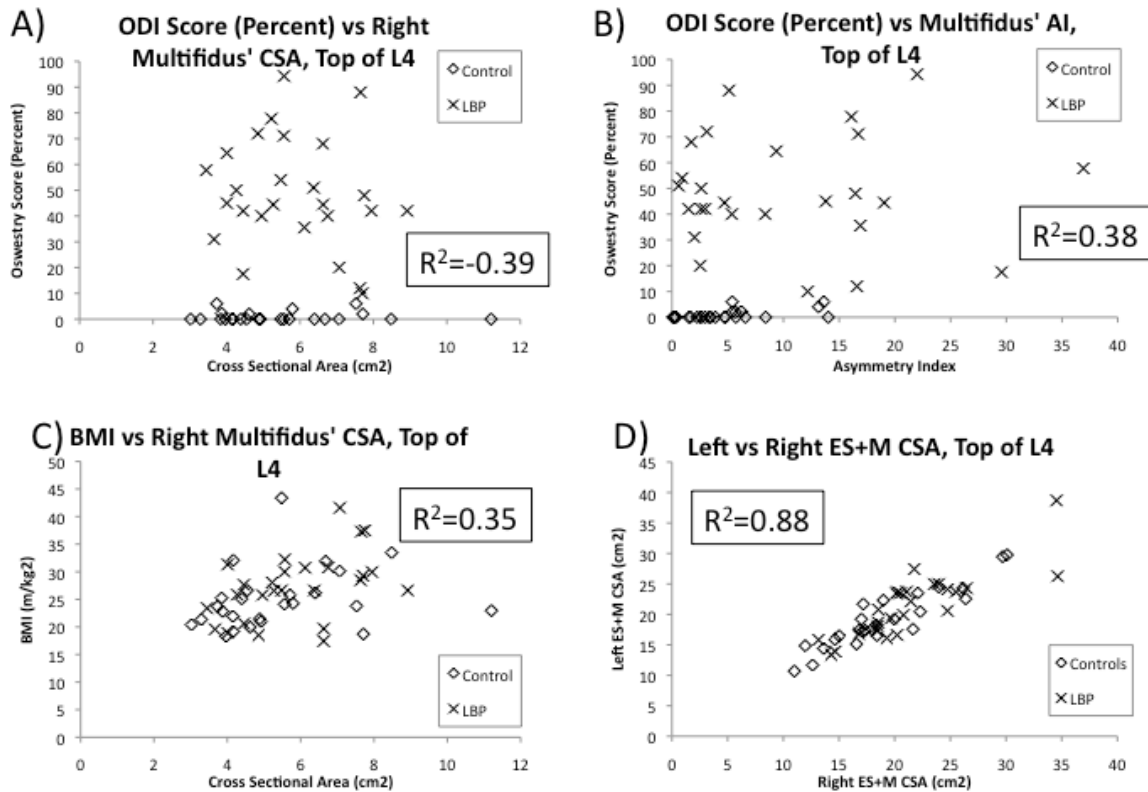


Figure 6.3 Correlations plots between ODI and CSA (A), ODI and asymmetry (B), BMI and multifidus CSA, and left versus right ES+M cross sectional area. All measures were made along the top of L4. Pearson's correlation coefficient (box in each plot) are also provided.

Large correlations between CSA and weight, and CSA and BMI were observed for the erector spinae ($R^2=0.41$ and $R^2=0.49$ for the left and right ES+M at the top of L4 and $R^2=0.36$ and $R^2=0.46$ for the left and right ES+M at the bottom of L4) and multifidus ($R^2=0.43$ and $R^2=0.35$ for the left and right multifidus at the top of L4 and $R^2=0.44$ and $R^2=0.47$ for the left and right multifidus at the bottom of L4 (**fig 6.3C**). There were many high correlations between the left and right values, such as left and right ES+M at the top

of L4 ($R^2=0.88$, **fig 6.3D**), left and right multifidus at the bottom of L4 ($R^2=0.88$), left and right psoas at the top ($R^2=0.94$) and bottom ($R^2=0.96$) of L4, indicating that inter-subject variability is greater than within-subject left-right variability. The same left-right comparison for the LBP group only showed lower correlation ($R^2=0.82$) than that of controls alone ($R^2=0.92$) indicating greater asymmetry in the LBP group.

The most significant comparisons for the multifidus ROI and anthropomorphic data were between the left multifidus at the top of L4, whose correlations for weight and BMI are 0.40 and 0.63, respectively. A similar comparison between the left ES+M and weight (not shown) revealed a correlation of $R^2=0.61$. Age did not correlate with CSA or asymmetry. There was very little dependence of muscle/ROI size and age; there was only one correlation above 0.20 ($R^2=0.23$ for age vs. right multifidus at the bottom of L4) for any muscle CSA and age. Also, there were low correlation coefficients between most CSA and Godin activity scores. The exceptions are the psoas, which, at the top of L4, had values of $R^2=0.20$ and $R^2=0.19$, for the left, and right, respectively, and at the bottom of L4 had values of $R^2=0.29$ and $R^2=0.31$, for the left, and right, respectively. Thus, there were no significant effects of age, activity level, or height.

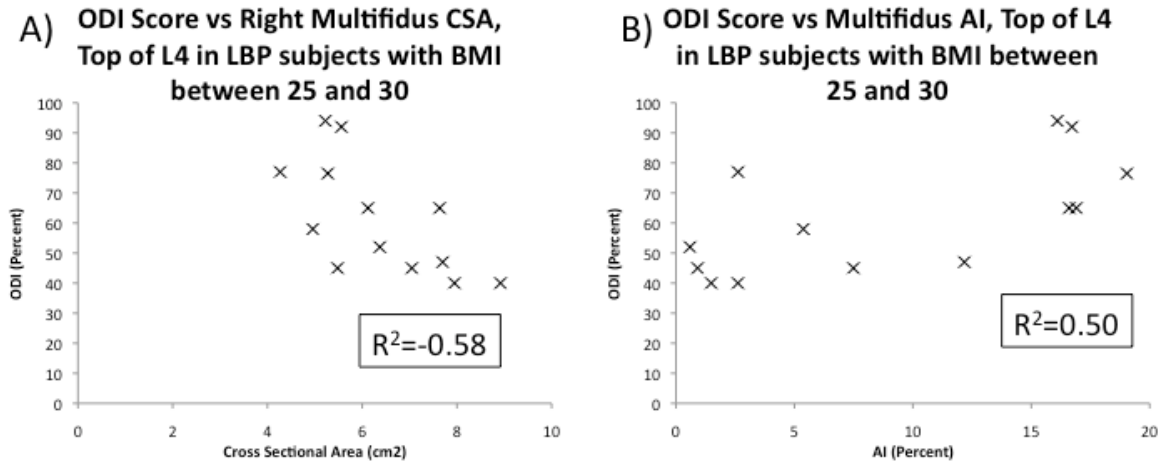


Figure 6.4 Correlations plots between (A) ODI and cross sectional area, and (B) ODI and asymmetry index. Pearson’s correlation coefficients (R^2) are also shown

The relation between the right multifidus’ CSA at the top of L4 and ODI score, goes from $R^2 = -0.35$ to $R^2 = -0.58$ (fig 6.4A). Figure 6.4B shows a similar comparison as shown in figure 6.4A (only the ‘Pre-Obese’ subjects). R^2 goes from 0.35 (fig 6.3B) to 0.50 (fig 6.4B). When the effects of BMI are minimized, the effects of LBP are revealed, and are greater than when BMI is not considered.

6.8. Discussion

Some of the primary findings of this study include a confirmation that the lower section of L4 is both larger, and shows a greater correlation with LBP symptoms, as measured by the ODI and VAS. Also, the multifidus is the most reliable target muscle for ROI assessment when correlating with LBP symptoms. CSA AI of the multifidus shows the strongest correlation (stronger than raw CSA values or any values of other target ROIs such as the QL or psoas). CSA for many of the target ROIs seem to scale with subject BMI or weight, but not other anthropomorphic data.

The mean CSA values for the multifidus and ES+M were similar to those reported elsewhere^{23,32} and had approximately the same variability. For almost all muscles, the CSA was greater at the lower endplate of L4 than the upper endplate, which is consistent with the results from a Hides study, which showed an incremental increase in multifidus CSA from L2 to L5³⁵. Only the psoas and the QL, for some comparisons, have different CSAs based on gender. This means that combining data from the genders is valid for ES+M or multifidus CSA. If percent difference is used, as shown elsewhere¹⁸, gender can be combined for any muscle.

Our study used axial images rather than oblique-axial images aligned with the discs, as done in other studies²⁴. Previous studies showed that oblique-axial slice orientation was not important in assessing spinal stenosis³⁶. Also, since spinal curvature is different for each subject, and muscle CSA may be different for different angles, using straight axial comparisons removes one subjective element. Fatty infiltration was included since fat exclusion would have been both difficult and subjective, in many of the subjects. Using straight axial images, and the inclusion of fat deposits makes our results easier to replicate.

Muscle volume³² and CSA are lower in subjects with minimal symptoms of LBP (with a mean ODI score of 15) at the L4 level. There were very few significant differences between the injured and uninjured groups for any of the muscles tested here. However, our LBP group had a wide range of VAS and ODI scores. ODI ranged from 12 to 94 with a mean±SD of 48±21. The highest correlation was between the ODI scores and ES+M CSA at the bottom of L4. There were also high correlations between ES+M CSA

and weight and ES+M compared to BMI, as well as multifidus versus BMI comparisons. The high correlation is not likely due only to the possibility that LBP subjects are less active and would have a higher BMI. This is because there is an equally high correlation between muscle groups' CSA and BMI in the *control group alone*, so the effect is only a direct effect of BMI or weight, not LBP symptom-induced changes in weight or BMI. Also there was not a high correlation between ODI score and BMI or ODI score and weight, which would be expected if there were a large effect of LBP-dependent weight gain. It should be noted that many studies have found differences between LBP symptomatic group and controls even without taking BMI into account¹⁸⁻²⁷. When symptomatic subjects with BMIs considered to be 'pre-obese' with BMI's between 24.99 and 30.00 were considered, there were high correlations between ODI and many ROI's CSA, as well as VAS and some CSA values, much higher than when the whole group is considered, or when all subjects were considered, based on measures of right multifidus and both ES+M.

Hides *et al.* showed a 17% decrease in multifidus CSA in the injured side¹⁸, and an 18% decrease in muscle volume in the injured side³², where this study noted percent change values of approximately 20% for the LBP population (from 20.8% to 22%). However, they used a slightly different calculation for percent change, called 'Percentage difference' (% Difference)^{20,37}, which is

$$\%Difference = \frac{|CSA_l - CSA_s|}{CSA_l} \quad (6.2)$$

where CSA_l is the CSA from the larger side and CSA_s is from the smaller side. An approximate comparison between our AI to Hides' % Difference can be done by % Difference = $2 \times AI$. As such, our LBP groups' AI is similar to those found elsewhere^{20,37}.

The Oswestry questionnaire, rather than the Roland-Morris questionnaire, was appropriate for our symptomatic population. The ODI is believed a better measure than the Roland-Morris disability questionnaire (RDQ) at detecting disability in more severe cases, while the RDQ is better than the ODI in more mild cases³³. Our subjects' symptoms were greater than those reported by Beneck and Kulig. Our LBP group had an average ODI score of 48, while Beneck and Kulig's LBP group was 14³². Further, our mean ODI score (48) would be categorized as 'Severe Disability' if it were a single subject.

CSA is affected by both the symptoms of LBP (**fig 6.3A**) and with weight/BMI (**fig 6.3C**). BMI values between 25.00 and 29.99 are considered 'Pre-Obese', according to the World Health Organization³⁴. The subjects shown in **figure 6.4** are data from LBP subjects with BMIs in the 'Pre-Obese' range. This mitigates the effect of BMI.

We noted a significant difference between the controls and LBP groups for the lower endplate of L4, when both sexes were combined (**table 6.2**).

It is not surprising that the multifidus was the most reliable correlation to LBP. It is considered a 'local' muscle group, connected directly the lumbar vertebrae, whereas other muscle groups such as the erector spinae are considered 'global' musculature, which act to transfer loads from the thoracic region to areas inferior to the lumbar spine³⁸.

6.9. Study Limitations

This study had a moderate sample size of 51, which is greater than some^{18,22,32} and less than others¹⁶ although pilot results indicate that our power was sufficient.

The primary factor that wasn't accounted for was time post-injury. All of our subjects had symptoms, which many consider chronic (9 months to 6 years). But, since some subjects only gave approximate timeframes, our CSA and asymmetry metrics could not be correlated to time after injury.

6.10. Conclusions

This study is unique in determining the relationship between LBP and muscle CSA, and CSA asymmetry, taking into consideration gender and anthropometric differences. The multifidus and ES+M are not different between genders, but the psoas and QL are. CSA asymmetry shows more utility than CSA alone in LBP. As multifidus and ES+M were correlated with BMI and weight it is essential to take these into consideration when using muscle CSA to evaluate LBP.

6.11. References

1. Chaiamnuay P, Darmawan J, Muirden KD, Assawatanabodee P. Epidemiology of rheumatic disease in rural Thailand: a WHO-ILAR COPCORD study. Community Oriented Programme for the Control of Rheumatic Disease. *J Rheumatol* 1998;25(7):1382-7.
2. Hoy D, Toole MJ, Morgan D, Morgan C. Low back pain in rural Tibet. *Lancet* 2003;361(9353):225-6.
3. Rapoport J, Jacobs P, Bell NR, Klarenbach S. Refining the measurement of the economic burden of chronic diseases in Canada. *Chronic Dis Can* 2004;25(1):13-21.
4. Jin K, Sorock GS, Courtney TK. Prevalence of low back pain in three occupational groups in Shanghai, People's Republic of China. *J Safety Res* 2004;35(1):23-8.
5. Rubin DI. Epidemiology and risk factors for spine pain. *Neurol Clin* 2007;25(2):353-71.
6. Dagenais S, Caro J, Haldeman S. A systematic review of low back pain cost of illness studies in the United States and internationally. *Spine J* 2008;8(1):8-20.
7. Lin CW, Haas M, Maher CG, Machado LA, van Tulder MW. Cost-effectiveness of guideline-endorsed treatments for low back pain: a systematic review. *Eur Spine J* 2011;20(7):1024-38.
8. Luo X, Pietrobon R, Sun SX, Liu GG, Hey L. Estimates and patterns of direct health care expenditures among individuals with back pain in the United States. *Spine (Phila Pa 1976)* 2004;29(1):79-86.
9. Indrakanti SS, Weber MH, Takemoto SK, Hu SS, Polly D, Berven SH. Value-based care in the management of spinal disorders: a systematic review of cost-utility analysis. *Clin Orthop Relat Res* 2012;470(4):1106-23.
10. Deyo RA, Weinstein JN. Low back pain. *N Engl J Med* 2001;344(5):363-70.
11. Koes BW, van Tulder MW, Thomas S. Diagnosis and treatment of low back pain. *BMJ* 2006;332(7555):1430-4.
12. Yoshihara K, Shirai Y, Nakayama Y, Uesaka S. Histochemical changes in the multifidus muscle in patients with lumbar intervertebral disc herniation. *Spine (Phila Pa 1976)* 2001;26(6):622-6.
13. Bergmark A. Stability of the lumbar spine. A study in mechanical engineering. *Acta Orthop Scand Suppl* 1989;230:1-54.
14. Panjabi MM. The stabilizing system of the spine. Part I. Function, dysfunction, adaptation, and enhancement. *J Spinal Disord* 1992;5(4):383-9; discussion 97.
15. Cresswell AG, Thorstensson A. The role of the abdominal musculature in the elevation of the intra-abdominal pressure during specified tasks. *Ergonomics* 1989;32(10):1237-46.

16. Kader DF, Wardlaw D, Smith FW. Correlation between the MRI changes in the lumbar multifidus muscles and leg pain. *Clin Radiol* 2000;55(2):145-9.
17. Mengiardi B, Schmid MR, Boos N, Pfirrmann CW, Brunner F, Elfering A, Hodler J. Fat content of lumbar paraspinal muscles in patients with chronic low back pain and in asymptomatic volunteers: quantification with MR spectroscopy. *Radiology* 2006;240(3):786-92.
18. Hides J, Gilmore C, Stanton W, Bohlscheid E. Multifidus size and symmetry among chronic LBP and healthy asymptomatic subjects. *Man Ther* 2008;13(1):43-9.
19. Hides JA, Lambrecht G, Richardson CA, Stanton WR, Armbrecht G, Pruettt C, Damann V, Felsenberg D, Belavy DL. The effects of rehabilitation on the muscles of the trunk following prolonged bed rest. *Eur Spine J* 2011;20(5):808-18.
20. Hides JA, Stanton WR, McMahan S, Sims K, Richardson CA. Effect of stabilization training on multifidus muscle cross-sectional area among young elite cricketers with low back pain. *J Orthop Sports Phys Ther* 2008;38(3):101-8.
21. Hides JA, Stokes MJ, Saide M, Jull GA, Cooper DH. Evidence of lumbar multifidus muscle wasting ipsilateral to symptoms in patients with acute/subacute low back pain. *Spine (Phila Pa 1976)* 1994;19(2):165-72.
22. Hyun JK, Lee JY, Lee SJ, Jeon JY. Asymmetric atrophy of multifidus muscle in patients with unilateral lumbosacral radiculopathy. *Spine (Phila Pa 1976)* 2007;32(21):E598-602.
23. Kim WH, Lee SH, Lee DY. Changes in the cross-sectional area of multifidus and psoas in unilateral sciatica caused by lumbar disc herniation. *J Korean Neurosurg Soc* 2011;50(3):201-4.
24. Lee HI, Song J, Lee HS, Kang JY, Kim M, Ryu JS. Association between Cross-sectional Areas of Lumbar Muscles on Magnetic Resonance Imaging and Chronicity of Low Back Pain. *Ann Rehabil Med* 2011;35(6):852-9.
25. Lescher S, Bender B, Eifler R, Haas F, Gruber K, Felber S. Isometric non-machine-based prevention training program: effects on the cross-sectional area of the paravertebral muscles on magnetic resonance imaging. *Clin Neuroradiol* 2011;21(4):217-22.
26. Shafaq N, Suzuki A, Matsumura A, Terai H, Toyoda H, Yasuda H, Ibrahim M, Nakamura H. Asymmetric Degeneration of Paravertebral Muscles in Patients with Degenerative Lumbar Scoliosis. *Spine (Phila Pa 1976)* 2012.
27. Wallwork TL, Stanton WR, Freke M, Hides JA. The effect of chronic low back pain on size and contraction of the lumbar multifidus muscle. *Man Ther* 2009;14(5):496-500.
28. Niemelainen R, Briand MM, Battie MC. Substantial asymmetry in paraspinal muscle cross-sectional area in healthy adults questions its value as a marker of low back pain and pathology. *Spine (Phila Pa 1976)* 2011;36(25):2152-7.
29. Yoshihara K, Nakayama Y, Fujii N, Aoki T, Ito H. Atrophy of the multifidus muscle in patients with lumbar disk herniation: histochemical and electromyographic study. *Orthopedics* 2003;26(5):493-5.
30. Enomoto M, Ukegawa D, Sakaki K, Tomizawa S, Arai Y, Kawabata S, Kato T, Yoshii T, Shinomiya K, Okawa A. Increase of Paravertebral Muscle Activity in Lumbar Kyphosis Patients by Surface

Electromyography Compared With Lumbar Spinal Canal Stenosis Patients and Healthy Volunteers. *J Spinal Disord Tech* 2012.

31. Clark BC, Walkowski S, Conatser RR, Eland DC, Howell JN. Muscle functional magnetic resonance imaging and acute low back pain: a pilot study to characterize lumbar muscle activity asymmetries and examine the effects of osteopathic manipulative treatment. *Osteopath Med Prim Care* 2009;3:7.

32. Beneck GJ, Kulig K. Multifidus atrophy is localized and bilateral in active persons with chronic unilateral low back pain. *Arch Phys Med Rehabil* 2012;93(2):300-6.

33. Fairbank JC, Couper J, Davies JB, O'Brien JP. The Oswestry low back pain disability questionnaire. *Physiotherapy* 1980;66(8):271-3.

34. World Health Organization 2012. Available from: URL: http://apps.who.int/bmi/index.jsp?introPage=intro_3.html.

35. Hides JA, Richardson CA, Jull GA. Magnetic resonance imaging and ultrasonography of the lumbar multifidus muscle. Comparison of two different modalities. *Spine (Phila Pa 1976)* 1995;20(1):54-8.

36. Henderson L, Kulik G, Richarme D, Theumann N, Schizas C. Is spinal stenosis assessment dependent on slice orientation? A magnetic resonance imaging study. *Eur Spine J* 2011.

37. Hides JA, Richardson CA, Jull GA. Multifidus muscle recovery is not automatic after resolution of acute, first-episode low back pain. *Spine (Phila Pa 1976)* 1996;21(23):2763-9.

38. Sullivan MS. Back support mechanisms during manual lifting. *Phys Ther* 1989;69(1):38-45.

Chapter 7 . Alterations in resting state BOLD MRI fractal dimension after Swedish massage.

Jones GEG, Wong R, Shipwright S, Dryden T, Sagar SM, Wardlaw GM, Kumbhare DA, Noseworthy MD.

7.1. Context of Paper

To the author's knowledge, analysis of resting state BOLD using the FD measure in the lumbar erector spinae and multifidus (ES+M) has not been published. This study determined the resting state BOLD FD using three types of FD analysis and determined the changes to FD immediately after Swedish massage therapy (MT).

Since some of the subject population received MT for their CLBP, the effect of MT on BOLD FD should be quantified. Note that even immediately after MT, there was no significant effect of MT on the FD_{RDslow} or FD_{RDfast} , but a significant effect on FD_{PS} . As a result, when determining the effect of LBP symptoms on BOLD FD measures (in the succeeding chapter), subjects who received MT within 6 months prior to MRI were discarded. Their data was not used even though there was no effect on two of the three FD measures *immediately* after MT (data from this manuscript/chapter). None of the

LBP subjects in chapter 8 received MT *immediately* before MRI, and some received MT *months* before their MRI.

Also, the results from this manuscript/chapter and those shown in chapter 8 are the first to study BOLD FD in the erector spinae, and as chapter 8 describes, there was no effect of LBP on any FD measures. The results from *this* manuscript/chapter confirms that FD in the lower back is sensitive to a treatment (FD_{PS}). This is an important finding, since the next chapter finds that BOLD FD does not resolve LBP symptoms. We confirm in this chapter that FD in the skeletal muscle/lower back *is* sensitive to something, just not LBP.

7.2. Declaration Statement

The concept and hypotheses for this paper was developed by Raimond Wong (RW), Michael D. Noseworthy (MDN), Trish Dryden (TD) and Stephen M. Sagar (SMS). Massage therapy was designed by Stacey Shipwright (SS) and TD and performed by SS. MR scanning of patients was done by MRI technologists in the Imaging Research Centre (IRC) at St. Joseph's Healthcare, according to technical suggestions provided by MDN and Graham M. Wardlaw (GMW). MDN and GMW did Matlab programming for image analysis. Gavin EG Jones (GEGJ) wrote the entire first draft of the manuscript and performed all image and statistical analysis. Guidance, advice, proofreading and editing was provided by MDN, Dinesh A. Kumbhare (DAK), RW, and GMW. The manuscript has been submitted to the American Journal of Physical Medicine and Rehabilitation on May 31st 2012.

7.3. Abstract

Objective: Blood oxygen level dependent (BOLD) magnetic resonance (MR) signal can be used to probe regional microvascular function. BOLD signal complexity in time can vary due to altered blood flow or volume, or through metabolic change. As massage therapy is known to change muscle metabolism and microvasculature this study was done to determine whether non-invasive BOLD imaging and its subsequent change in complexity can visualize the effect of Swedish massage.

Design: Resting state BOLD MRI was acquired before and after Swedish massage, which included the effleurage and petrissage techniques in 6 healthy subjects. The target region was the L4 area of the erector spinae and multifidus (ES+M) muscles. BOLD data was acquired with TE/TR=35/250ms, 3 slices, 2400 time points. Signal complexity was evaluated using fractal dimension relative dispersion (FD_{RD}) and power spectral (FD_{PS}) mapping techniques.

Results and Conclusions: There was a significant decrease ($p<0.01$) in complexity of FD_{PS} from 1.16 ± 0.12 to 1.08 ± 0.09 after massage. Lower FD has been theorized to be the result of increased low frequency fluctuations in microvasculature, perhaps due to elevated vascular pulsatility and hence greater perfusion. Thus, we believe this is the first time the effect of therapeutic massage on muscle has been imaged.

7.4. Key Words

Massage, muscle, MRI, signal complexity

7.5. Introduction

Massage therapy (MT) has been practiced for many years. The concept of using Swedish MT originated over a century and a half ago¹, but the physiological and psychological correlates have been studied in detail only recently. There has been an exponential increase in MT related publications in scientific journals within the past twenty years, albeit from small initial numbers². Despite a growing evidence base, there still appears to be fewer publications than other psychosomatic phenomena, compared to psychotherapy, for example. There are several commonly understood and evidence based benefits of MT, including the reduction of anxiety and depression³, and reduction in muscular tension^{4,5}. Further, MT is believed to be related to many psychological and physiologic effects, from amelioration of discomfort in patients with breast cancer, to altering blood pressure, to reducing low birth weight, and premature birth^{6,7}. The explicit underlying mechanisms for these and other benefits are not yet well understood. Massage has also been attributed to increased local blood flow, as measured by infrared spectroscopy^{8,9} and ultrasound¹⁰.

Several different techniques are commonly used for Swedish MT, some of the specific techniques believed to influence circulation are effleurage, petrissage and tapotement. Effleurage is a slow rhythmic stroking along the skin, from the distal to proximal direction. It is believed to alter blood flow and accelerate lymphatic drainage¹¹⁻¹³. Petrissage (from French pétrir, "to knead") are massage movements using fingers, hands, thumbs, palms, which apply deep pressure, which alternately compresses and

releases the skin and underlying muscle tissue. Kneading, wringing, skin rolling and picking-up are various common forms of petrissage movements¹⁴. Although it has been long theorized that both effleurage and petrissage increase blood flow, there is a lack of clear evidence in the research to date and there are numerous methodological variations and limitations¹⁵. Tapotement is a light percussive movement by opposite hands at a high frequency. The tapping is generally believed to alter skin surface level circulation. However, Shoemaker *et al.*¹⁶ did not observe an increase in local blood flow after MT, which included tapotement. MT in this study uses effleurage and petrissage, and avoids tapotement.

The current study focuses on measuring/visualising changes in healthy lower back muscle microvascular dynamics after Swedish MT, as measured by changes in magnetic resonance imaging (MRI) blood oxygen level dependent (BOLD) signal complexity. The BOLD signal is related to the ratio of oxygenated to deoxygenated haemoglobin. As such, the BOLD signal reflects a complex change in blood flow, volume and metabolism which is best characterized using a temporal fractal dimension (FD), an indicator of both self-affinity and complexity¹⁷. A self-similar structure has identical properties at progressively greater resolution. Self-affinity is analogous to self-similarity, without being exact replicas at all geometric scales. Structures with increasing self-similarity or self-affinity have increasing complexity. Fractal dimension is measured on a scale between 1.0 and 1.5, where values closer to 1.0 are simple, and values closer to 1.5 are more chaotic or complex¹⁸. It is believed that complexity and self-affinity are related. A sinusoidal wave, for example, has a FD value close to 1.0 whereas white noise

approaches 1.5. Therefore we hypothesized perfusion associated changes resulting from Swedish MT would reflect in changes in BOLD FD, where values closer to 1.0 reflect greater blood flow than higher FD values.

7.6. Materials and Methods

In a study approved by our institutional research ethics board three male and three female subjects (mean age 39 ± 17 years) underwent BOLD MRI immediately prior to and immediately following Swedish massage. Participants had no recent (3 years prior to scanning and massage) history of lower back pain or injury, had not received a professional massage in the 6 months preceding their inclusion in this project, and females were post-menopausal and not on hormone replacement therapy. Following subject consent, pre-massage MRI BOLD scanning was performed (30 minutes; details below). This was followed by massage therapy (MT; 30 minutes, detailed below) and immediately a post-MT BOLD MRI scan (30 minutes). The entire procedure took 1.75hrs.

7.6.1. Massage Therapy (MT)

MT was administered immediately following the first (pre) scan by a registered massage therapist. Swedish massage was administered to the muscles of the dorsal trunk between the lower neck (T1) and the coccyx. General techniques were applied to the entire back region and specific techniques to the mid- to low-back and gluteal region.

Note that the muscles targeted for imaging (lumbar erector spinae and multifidus) received MT.

The initial general techniques consisted of static contact to the upper and lower back, stroking followed by effleurage (light pressure, increasing with each stroke) applied in the direction of the neck and upper back to lower back.

The middle phase (specific techniques) consisted of general light petrissage, extending to more specific and deeper petrissage to the upper back, mid back and lower back, in the lumbar paraspinals, quadratus lumborum, gluteal muscles, rhomboids, erector spinae, levator scapula, latissimus dorsi, and trapezius, between T1 and the coccyx. Next, from T1 to the coccyx, friction and/or muscle stripping was administered, using moderate to deep pressure. The closing phase echoed the initial phase (general techniques) and consisted of effleurage, stroking followed by static contact.

7.6.2. Magnetic Resonance Imaging (MRI)

Imaging was performed supine using a 3T GE Signa short bore MRI system (GE Healthcare, Milwaukee, WI) and a 6 channel neck/spine array radio-frequency (RF) coil. The supine position was chosen, with legs slightly elevated at the knees using a curved foam pad, to keep the back muscles slightly elevated from the MRI bed. Furthermore, the supine position avoided any respiratory-associated motion contamination in the lumbar region. Imaging included anatomic axial T1-weighted (T1W) and sagittal T2-weighted (T2W) images and blood oxygen level dependent (BOLD) images. The T2W images were acquired to rule out underlying pathology and hence were only acquired in the pre-

massage imaging session. The T2W images were acquired using a fast recovery fast spin echo (FRFSE) with TR/TE=3200/85ms, ETL=19, receiver bandwidth (rbw) = 41kHz, A-P frequency direction, NEX=6, matrix=416x256, field of view (FOV)=28cm, 4mm slice thickness, 1mm spacing, 30 slices. Axial T1W images were acquired pre and post massage and were prescribed to match BOLD images (described below). These were acquired using a FSE-XL sequence centered on L3 (TR/TE=500/8.78ms, matrix=320x224, interpolated to 512x512, 10mm thick, 0mm skip, 22cm FOV, ETL=3, NEX=2). Functional imaging using BOLD signal was done pre and post massage using gradient echo, echo planar imaging (GE-EPI) with TR/TE=250/35ms, matrix=64x64, rbw=250kHz, 3 slices with identical location as the axial T1W and 2400 time points (10 minute duration).

7.6.3. Image Analysis

BOLD data was analyzed using an in-house program written using Matlab 2010a (Mathworks, Natick MA). BOLD datasets were analyzed both by a power spectrum and relative dispersion (or coefficient of variation) methods. The power spectrum fractal dimension (FD_{PS}) calculation was done based on Schepers *et al.*¹⁹. In short, the data was converted from the time to the frequency domain, using a fast Fourier transform (FFT), and fractal dimension (FD_{PS}) was calculated from:

$$|A|^2 = \frac{1}{f^\beta}$$

$$FD_{PS} = 2 - \frac{(\beta + 1)}{2}$$

Where A is the amplitude of the BOLD (T2* weighted) signal in the frequency domain and β is the spectral index¹⁷.

Alternatively, FD was also calculated by using the relative dispersion method (FD_{RD}). Here, relative dispersion (RD) is defined as the standard deviation (σ) divided by the mean (μ) and FD_{RD} is calculated based on:

$$RD(m) = RD(m_{ref}) \times \left(\frac{m}{m_{ref}} \right)^{1-FD_{RD}}$$

Here, the RD is calculated at multiple scales (m), and the reference scale (m_{ref}) is set to 1. Previous work has noted two FD_{RD} components in skeletal muscle (slow and fast). Here we calculated $FD_{RD-slow}$ from observations at greater timescales (between 4 and 64 seconds long), and $FD_{RD-fast}$ calculations are based on data between 0.25 and 2 seconds long.

Regions of interest (ROIs) were drawn such that the erector spinae and lumbar multifidus (ES+M) muscles were the targets at the L4 level. ROIs were drawn on the BOLD image before FD calculation. A 2-way repeated measures ANOVA, with the two

factors being laterality (i.e. left vs. right ES+M muscles) and treatment (i.e. before and after MT) was performed on muscle FD data.

7.7. Results

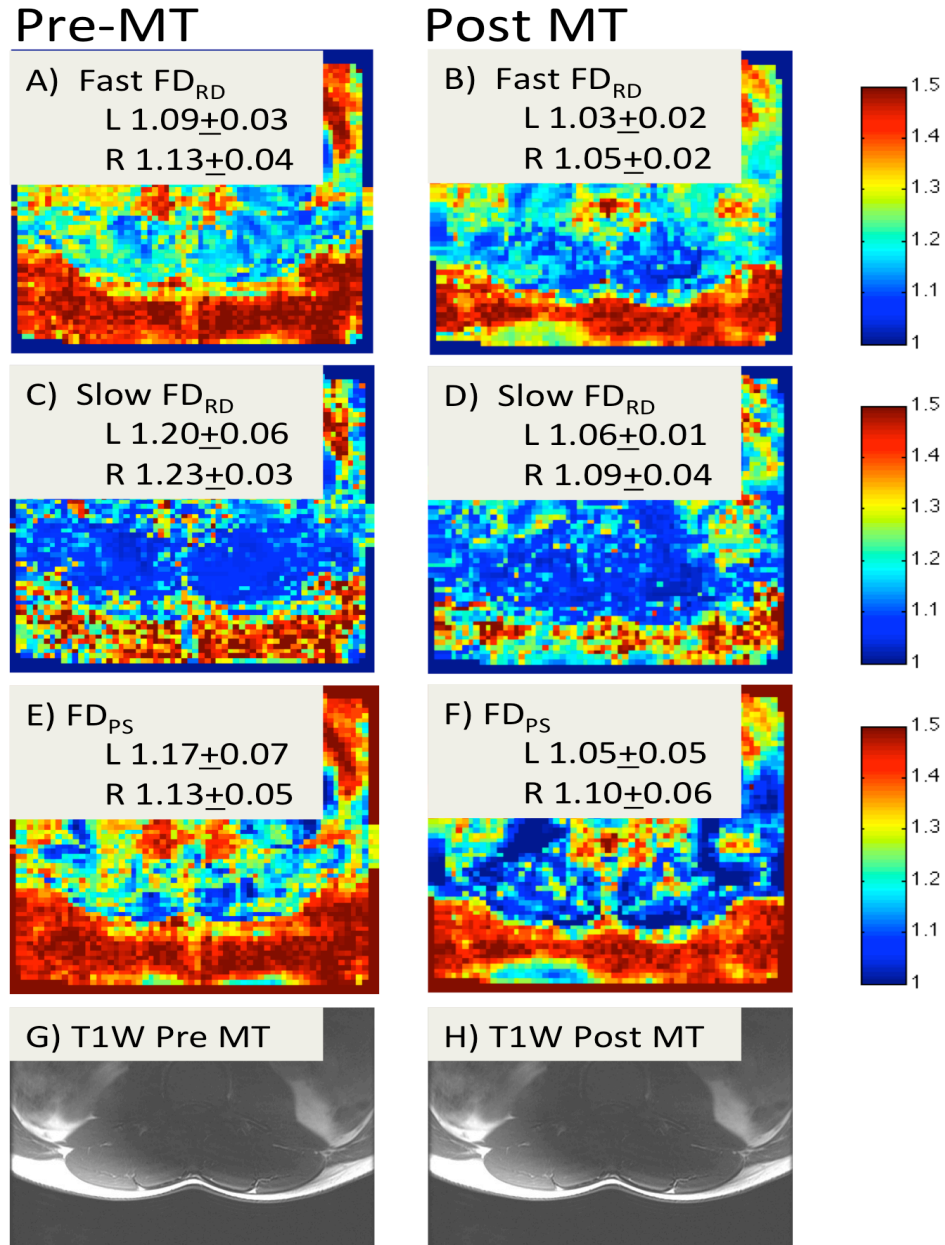


Figure 7.1 Fractal dimension maps and corresponding axial T1W images at L4 are shown from a healthy 23yr old male with no history of low back pain. A and B show maps of the fast component of FD_{RD} , C and D are slow FD_{RD} component, E and F are power spectrum FD maps (FD_{PS}), and G and H are T1W images. The FD_{PS} is clearly reduced post MT. Although the fast FD_{RD} component appears reduced in this subject neither it nor the slow FD_{RD} component were significantly different in pre compared to most MT.

Example FD maps of the target lower back area are presented in **fig. 7.1**. Overall, from the parametric FD maps, the ES+M appeared to have reduced BOLD FD after massage treatment, for both power spectrum (FD_{PS}) and relative dispersion (FD_{RD}) analysis methods. However, group analysis showed only a statistically significant main effect of massage treatment for FD_{PS} [2 way repeated measures ANOVA, using both laterality (left vs. right) and effect of massage as repeated factors] (**fig. 7.2**).

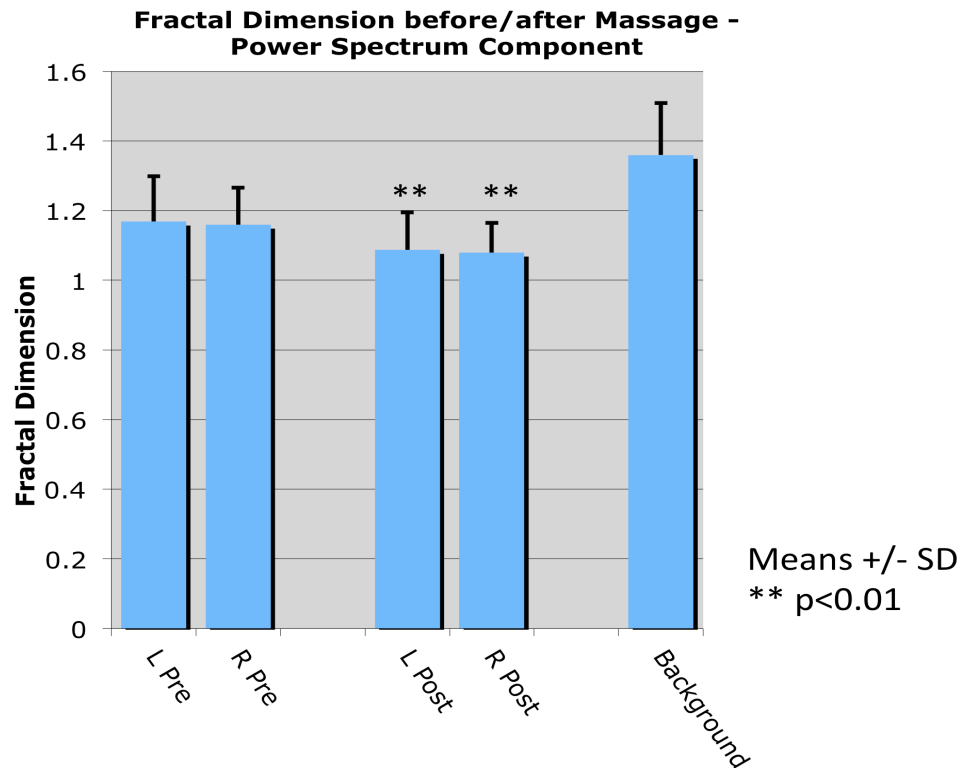


Figure 7.2 Plots fractal dimension (FD) power spectrum (PS) of the right and left ES+M muscle groups before massage treatment (MT). Values are means \pm standard deviation (** $p < 0.01$).

There was no significant effect of massage on either the fast or slow FD_{RD} components of the BOLD signal (**fig. 7.3**). No significant laterality effect was noted for any of the FD methods tested.

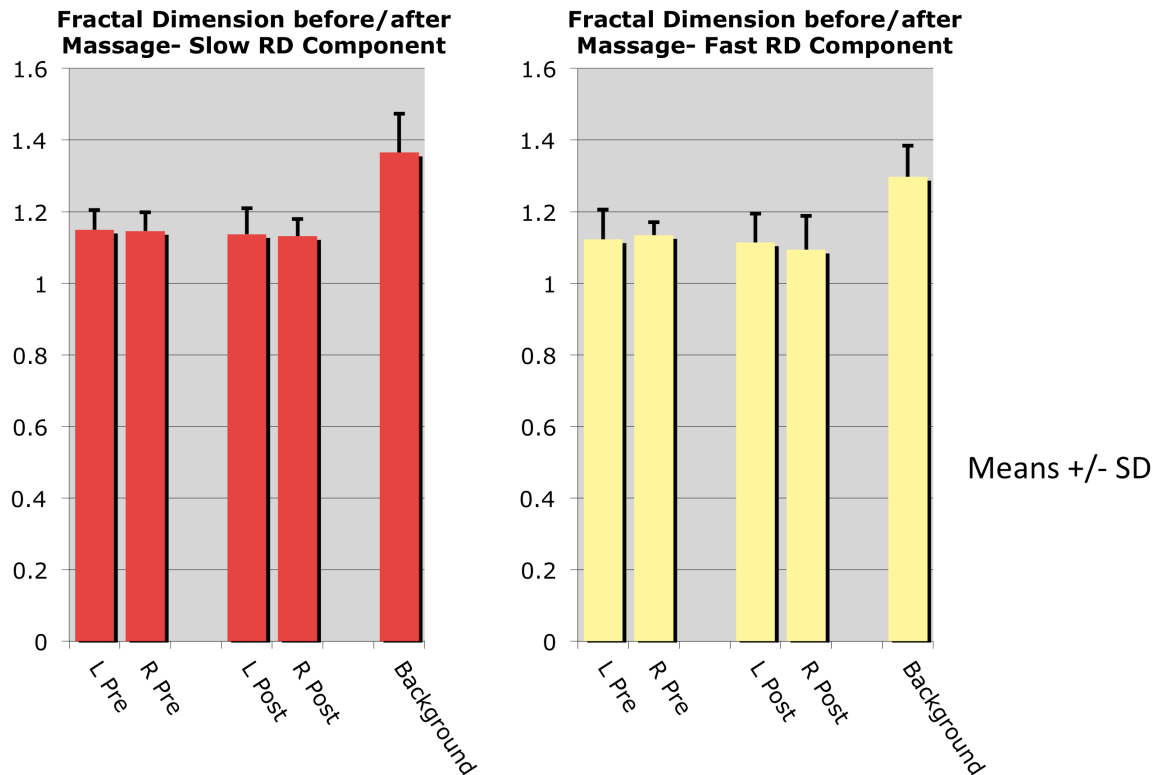


Figure 7.3 Plots of fast and slow components of fractal dimension (FD) relative dispersion (RD) of the right and left ES+M muscle groups before massage treatment (MT). Data are Means +/- SD, no significant effects of right/left or pre/post MT (2 way repeated measures ANOVA, background not included in ANOVA).

As a check of MRI scanner consistency, FD calculations were done on a ROI in the BOLD image background (i.e. air in the image around the person)(**figs. 7.2 and 7.3**). This consistently showed higher FD values (near 1.4), characteristic of scanner electronic (near white) noise, which is complex and aperiodic. Further, background ROIs were significantly higher than either the pre or post MT ES+M ROIs (1 way ANOVA). No differences in scanner noise FD were noted pre vs. post massage.

7.8. Discussion

Self similarity occurs when a structure has the same appearance at differing spatial scale, or in the time domain, at different sample size.

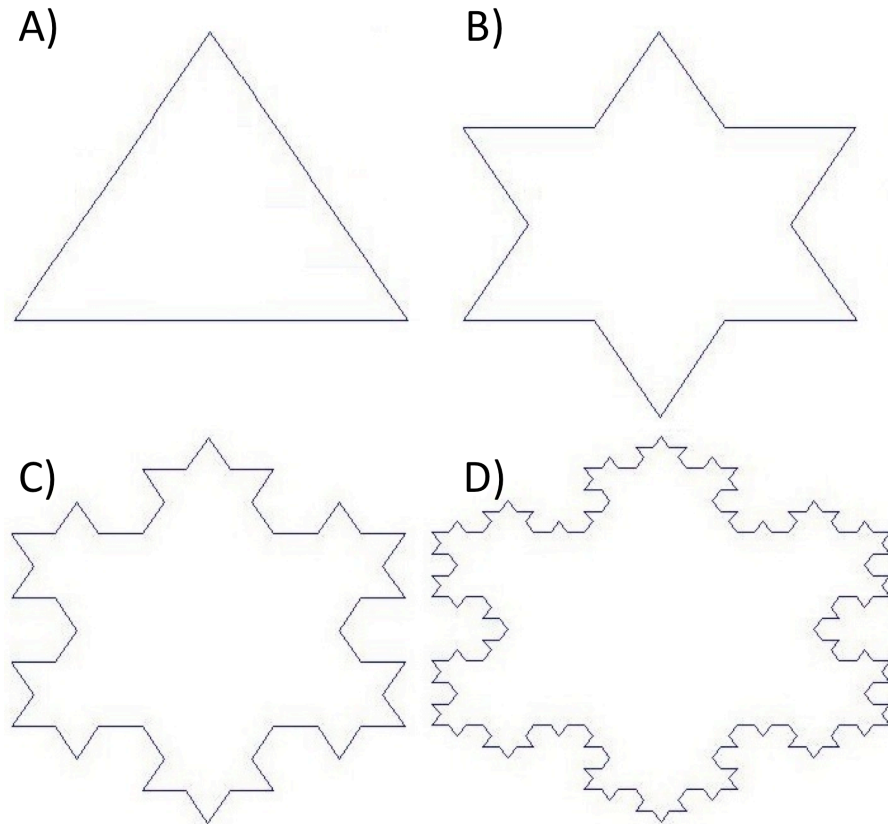


Figure 7.4 The ‘Koch snowflake’ where shapes have increasing complexity, self similarity and self affinity, and hence increasing FD from A to D. Plots were produced using Matlab (Mathworks, Natick, MA).

Self similarity can be shown pictorially by the “Koch’s Snowflake” (fig. 7.4) where each structure shown in figs. 7.4A-D has the property of self similarity at any scale, with progressively higher complexity and hence higher FD. This spatial calculation

can similarly be performed on time domain data (such as BOLD signals). A low value for FD means lower BOLD signal complexity. In microvasculature lower complexity may represent regular or rhythmic flow and tissue oxygenation, which could be achieved through higher perfusion rates. We found a bilateral reduction in FD_{PS} , post massage (**Fig. 7.2**) that was qualitatively noticeable on FD_{PS} maps (**Fig. 7.1**). Weerapong *et al.* believed that both effluerage and petrissage enhance venous return²⁰. Furthermore, using infrared thermometry, MT which includes both petrissage and effleurance has been shown to increase blood flow⁸. MT has shown to increase blood flow in diabetic subjects with peripheral arterial disease²¹. A vibration inducing massage machine has been shown to increase local blood flow²². Yet others have found increases in blood flow with MT, however those were only at the skin level not in deep muscle. Hinds *et al.* suspect this may be due to increased friction associated with MT, and as a consequence increase in local blood flow to dissipate the heat^{23,24}.

Conversely, there is some indirect evidence supporting the idea that muscle blood flow is decreased after MT. For example, preterm females are more relaxed during and after moderately intense but not light MT, as measured by increased parasympathetic activity based on EKG activity²⁵⁻²⁷. However, the authors did not postulate the effect on muscle blood flow. Infants displayed increased parasympathetic activation, including increased vagus nerve activation, after massage^{24, 26}. Decreased brachial artery blood flow and increased muscle lactic acid concentration with consequent decreased pH were observed in massage subjects compared to non-massaged controls after forearm exercise²⁸. Although there are studies consistent with post-MT decreased muscle blood

flow, many are due to *indirect* measures. There appear to be studies confirming increased blood flow *directly*, which would make comparisons to the current study more relevant. For example, Field *et al.*²⁶ showed there is increased post-MT heart rate in preterm infants, which could be consistent with increased muscular blood flow.

There are many differences in the type and duration of MT, the subject groups, location of the massage, and other factors. For example, Wiltshire *et al.*²⁸ showed decreased blood flow and greater lactic acid buildup in the forearms of healthy males in their twenties after a forearm grip exercise and then forearm massage. Their data should not be directly compared to Button *et al.*²², who showed that 30 minutes of vibratory machine stimulation increased blood flow in the calves of healthy subjects, compared to placebo-controls. Also, Castro-Sanchez *et al.*²¹ concluded that there was an increase in lower limb blood flow with type 2 diabetic patients. The closest study on the lower back determined that there was decreased systolic and diastolic blood pressure of Caucasian hypertensive subjects after massage²⁹.

A lower FD_{PS} implies increased muscle microvascular perfusion. We wanted to verify lower FD_{PS} was due to the MT and not something else. First, MT was consistent between left and right sides of the subjects (i.e. there was no significant effect of laterality, **fig. 2**) indicating balanced treatment by the massage therapist. The background FD values from both FD_{PS} and FD_{RD} (**fig.2**) were significantly greater (Student's T-test, $p < 0.05$) than both the pre- and post-MT data indicating that FD is a reliable measure and not something due to MRI scanner variation. Furthermore, there was no noticeable

background effect on (i.e. image noise) FD values, showing the MRI scanner was not the source of FD differences.

We have shown that the FD_{PS} method is more sensitive to changes after MT than FD_{RD} methods. Eke *et al.*^{17, 30} has shown that depending on how data appear in the frequency domain, it can be characterized as fractional Brownian motion (fBm) or fractional Gaussian noise (fGn). If temporal data can be classified as fGn, then dispersional analysis should be used (i.e. FD_{RD} method), while if data are fBm, then bridge detrended scaled windowed variance (bdSWV) should be used. Both bdSWV and dispersional analysis are in the time domain. Our study did not characterize this data as either fGn or fBm, so that may be the origin of the limitation with our FD_{RD} method.

Compared to conventional MRI sequences, the use of BOLD FD analysis is potentially of great value across various forms of pathology, showing unique functional colour maps that reflect sensitive changes in microvascular activity. Many disorders include a microvascular component, such as diabetes³¹, compartment syndrome³²⁻³⁴, and cancer³⁵⁻³⁹. In fact BOLD FD was shown to highlight potential intratumour microvascular activity⁴⁰. Similarly, this microvascular functional information could be applied to muscle, yielding much more than anatomical information. For example, imaging using conventional sequences is not always useful in characterizing lower back pain. Last and Hulbert stated: “imaging has limited utility because most patients with chronic low back pain have nonspecific findings on imaging studies, and asymptomatic patients often have abnormal findings”⁴¹. Given BOLD FD’s sensitivity to tissue microvascular changes, the functional information generated may prove to be much more

powerful in assessing tissue status, before and after intervention – using techniques such as massage. Ultimately, BOLD FD values reflect changes in tissue microvasculature, hence blood flow/oxygenation variation. Here we show whether changes in BOLD FD occur immediately after MT in the erector spinae and multifidus muscles at the L4 level. Our data support the theory that MT results in increased blood flow, based on decreased FD_{PS} .

7.9. Conclusion

The results from this study are consistent with previous studies^{8, 16, 20, 42} which found that there was a slight significant change in blood flow after Swedish MT using primarily effleurage and petrissage. For our tests, the FD_{PS} was more sensitive than either FD_{RD} method.

7.10. References

1. Ling P. *Gymnastikens Allmanna Grunder*. Stockholm: Upsala : Palmblad & Comp.; 1834.
2. Moyer CA, Dryden T, Shipwright S. Directions and dilemmas in massage therapy research: a workshop report from the 2009 north american research conference on complementary and integrative medicine. *Int J Ther Massage Bodywork* 2009; 2:15-27.
3. Moyer CA, Rounds J, Hannum JW. A meta-analysis of massage therapy research. *Psychol Bull* 2004; 130:3-18.
4. Furlan AD, Imamura M, Dryden T, Irvin E. Massage for low-back pain. *Cochrane Database Syst Rev* 2008(4):CD001929.
5. Furlan AD, Imamura M, Dryden T, Irvin E. Massage for low back pain: an updated systematic review within the framework of the Cochrane Back Review Group. *Spine (Phila Pa 1976)* 2009; 34:1669-1684.
6. Lund I, Lundeberg T, Kurosawa M, Uvnas-Moberg K. Sensory stimulation (massage) reduces blood pressure in unanaesthetized rats. *J Auton Nerv Syst* 1999; 78:30-37.
7. Sagar SM, Dryden T, Myers C. Research on therapeutic massage for cancer patients: potential biologic mechanisms. *J Soc Integr Oncol* 2007; 5:155-162.
8. Sefton JM, Yarar C, Berry JW, Pascoe DD. Therapeutic massage of the neck and shoulders produces changes in peripheral blood flow when assessed with dynamic infrared thermography. *J Altern Complement Med* 2010; 16:723-732.
9. Mori H, Ohsawa H, Tanaka TH, Taniwaki E, Leisman G, Nishijo K. Effect of massage on blood flow and muscle fatigue following isometric lumbar exercise. *Med Sci Monit* 2004; 10:CR173-178.
10. Noble JG, Lee V, Griffith-Noble F. Therapeutic ultrasound: the effects upon cutaneous blood flow in humans. *Ultrasound Med Biol* 2007; 33:279-285.
11. Goats GC. Massage--the scientific basis of an ancient art: Part 2. Physiological and therapeutic effects. *Br J Sports Med* 1994; 28:153-156.

12. Goats GC. Massage--the scientific basis of an ancient art: Part 1. The techniques. *Br J Sports Med* 1994; 28:149-152.
13. Wakim KG. Physiologic effects of massage. In: Licht S, editor. *Massage, Manipulation and Traction*. New York, NY: Robert E. Krieger Publishing Company; 1976. p 38–43.
14. Cherkin DC, Sherman KJ, Kahn J, Erro JH, Deyo RA, Haneuse SJ, Haneuse SJ, Cook AJ. Effectiveness of focused structural massage and relaxation massage for chronic low back pain: protocol for a randomized controlled trial. *Trials* 2009;10:96.
15. Galloway S, Hunter A, Watt JM. Athletes. In: Dryden T, Moyer C, editors. *Massage Therapy Integrating Research and Practice, Human Kinetics*. 2012. p103-111.
16. Shoemaker JK, Tiidus PM, Mader R. Failure of manual massage to alter limb blood flow: measures by Doppler ultrasound. *Med Sci Sports Exerc* 1997; 29:610-614.
17. Eke A, Herman P, Bassingthwaighte JB, Raymond GM, Percival DB, Cannon M, Balla I, Ikrényi C. Physiological time series: distinguishing fractal noises from motions. *Pflugers Arch* 2000; 439:403-415.
18. Basstingthwaite. Fractal Measures of Heterogeniety and Correlation. In: Bassingthwaighte JB, Liebovitch LS, West BJ, editors. *Fractal Physiology*. New York, NY: Oxford Publishing; 1994. p 63-106.
19. Schepers HE, Van Beek JHGM, Bassingthwaite JBl. Four methods to estimate the fractal dimension from self-affine signals. *IEEE Eng Med Biol* 1992; 11:5764.
20. Weerapong P, Hume PA, Kolt GS. The mechanisms of massage and effects on performance, muscle recovery and injury prevention. *Sports Med* 2005; 35:235-256.
21. Castro-Sanchez AM, Moreno-Lorenzo C, Mataran-Penarrocha GA, Feriche-Fernandez-Castanys B, Granados-Gamez G, Quesada-Rubio JM. Connective Tissue Reflex Massage for Type 2 Diabetic Patients with Peripheral Arterial Disease: Randomized Controlled Trial. *Evid Based Complement Alternat Med* 2009.
22. Button C, Anderson N, Bradford C, Cotter JD, Ainslie PN. The effect of multidirectional mechanical vibration on peripheral circulation of humans. *Clin Physiol Funct Imaging* 2007; 27:211-216.
23. Hinds T, McEwan I, Perkes J, Dawson E, Ball D, George K. Effects of massage on limb and skin blood flow after quadriceps exercise. *Med Sci Sports Exerc* 2004; 36:1308-1313.
24. Field T, Diego M, Hernandez-Reif M. Moderate pressure is essential for massage therapy effects. *Int J Neurosci* 2010; 120:381-385.

25. Diego MA, Field T. Moderate pressure massage elicits a parasympathetic nervous system response. *Int J Neurosci* 2009; 119:630-638.
26. Diego MA, Field T, Hernandez-Reif M, Deeds O, Ascencio A, Begert G. Preterm infant massage elicits consistent increases in vagal activity and gastric motility that are associated with greater weight gain. *Acta Paediatr* 2007; 96:1588-1591.
27. Field T. Pregnancy and labor massage. *Expert Rev Obstet Gynecol* 2010; 5:177-1781.
28. Wiltshire EV, Poitras V, Pak M, Hong T, Rayner J, Tschakovsky ME. Massage impairs postexercise muscle blood flow and "lactic acid" removal. *Med Sci Sports Exerc* 2010; 42:1062-1071.
29. Olney CM. The effect of therapeutic back massage in hypertensive persons: a preliminary study. *Biol Res Nurs* 2005; 7:98-105.
30. Eke A, Herman P, Kocsis L, Kozak LR. Fractal characterization of complexity in temporal physiological signals. *Physiol Meas* 2002; 23:R1-R38.
31. De Boer MP, Meijer RI, Wijnstok NJ, Jonk AM, Houben AJ, Stehouwer CD, Smulders YM, Eringa EC, Serné EH. Microvascular dysfunction: a potential mechanism in the pathogenesis of obesity-associated insulin resistance and hypertension. *Microcirculation* 2012; 19:5-18.
32. Botte MJ, Fronck J, Pedowitz RA, Hoenecke HR, Jr., Abrams RA, Hamer ML. Exertional compartment syndrome of the upper extremity. *Hand Clin* 1998; 14:477-482.
33. Duran WN, Takenaka H, Hobson RW, 2nd. Microvascular pathophysiology of skeletal muscle ischemia-reperfusion. *Semin Vasc Surg* 1998; 11:203-214.
34. Blaisdell FW. The pathophysiology of skeletal muscle ischemia and the reperfusion syndrome: a review. *Cardiovasc Surg* 2002; 10:620-630.
35. Ziche M, Morbidelli L. Molecular regulation of tumour angiogenesis by nitric oxide. *Eur Cytokine Netw* 2009; 20:164-170.
36. Wong ML, Prawira A, Kaye AH, Hovens CM. Tumour angiogenesis: its mechanism and therapeutic implications in malignant gliomas. *J Clin Neurosci* 2009; 16:1119-1130.
37. Keppler D, Sameni M, Moin K, Mikkelsen T, Diglio CA, Sloane BF. Tumor progression and angiogenesis: cathepsin B & Co. *Biochem Cell Biol* 1996; 74:799-810.

38. Folkman J. Tumor angiogenesis. *Adv Cancer Res* 1985; 43:175-203.
39. Shing Y, Folkman J, Haudenschild C, Lund D, Crum R, Klagsbrun M. Angiogenesis is stimulated by a tumor-derived endothelial cell growth factor. *J Cell Biochem* 1985; 29:275-287.
40. Wardlaw G, Wong R, Noseworthy MD. Identification of intratumour low frequency microvascular components via BOLD signal fractal dimension mapping. *Phys Med* 2008; 24:87-91.
41. Last AR, Hulbert K. Chronic low back pain: evaluation and management. *Am Fam Physician* 2009; 79:1067-1074.
42. Cunningham JE, Kelechi T, Sterba K, Barthelemy N, Falkowski P, Chin SH. Case report of a patient with chemotherapy-induced peripheral neuropathy treated with manual therapy (massage). *Support Care Cancer* 2011; 19:1473-1476.

Chapter 8 . BOLD FD in the erector spinae in subjects with and without LBP

Gavin E.G. Jones, M.Sc., Dinesh A. Kumbhare, M.Sc., M.D., FRCPC, Srinivasan Harish MBBS, FRCPC, and Michael D. Noseworthy, PhD, P.Eng.

8.1. Preamble

This chapter is a manuscript in preparation. Data analysis is complete and manuscript submission will be discussed in subsequent months. Many of the basic reviews of BOLD-MRI and fractal dimension analysis are not included in the introduction (chapter 8.2) since that material is part of chapter 2.3.

8.2. Introduction

The ES+M is altered in subjects with lower back pain as previously noted in earlier chapters. Structural changes have been observed based on DTI and CSA measures (Chapters 5, 6 and 9). In addition to structural differences in the multifidus and erector spinae with LBP, there are also functional differences; subjects with low back pain have more active erector spinae than controls during Swiss ball exercises (Bressel *et al.* 2012), during back exercises (Colado *et al.* 2011), and during normal walking paradigms (Hanada *et al.* 2011), based on EMG measurements. Also, the induction of pain in

asymptomatic subjects alters the EMG signal from the lumbar multifidus (Keisel *et al.* 2012). Since functional activity of the erector spinae is altered with low back pain, and the sensation of pain is also associated with changes in erector spinae activity, it is possible there are changes in local perfusion that are associated with the symptoms of low back pain.

Perfusion is commonly assessed using intravenous contrast agents. However, the bony region of this area of the back would make acquisition of MR perfusion data a challenge. Also, all contrast-based perfusion methods are a snap-shot into local blood flow which may or may not reflect microvascular flow over prolonged time. Furthermore, we wanted to develop a non-invasive method to look at musculature that does not rely on intravenous injections. As an alternative, MRI BOLD imaging was hypothesized to be a useful approach. BOLD signal, which results from the ratio of oxy to deoxyhaemoglobin, reflects a complex signal containing contributions from local blood volume, perfusion, haematocrit and local metabolism. Although changes in the BOLD signal have not been used to measure changes in the lumbar erector spinae, BOLD imaging has proven to be useful for several clinically relevant purposes.

BOLD has shown utility in cancer (Barrett *et al* 2007; Padhani *et al* 2007). Cancerous tissue often initiates abnormal angiogenesis through the release of several angiogenic factors including vascular endothelial cell growth factor (VEGF). This can lead to a tumour ‘concentration’ of blood vessels greater than surrounding normal tissue. Changes in the BOLD signal are attributed to increased local blood volume, and closely match the outline of tumours (Lüdemann *et al.* 2006). Changes in the fractal dimension

(see Chapter 2.3) of the BOLD signal may be associated with tumours (Wardlaw *et al.* 2008). This may have to do with the disorganized, haphazard organization of the tumor vasculature compared to normal tissue as well as increased perfusion. One common thread between cancer and BOLD signal is the increased perfusion, blood flow and volume (all attributable to angiogenic processes) and increased metabolism.

Arthritis is another disease having inflammatory responses that can lead to aberrant angiogenesis and resulting increased perfusion, blood flow and volume. As such BOLD imaging has shown utility in arthritis (Doria and Dick 2005). Healthy musculature has also been evaluated using the BOLD signal (Noseworthy *et al.* 2003). Furthermore, modulation due to vasoactive compounds has shown muscle BOLD is highly sensitive to microvasculature (Bulte *et al.* 2006).

BOLD signal is often measured in cancer, muscle and arthritis studies using paradigms similar to functional MRI brain imaging. However the paradigms are often done via hyperoxia or carbogen cycling, the result of which is analyzed using standard generalized linear models (GLM). We proposed that the BOLD signal, being a complex signal, may be measured using an index of complexity, the fractal dimension (FD). Here low FD indicates periodicity and likely higher perfusion. Alternatively, higher FD indicates a muscle with minimal perfusion, likely with reduced activity. We suggest BOLD FD could be used to demonstrate local perfusion changes, possibly resulting from chronic pain within the ES+M target. A difference in BOLD FD in subjects with CLBP compared to controls is consistent with a difference in blood flow in the ES+M.

8.3. Materials and Methods

8.3.1. Subject population

Twenty two subjects (twelve females, ten males) with LBP and 21 (ten females, eleven males) control subjects were scanned. The two groups' demographic characteristics were not significantly different from each other, but the ODI and VAS scores were significantly higher in the LBP group than controls; ODI LBP: 44.6 ± 23.4 , ODI controls: 1.8 ± 3.6 , VAS LBP: 6.3 ± 2.7 , VAS controls: 0.1 ± 0.3 .

8.3.2. MRI parameters and offline analysis

MRI parameters were identical to those used in chapter 7 (FD in subjects with MT). In short, subjects were scanned in a supine position on a GE 3T Signa MRI (GE Healthcare, Milwaukee, WI), using a 12-channel neck/spine RF coil. Axial and sagittal T1W and T2W images were acquired to verify there were no bony abnormalities or other extreme pathology. No subjects failed this routine radiological examination. For BOLD scans 3 slices, covering L4 were acquired with gradient echo/echo planar imaging and TR/TE of 250/35ms, matrix 64×64 for 2400 time points (scan length = 10 minutes).

Regions of interest (ROI) were the erector spinae muscles and a background ROI outside the body, drawn on the BOLD FD image. FD was then calculated using the FD_{PS} method (Eq 2.6 and 2.7) and FD_{RD} method (Eq 2.8) as described in chapter 2. Analysis was performed using in-house programs written in Matlab (Mathworks, Natick, MA).

8.3.3. Statistical analysis

Tests for normality within each ROI was made with Jarque-Bera test, which takes into consideration both skewness and Kurtosis, and a test for normality within each group was made with the Shapiro-Wilk test (SPSS 12.0, IBM). Comparisons between groups were performed with ANOVA with left and right ES+M and LBP/control as factors.

To determine the relationship between FD and another continuous measures such as age, ODI score or BMI, Pearson's correlation coefficient was calculated.

8.4. Results

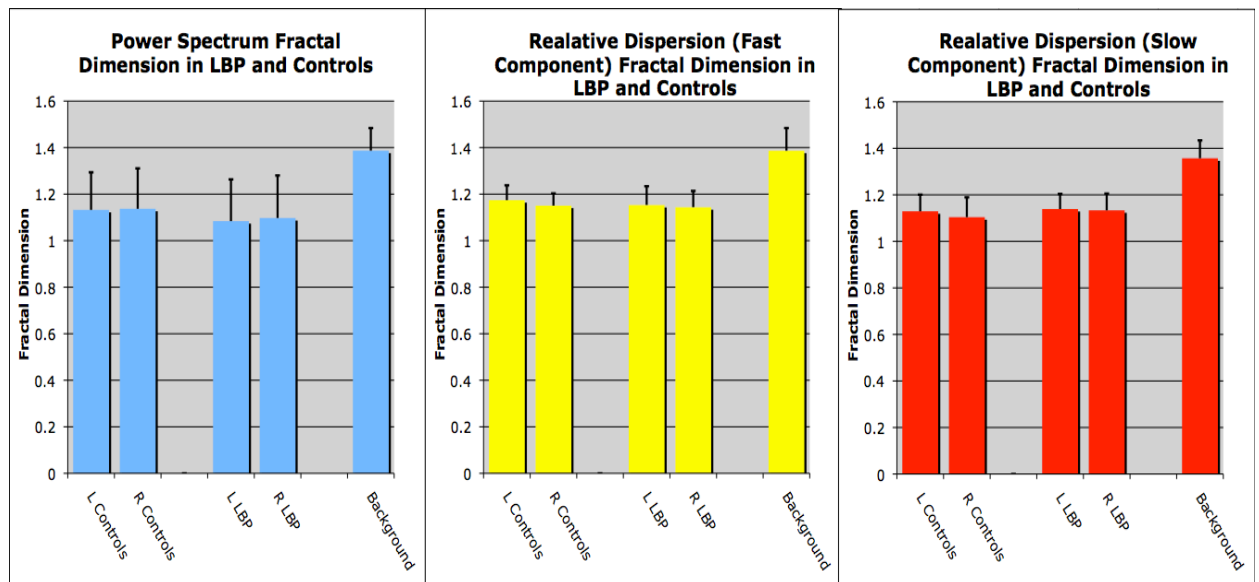


Figure 8.1 BOLD FD in subjects with and without LBP.

BOLD FD using the FD_{PS} , $FD_{RD-fast}$, and $FD_{RD-slow}$ methods are shown in figure 8.2. For all three FD calculations, there were no significant differences between the LBP and control groups, nor any difference between left and right ES+M ($p>0.05$). However,

for each of the three FD calculations, the background was significantly greater than all other values ($p < 0.05$). This indicates the FD measure is not a mathematical artifact since BOLD signal is more complex and random outside the body (i.e. in regions of white noise caused by the MRI scanner system), where no perfusion is expected. From tissue ROIs the FD is lower, indicating biological temporal variations such as perfusion and metabolic fluctuation.

To make correlations between FD and either demographic information or symptoms of LBP (ODI and VAS scores), the right and left FD values were averaged. Justification for averaging left and right FD values is that the asymmetry index values were very low, with many under 2, indicating FD values were highly symmetric, more so than CSA and DTI FA AI. There was very little correlation between FD_{PS} and anthropomorphic data (either age, weight, height, Godin Score, VAS, or ODI score). The highest value was $R^2=0.19$ (between FD_{PS} and Godin Score), and many of the other comparisons yielded much lower values. When all subjects (LBP and controls) were included, the correlation comparing FD_{PS} and BMI is $R^2=0.24$ as seen in figure 8.2 below which was much higher than comparisons between FD_{PS} and other anthropomorphic data.

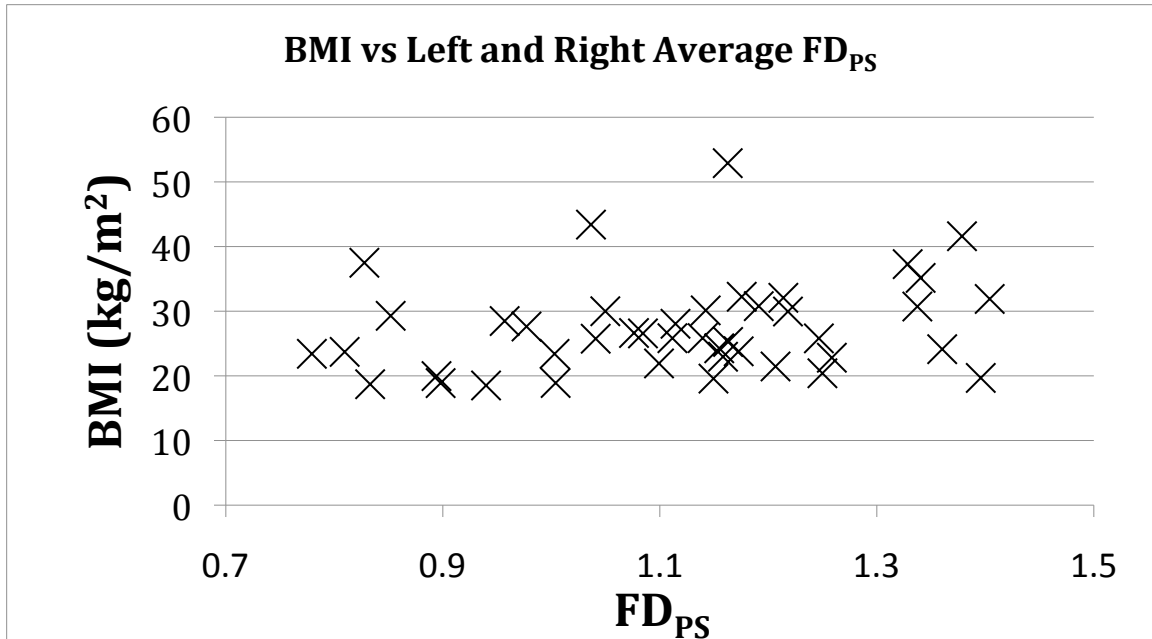


Figure 8.2 Scatter plot of BMI vs. Mean (left and right) BOLD FD_{PS} in all subjects.

The correlation between FD_{PS} and ODI score (which is the gold standard for LBP symptoms) was only $R^2=0.03$.

It is possible that there is a greater relationship between ODI and FD_{PS} for subjects within certain BMI ranges rather than the population taken as a whole. Table 8.1 shows the correlation coefficients between ODI and FD_{PS} for BMI broken down into ranges listed by the World Health Organization (WHO 1995).

BMI (kg/m ²)	Pearson's R ²	n
18-25	-0.16	18
25-30	-0.1	13
30-35	-0.029	6
35-40	-0.29	3
>40	0.36	3
ALL BMIs	-0.03	43

Table 8.1 Pearson's correlation coefficient (R²) for subjects (LBP and controls) for different BMI categories, and the sample sizes (n).

The greatest correlation values were for subjects with BMIs between 18 and 25. There were other high correlations, but the sample sizes are small. The correlation between ODI and FD_{PS} in all subjects and in only those with BMIs between 18 and 25 is shown in figure 8.3, below.

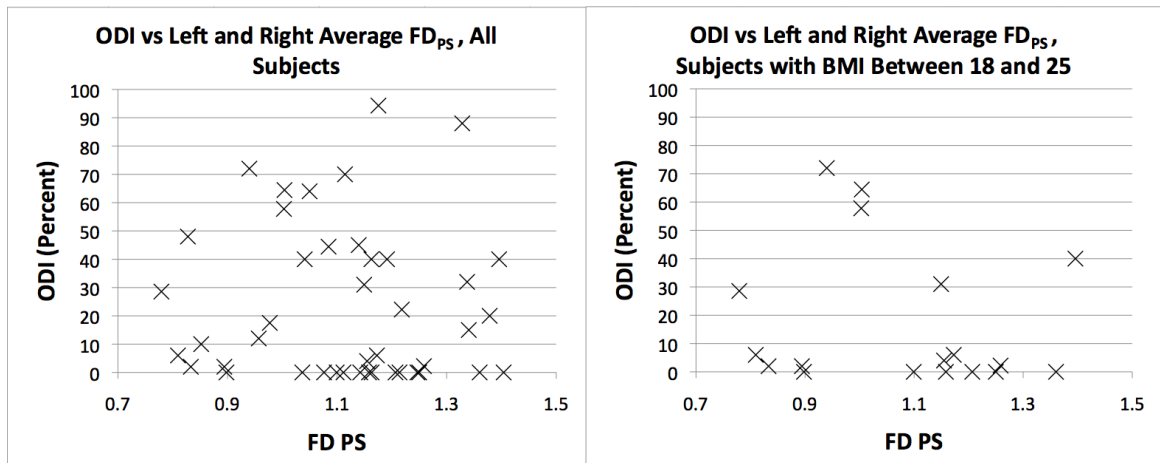


Figure 8.3 Scatter plot of ODI vs. Mean (left and right) BOLD FD_{PS} in all subjects for all subjects (R²=0.03) and for subjects with BMI between 18 and 25 (R²=0.16).

8.5. Discussion

Analyzing the BOLD signal has proven useful in other applications (Barrett *et al.* 2007; Padhani *et al.* 2007; Doria and Dick 2005). Here we did not find FD measures were different between LBP subjects and controls. Furthermore, there was no correlation between FD values and any other measured factor, such as anthropometric characteristics or symptoms of LBP, as measured by ODI or VAS.

LBP has been shown to cause changes in the erector spinae, such as gross structural changes measured by muscle CSA (Niemelainen *et al.* 2011; Beneck and Kulig 2012), and changes in tonic activity during tasks (Enomoto *et al.* 2012; Kolich *et al.* 2000; Tanaka *et al.* 2002).

It is likely that the lumbar multifidus contains a large proportion of fibres that are oxidative in nature, based on their requirement of tonic activity. This implies that the BOLD signal is larger than would be expected if the fibres were largely glycolytic.

The fact that there are functional changes to the lumbar erector spinae did not translate into changes in the BOLD FD values. There are several possible reasons for the lack of observed changes in BOLD FD. It is possible there is not such a great increase in tonic activity in the patient who suffers from CLBP that increased blood supply is required. Furthermore, the subject is lying quiescent in a supine position, and is not required to have activated erector spinae, as is required during standing upright. Typically, differences between control and LBP subjects are revealed in EMG activity

when a task is performed. It may be useful in the future to determine whether there are differences in BOLD FD after several tasks which stress lower back activity, such as lumbar raises, planks, or standing on an unstable surface (Ramprasad *et al.* 2011) then immediately measuring the changes in BOLD FD. Since it is presumed that blood flow is correlated with FD, then there is no change in blood flow with the symptoms of LBP in subjects suffering from CLBP.

Chapter 9. Combined Measures

9.1. Overview

Both DTI and CSA have shown to be sensitive to LBP symptoms, but BOLD FD_{PS} showed only slight correlation to LBP symptoms. There were several promising observations, similar in both DTI and T2W CSA scans:

- i. The absolute value of a metric does not change significantly comparing the control and LBP groups, however there is greater asymmetry in the LBP group than controls (FA AI for DTI scans and CSA AI for T2W images).
- ii. Correlation has revealed relationships between a dependent factor such as FA AI or CSA AI with the symptoms of LBP. There is a wide variety of severity of symptoms in the LBP group. When correlating FA AI or CSA AI to the symptoms of LBP, as measured by ODI, both measures show correlations with $R^2=0.35$ to 0.40 .
- iii. ODI score was found to correlate with VAS at a level of greater than $R^2=0.90$ for the populations used for DTI and T2W scanning, indicating that the underlying phenomena they both measure is similar. This is not surprising, since the subject samples are almost identical for the different studies. In other words, with three exceptions, the same subjects were used for all three scan/analysis types.

- iv. Correlations ranging from $R^2=0.30$ to 0.40 was found when comparing BMI and either FA AI or CSA AI or weight and either FA AI or CSA AI.
- v. The correlation between ODI and FA AI or CSA AI increased only when certain categories of BMI were used, typically below 40 kg/m^2 .
- vi. There were no other correlations above 0.25 found between FA AI or CSA AI or any other demographic characteristic, such as height, age, or level of physical activity (as measured by Godin score).

These observations indicate that the trends measured are likely genuine for both DTI and T2W scans. Also, a combination of the data may provide useful. Further, data from both DTI and T2W show the same reliance on BMI but not on other factors, so the limits or categories placed on this combined factor will not have to choose between diverging trends. In other words, the same BMI categories are most reliable for both DTI and T2W data.

Since there are so many similarities, one might ask if they are measuring the same phenomena. This seems unlikely since the correlation coefficient between DTI FA AI and CSA AI was $R^2=-0.05$.

Only the most efficacious measures from each of the different MR scans will be tested in combination to see if, together, they are more closely related to the current clinical standards, the ODI or VAS. For DTI measures, the FA AI in the multifidus of both sexes can be used. For CSA, the multifidus CSA AI at the top endplate of L4 of both sexes can be used. For BOLD FD, mean (left and right) FD PS can be used.

Since both FA AI and CSA AI are both normalized data which scale from 0-100, they can be summed, product or difference taken with equal contribution from each measure. This cannot be said of FD_{PS} , which scales from 1.0 to 1.5 and must be normalized to fit a value between 0 and 100, to ensure there is equal contribution from FD_{PS} .

9.2. Combination of Data

Several different measures were tested, using simple mathematical relationships such as multiplying measures together, such as $[FA\ AI]*[CSA\ AI]$ or averaging measures, such as $[(FA\ AI)+(CSA\ AI)]/2$.

Combination measures using BOLD FD_{PS} were calculated but those using BOLD FD_{PS} are problematic, since FD_{PS} only scales between 1 and 1.5 while other AI measures scale between 0 and 100. If normalized BOLD FD_{PS} were used (altered to scale between 0 and 100 rather than 1.0 and 1.5), then its contribution would be too high compared to the other scans. This is because even though FA AI and CSA AI theoretically scale between 0 and 100, in practice the AI values were very low; the CSA AI for all subjects was 8.62 and FA AI for all subjects was 3.97. By comparison, the mean normalized FD_{PS} was 73.17. Also, using FD was not likely to add accuracy to the combined index; FD_{PS} correlated with ODI score only with a level of $R^2=-0.03$, and there was no significant difference between the LBP and control groups when comparing mean FD_{PS} . Several different calculations were tested, and are listed below:

$$Index1 = \frac{CSA_{AI} + FA_{AI} + FD_{PS}}{3} \quad (9.1)$$

$$Index2 = \frac{CSA_{AI} + FA_{AI} + FD_{PS-Norm}}{3} \quad (9.2)$$

$$Index3 = CSA_{AI} \times FA_{AI} \times FD_{PS} \quad (9.3)$$

$$Index4 = CSA_{AI} \times FA_{AI} \quad (9.4)$$

$$Index5 = \frac{CSA_{AI} + FA_{AI}}{2} \quad (9.5)$$

$$Index6 = |CSA_{AI} - FA_{AI}| \quad (9.6)$$

$FD_{PS-Norm}$ is a normalized FA, which scales from 66-100 instead of 1.0-1.5. It is calculated simply as:

$$FD_{PS-Norm} = (FD_{PS} - 1.0) \times 150 \quad (9.7)$$

Two or more measures may contribute to the variability, which correlates to ODI, and together, there may be improvement. This is the rationale for the simple averages in indices 1, 2 and 5. Although taking the product of two measures (from indices 3 and 4) is uncommon in physiological measures, such an effect has been shown between hearing impairment and the product of age and smoking (Noorhasim and Rampal 1998) physical activity and body size on breast cancer risk (McCullough *et al.* 2012), circadian genes and breast cancer risk in shift workers (Monsees *et al.* 2012), and obesity and vitamin D deficiency on insulin resistance (Kabadi *et al.* 2012). Each possible index is evaluated based on the correlation with the ODI and VAS measures. Table 9.1 below shows Pearson's correlation coefficient (R^2) for each Index (1-6) vs. either ODI or VAS.

	ODI	VAS
Index #1	0.37	0.37
Index #2	0.21	0.22
Index #3	0.20	0.25
Index #4	0.29	0.34
Index #5	0.37	0.37
Index #6	0.39	0.38

Table 9.1 Pearson’s Correlation Coefficient for each index vs ODI or VAS.

It appears that the highest correlations are for equations 9.5 and 9.6. Also, since both FA AI and CSA AI show correlation with BMI and both index #5 and #6 are comprised of FA AI and CSA AI measures, Pearson’s correlation coefficient was calculated between index #5 and ODI and index #6 and ODI for LBP subjects with BMIs in various categories as seen in table 9.2.

BMI Range	Index #	R ²	
		ODI SCORE	n
18-25	5	0.88	7
	6	0.51	
26-30	5	0.43	8
	6	-0.39	
31-39	5	0.18	7
	6	-0.11	
18-30	5	0.67	15
	6	0.15	

Table 9.2 Pearson’s correlation coefficient (R²) for Indices #5 and #6. Only LBP subjects are used, and correlation are broken down into BMI categories. The last row are R² for BMIs between 18 and 30, the most reliable group, although it is not a WHO category.

9.2.1. Justification for Using only LBP Subjects in BMI Categorized

Correlations Between Index and ODI

Only LBP subjects were used for comparisons in table 9.2 since control subjects typically had very low (zero or close to zero) ODI values. Control subjects typically cluster around the origin. An example can be seen in figure 9.1. Such data would artificially inflate correlation coefficient values. So then a high correlation might mean that there are more control subjects in that BMI category, and might not reveal an actual relationship between the index value and ODI for that BMI category. Note that there was one subject with a BMI of greater than 40, so the correlation between Indices and ODI could not be calculated for that BMI category.

9.2.2. Comparisons Among Indices and ODI – BMI categories

It is obvious from table 9.2 that index #5 appears to be the most useful. Although the R² were similar for Index #5 and #6 in table 9.1, when groups were broken down into

BMI categories, the correlations were higher for Index #5, especially for lower BMIs. The relationship between ODI and Index #5 decreases with increasing BMIs from $R^2=0.88$ down to 0.18, while the correlation between Index #6 and ODI is even negative for some categories (asymmetry is greater in subjects with less severe symptoms). Further, Index #5 makes more sense than Index #6. It is a standard mean of FA AI and CSA AI, while Index #6 is a difference between the two. For this reason, Index #5 is the mean of CSA AI and DTI FA AI, and can be renamed the *JONES-NOSEWORTHY-KUMBHARE INDEX*, *JNK INDEX*, and will be used and is the best measure of combination of the DTI and CSA measures used in this study. The correlation between the JNK Index and ODI for all subjects is seen in figure 9.1 and only for those with BMIs between 18 and 25 in figure 9.2.

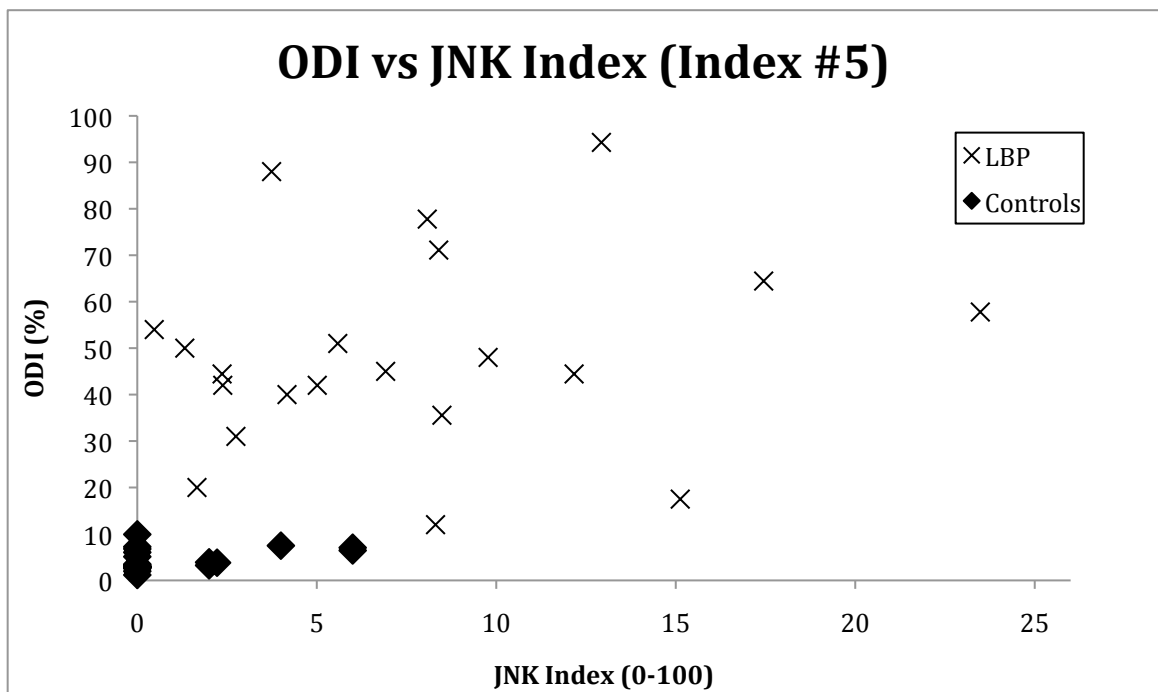


Figure 9.1 ODI vs. JNK Index (equally weighted mean of FA AI and CSA AI) for all subjects. $R^2=0.37$ for all subjects.

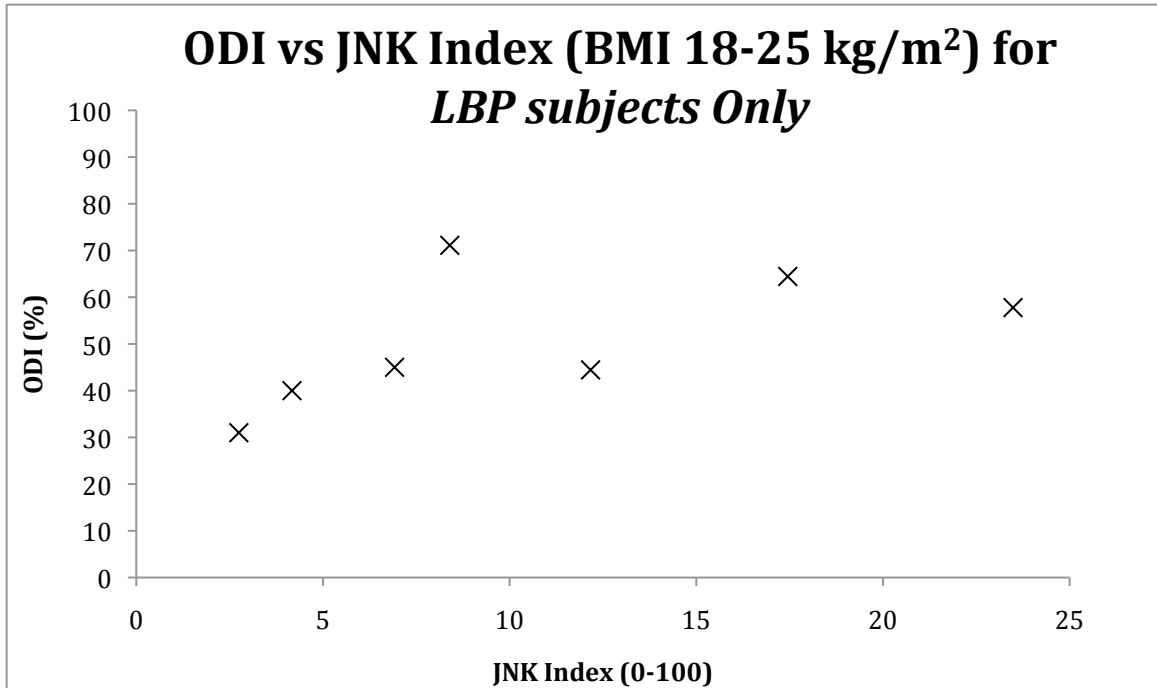


Figure 9.2 ODI vs. JNK Index for LBP subjects only, with BMI between 18 and 25. R²=0.88 for this group.

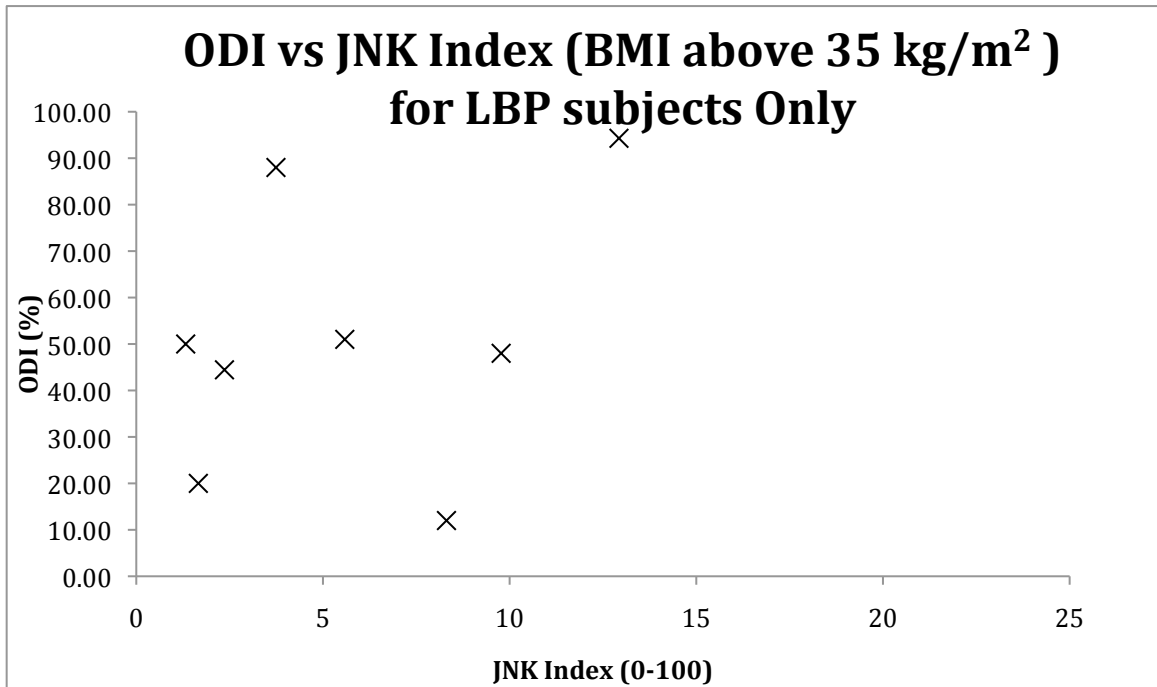


Figure 9.3 ODI vs. JNK Index for LBP subjects only, with BMI above 30 kg/m². R²=0.18 for this group.

Figure 9.3 shows the scatter plot of ODI vs. JNK index for subjects with BMI above 35 kg/m². BMI above 35 kg/m² is the least reliable category, with $R^2=0.18$, compared to figure 9.2, with $R^2=0.88$.

Chapter 10 . Future Directions

10.1. Study Limitations

The MR scan types used in this thesis cross the spectrum from widely used (T2W imaging) to novel (fractal analysis of the BOLD signal).

Cross sectional area of T2W images are well studied, and have been reported in the lumbar erector spinae and multifidus using MRI (Hides *et al.* 1995; Kader *et al.* 2000; Lee *et al.* 2011; Beneck and Kulig 2012; Shafaq *et al.* 2012). T2W images were originally collected as a measure to establish content validity; to confirm that our subjects are similar to those reported elsewhere (Hides *et al.* 1995; Kader *et al.* 2000; Lee *et al.* 2011; Beneck and Kulig 2012; Shafaq *et al.* 2012).

DTI has been performed extensively in other tissues, such as the brain and CNS (Christidi *et al.* 2011; Asano *et al.* 2012; Kasahara *et al.* 2012; Lange *et al.* 2012; Zappala *et al.* 2012), and in skeletal muscle (Zaraiskaya *et al.* 2006; Damon 2008; Kan *et al.* 2009; Karampinos *et al.* 2009; Froeling *et al.* 2010; Kim *et al.* 2011; Cermak *et al.* 2012). However, there are no publications of DTI in the lumbar multifidus and/or erector spinae, let alone any that analyze the musculature in relation to LBP symptoms.

Fractal analysis of the BOLD signal is in its burgeoning stages both in the brain and skeletal muscle (Noseworthy *et al.* 2010). The unique aspect of BOLD FD is the functional changes in the musculature in subjects with LBP symptoms.

Since there are a wide variety of types of MRI scan types used here, the limitations for each are unique. For BOLD imaging with FD analysis, there is a logical jump, which says that a sinusoidal signal has lower FD values (which is true) and decreased complexity, but a sinusoidal signal in the frequency range required by perfusion approximately 1-2 Hz is not the only cause for decreased signal complexity. A flat line (no blood flow) has low complexity. As does a sinusoid at a different frequency, outside the physiological range. The assumption that the decreased complexity is due to increased contribution of perfusion can be tested in several ways:

1. Blood flow can be altered artificially, such as administration of heat or a local vasodilator via a surface patch, which would cause increased blood flow in the erector spinae, but not other areas or just on one side. The contralateral side and pre-heat administration can be controls.
2. Blood flow could have been measured with infrared spectroscopy or possibly contrast-enhanced ultrasound or MRI to confirm that changes (if they were found) were consistent with accepted measures.
3. Analyzing the BOLD signal to fit a sinusoid at the appropriate heart rate (HR), which could be found from pulse oximetry. The sine amplitude and residuals (from the data fit) could be calculated and compared to control data to determine if there was a change in blood flow as well as a comparison to any changes in FD data.

DTI could have benefitted from optimizing parameters **in the lower back**, such as b-value and/or number of encoding directions, which would result in greatest SNR, with

optimal scan time. Further, reducing scan time, by reducing NEX or TR so that there is still SNR greater than 20 (Damon 2008) and the results can correlate with the symptoms of LBP.

10.2. Recommendations for Proposed Work

This study was a first step to determine the utility for certain scans (such as lower back DTI and BOLD FD) for CLBP.

As described in the above section, there are specifics about to the FD measure which can be tested (listed 1-3 in above page).

Also, several empirical questions which should be addressed before these scans is used to affect clinical decisions:

- Is JNK more sensitive to certain types of LBP?
- Is JNK more sensitive to injuries that originate from certain I-S locations?
- Is there a critical time after injury to make measurements?
- There is a correlation between the symptoms of LBP and DTI/T2W results, but is there a causal relationship? Does LBP symptom severity cause the structural changes observed?
- Can it be combined with some other modality to improve sensitivity such as ultrasound estimate for Young's modulus or task-related EMG? – Are the results from just the DTI and T2W scans the only ones that can be combined?
- Is there a better way to combine the data rather than just a simple average

- Can the multiple sources of variability from the two measures (DTI and T2W) be identified, using a statistical technique such as principle component analysis (PCA)?
- Is the decreased effectiveness in subjects with BMIs greater than 35 due only to the inclusion of fat in the ROIs?
- Is the scan monetarily worthwhile? If there is an estimated cost of \$250 per scan, and the yearly cost per patient is \$5,500 (Jacobs et al. 2004), then the scans and analyses would have to result in only a 5% decrease in direct costs to break even.

Although promising, there are many regulatory, financial and legal barriers to widespread clinical use of these scans in North America. Even so, improvement in current diagnosis using DTI in lumbar dysfunction is timely and may be cost-effective. This is a thought reminiscent of that by Zhang *et al.* (2012) who suggest “*it would be worthwhile to validate the relationship between DTI metrics and the degenerative status of [intervertebral discs] IVDs ... on patients with degenerative discs in order to further explore the clinical usefulness and relevance of DTI.*”

Chapter 11. References

- Adhikari, A., S. Biswas and R. K. Gupta (2011). Drug utilization pattern in pregnant women in rural areas, India: cross-sectional observational study. *J Obstet Gynaecol Res* 37(12): 1813-1817.
- Andre, J. B. and R. Bammer (2010). Advanced diffusion-weighted magnetic resonance imaging techniques of the human spinal cord. *Top Magn Reson Imaging* 21(6): 367-378.
- Asano, Y., J. Shinoda, A. Okumura, T. Aki, S. Takenaka, K. Miwa, M. Yamada, T. Ito and K. Yokoyama (2012). Utility of fractional anisotropy imaging analyzed by statistical parametric mapping for detecting minute brain lesions in chronic-stage patients who had mild or moderate traumatic brain injury. *Neurol Med Chir (Tokyo)* 52(1): 31-40.
- Balbi, V., J. F. Budzik, A. Duhamel, A. Bera-Louville, V. Le Thuc and A. Cotten (2011). Tractography of lumbar nerve roots: initial results. *Eur Radiol* 21(6): 1153-1159.
- Bammer, R. and F. Fazekas (2003). Diffusion imaging of the human spinal cord and the vertebral column. *Top Magn Reson Imaging* 14(6): 461-476.
- Barakat, N., F. B. Mohamed, Hunter, L. N. (2012). Diffusion Tensor Imaging of the Normal Pediatric Spinal Cord Using an Inner Field of View Echo-Planar Imaging Sequence. *AJNR Am J Neuroradiol*.
- Barrett T, Brechbiel M, Bernardo M, Choyke P.L. (2007). MRI of tumor angiogenesis. *J Magn Reson Imaging* 26(2):b 235-249.
- Beneck, G. J. and K. Kulig (2012). Multifidus atrophy is localized and bilateral in active persons with chronic unilateral low back pain. *Arch Phys Med Rehabil* 93(2): 300-306.

Benoist, M., P. Boulu and G. Hayem (2012). Epidural steroid injections in the management of low-back pain with radiculopathy: an update of their efficacy and safety. *Eur Spine J* 21(2): 204-213.

Bergmark, A. (1989). Stability of the lumbar spine. A study in mechanical engineering. *Acta Orthop Scand Suppl* 230: 1-54.

Bressel E, Dolny DG, Vandenberg C, Cronin JB. (2012). Trunk muscle activity during spine stabilization exercises performed in a pool. *Phys Ther Sport*. May;13(2):67-72.

Broussard, D. M., J. K. Bhatia and G. E. Jones (1999). The dynamics of the vestibulo-ocular reflex after peripheral vestibular damage. I. Frequency-dependent asymmetry. *Exp Brain Res* 125(3): 353-364.

Callaghan P.T., O. Soderman O. (1983). Examination of the lamellar phase of aerosol OT: water using pulsed field gradient nuclear magnetic resonance. *J Chem Phys* 87:1737.

Cermak, N. M., M. D. Noseworthy, J. M. Bourgeois, M. A. Tarnopolsky and M. J. Gibala (2012). Diffusion tensor MRI to assess skeletal muscle disruption following eccentric exercise. *Muscle Nerve* 46(1): 42-50.

Chang, G., L. Chen and J. Mao (2007). Opioid tolerance and hyperalgesia. *Med Clin North Am* 91(2): 199-211.

Chou, R. (2012). ACP Journal Club. Risk-stratified primary care management of low back pain reduced disability. *Ann Intern Med* 156(4): JC2-07.

Chou, R., L. H. Huffman, S. American Pain and P. American College of (2007a). Medications for acute and chronic low back pain: a review of the evidence for an American Pain Society/American College of Physicians clinical practice guideline. *Ann Intern Med* 147(7): 505-514.

Chou, R., L. H. Huffman, S. American Pain and P. American College of (2007b). Nonpharmacologic therapies for acute and chronic low back pain: a review of the

evidence for an American Pain Society/American College of Physicians clinical practice guideline. *Ann Intern Med* 147(7): 492-504.

Christidi, F., E. D. Bigler, S. R. McCauley, K. P. Schnelle, T. L. Merkley, M. B. Mors, X. Li, M. Macleod, Z. Chu, J. V. Hunter, H. S. Levin, G. L. Clifton and E. A. Wilde (2011). Diffusion tensor imaging of the perforant pathway zone and its relation to memory function in patients with severe traumatic brain injury. *J Neurotrauma* 28(5): 711-725.

Chuang, L. H., M. O. Soares, H. Tilbrook, H. Cox, C. E. Hewitt, J. Aplin, A. Semlyen, A. Trehwela, I. Watt and D. J. Torgerson (2012). A Pragmatic Multi-centred Randomised Controlled Trial of Yoga for Chronic Low Back Pain: Economic Evaluation. *Spine (Phila Pa 1976)*.

Colado JC, Pablos C, Chulvi-Medrano I, Garcia-Masso X, Flandez J, Behm DG. (2011). The progression of paraspinal muscle recruitment intensity in localized and global strength training exercises is not based on instability alone. *Arch Phys Med Rehabil. Nov*;92(11):1875-83.

Cowan, S. M., K. L. Bennell, K. M. Crossley, P. W. Hodges and J. McConnell (2002). Physical therapy alters recruitment of the vasti in patellofemoral pain syndrome. *Med Sci Sports Exerc* 34(12): 1879-1885.

Cresswell, A. G., H. Grundstrom and A. Thorstensson (1992). Observations on intra-abdominal pressure and patterns of abdominal intra-muscular activity in man. *Acta Physiol Scand* 144(4): 409-418.

Cresswell, A. G., L. Oddsson and A. Thorstensson (1994). The influence of sudden perturbations on trunk muscle activity and intra-abdominal pressure while standing. *Exp Brain Res* 98(2): 336-341.

Dagenais, S., J. Caro and S. Haldeman (2008). A systematic review of low back pain cost of illness studies in the United States and internationally. *Spine J* 8(1): 8-20.

Damon, B. M. (2008). Effects of image noise in muscle diffusion tensor (DT)-MRI assessed using numerical simulations. *Magn Reson Med* 60(4): 934-944.

- Davis, K. G. and S. E. Kotowski (2005). Preliminary evidence of the short-term effectiveness of alternative treatments for low back pain. *Technol Health Care* 13(6): 453-462.
- Deville, W. L., D. A. van der Windt, A. Dzaferagic, P. D. Bezemer and L. M. Bouter (2000). The test of Lasegue: systematic review of the accuracy in diagnosing herniated discs. *Spine (Phila Pa 1976)* 25(9): 1140-1147.
- Deyo, R. A. and J. N. Weinstein (2001). Low back pain. *N Engl J Med* 344(5): 363-370.
- Don, A. S. and E. Carragee (2008). A brief overview of evidence-informed management of chronic low back pain with surgery. *Spine J* 8(1): 258-265.
- Doria, A. S. and Dick, P (2005). Region-of-interest-based analysis of clustered BOLD MRI data in experimental arthritis. *Acad Radiol.* 12(7):841-52.
- Drummond, M., D. Brixner, M. Gold, P. Kind, A. McGuire, E. Nord and G. Consensus Development (2009). Toward a consensus on the QALY. *Value Health* 12 Suppl 1: S31-35.
- Eguchi, Y., S. Ohtori, *et al.* (2011a). Quantitative evaluation and visualization of lumbar foraminal nerve root entrapment by using diffusion tensor imaging: preliminary results. *AJNR Am J Neuroradiol* 32(10): 1824-1829.
- Eguchi, Y., S. Ohtori, *et al.* (2011b). Diffusion magnetic resonance imaging to differentiate degenerative from infectious endplate abnormalities in the lumbar spine. *Spine (Phila Pa 1976)* 36(3): E198-202.
- Eisenberg, D.M., Post, D.E., Davis, R.B., Connelly, M.T., Legedza, A.T., Hrbek, A.L., Prosser, L.A., Buring, J.E., Inui, T.S., Cherkin, D.C. (2007). Addition of choice of complementary therapies to usual care for acute low back pain: a randomized controlled trial. *Spine (Phila Pa 1976)* 32(2): 151-158.
- Elliott, J., A. Pedler, P. Beattie and K. McMahon (2010). Diffusion-weighted magnetic resonance imaging for the healthy cervical multifidus: a potential method for

studying neck muscle physiology following spinal trauma. *J Orthop Sports Phys Ther* 40(11): 722-728.

Enomoto, M., Ukegawa, D., Sakaki, K., Tomizawa, S., Arai, Y., Kawabata, S., Kato, T., Yoshii, T., Shinomiya, K., Okawa, A. (2012). Increase of Paravertebral Muscle Activity in Lumbar Kyphosis Patients by Surface Electromyography Compared With Lumbar Spinal Canal Stenosis Patients and Healthy Volunteers. *J Spinal Disord Tech*.

Fairbank, J. C., J. Couper, J. B. Davies and J. P. O'Brien (1980). The Oswestry low back pain disability questionnaire. *Physiotherapy* 66(8): 271-273.

Foster, N. E., E. Thomas, A. Bishop, K. M. Dunn and C. J. Main (2010). Distinctiveness of psychological obstacles to recovery in low back pain patients in primary care. *Pain* 148(3): 398-406.

Froeling, M., J. Oudeman, S. van den Berg, K. Nicolay, M. Maas, G. J. Strijkers, M. R. Drost and A. J. Nederveen (2010). Reproducibility of diffusion tensor imaging in human forearm muscles at 3.0 T in a clinical setting. *Magn Reson Med* 64(4): 1182-1190.

Furlan, A. D., M. Imamura, T. Dryden and E. Irvin (2009). Massage for low back pain: an updated systematic review within the framework of the Cochrane Back Review Group. *Spine (Phila Pa 1976)* 34(16): 1669-1684.

Gagnier, J. J., M. W. van Tulder, B. Berman and C. Bombardier (2007). Herbal medicine for low back pain: a Cochrane review. *Spine (Phila Pa 1976)* 32(1): 82-92.

Gerstner, E. R. and A. G. Sorensen (2011). Diffusion and diffusion tensor imaging in brain cancer. *Semin Radiat Oncol* 21(2): 141-146.

Gold, M. R., J. E. Siegel, L. B. Russell and M. C. Weinstein (1996). *Cost-Effectiveness in Health and Medicine*. New York, Oxford University Press.

Gore, M., A. Sadosky, B. R. Stacey, K. S. Tai and D. Leslie (2012). The burden of chronic low back pain: clinical comorbidities, treatment patterns, and health care costs in usual care settings. *Spine (Phila Pa 1976)* 37(11): E668-677.

Haldeman, S. and S. Dagenais (2008). A supermarket approach to the evidence-informed management of chronic low back pain. *Spine J* 8(1): 1-7.

Hanada EY, Johnson M, Hubley-Kozey C. (2011). A comparison of trunk muscle activation amplitudes during gait in older adults with and without chronic low back pain. *PM R.* 3(10):920-8.

Henschke, N., R. W. Ostelo, M. W. van Tulder, J. W. Vlaeyen, S. Morley, W. J. Assendelft and C. J. Main (2010). Behavioural treatment for chronic low-back pain. *Cochrane Database Syst Rev*(7): CD002014.

Herdman, M., C. Gudex, A. Lloyd, M. Janssen, P. Kind, D. Parkin, G. Bonsel and X. Badia (2011). Development and preliminary testing of the new five-level version of EQ-5D (EQ-5D-5L). *Qual Life Res* 20(10): 1727-1736.

Hides, J., C. Gilmore, W. Stanton and E. Bohlscheid (2008). Multifidus size and symmetry among chronic LBP and healthy asymptomatic subjects. *Man Ther* 13(1): 43-49.

Hides, J. A., G. A. Jull and C. A. Richardson (2001). Long-term effects of specific stabilizing exercises for first-episode low back pain. *Spine (Phila Pa 1976)* 26(11): E243-248.

Hides, J. A., C. A. Richardson and G. A. Jull (1995). Magnetic resonance imaging and ultrasonography of the lumbar multifidus muscle. Comparison of two different modalities. *Spine (Phila Pa 1976)* 20(1): 54-58.

Hides, J. A., C. A. Richardson and G. A. Jull (1996). Multifidus muscle recovery is not automatic after resolution of acute, first-episode low back pain. *Spine (Phila Pa 1976)* 21(23): 2763-2769.

Hill, J. C., K. M. Dunn, C. J. Main and E. M. Hay (2010). Subgrouping low back pain: a comparison of the STarT Back Tool with the Orebro Musculoskeletal Pain Screening Questionnaire. *Eur J Pain* 14(1): 83-89.

Hill, J. C., D. G. Whitehurst, *et al.* (2011). Comparison of stratified primary care management for low back pain with current best practice (STarT Back): a randomised controlled trial. *Lancet* 378(9802): 1560-1571.

Hodges, P. W. (2003). Core stability exercise in chronic low back pain. *Orthop Clin North Am* 34(2): 245-254.

Hodges, P. W. and C. A. Richardson (1996). Inefficient muscular stabilization of the lumbar spine associated with low back pain. A motor control evaluation of transversus abdominis. *Spine (Phila Pa 1976)* 21(22): 2640-2650.

Hyun, J. K., J. Y. Lee, S. J. Lee and J. Y. Jeon (2007). Asymmetric atrophy of multifidus muscle in patients with unilateral lumbosacral radiculopathy. *Spine (Phila Pa 1976)* 32(21): E598-602.

Jacobs P, Schopflocher D, Klarenbach S, Golmohammadi K, Ohinmaa A. (2004). A health production function for persons with back problems: results from the Canadian Community Health Survey of 2000. *Oct 15;29(20):2304-8.*

Jang, S. H. (2011). Diffusion tensor imaging studies on corticospinal tract injury following traumatic brain injury: a review. *NeuroRehabilitation* 29(4): 339-345.

Jull, G., P. Trott, H. Potter, G. Zito, K. Niere, D. Shirley, J. Emberson, I. Marschner and C. Richardson (2002). A randomized controlled trial of exercise and manipulative therapy for cervicogenic headache. *Spine (Phila Pa 1976)* 27(17): 1835-1843; discussion 1843.

Kabadi SM, Lee BK, Liu L. (2012). Joint Effects of Obesity and Vitamin D Insufficiency on Insulin Resistance and Type 2 Diabetes: Results from the NHANES 2001-2006. *Diabetes Care*. Jun 29. [Epub ahead of print]

Kader, D. F., D. Wardlaw and F. W. Smith (2000). Correlation between the MRI changes in the lumbar multifidus muscles and leg pain. *Clin Radiol* 55(2): 145-149.

Kaigle, A. M., S. H. Holm and T. H. Hansson (1995). Experimental instability in the lumbar spine. *Spine (Phila Pa 1976)* 20(4): 421-430.

Kan, J. H., A. M. Heemskerk, Z. Ding, A. Gregory, G. Mencio, K. Spindler and B. M. Damon (2009). DTI-based muscle fiber tracking of the quadriceps mechanism in lateral patellar dislocation. *J Magn Reson Imaging* 29(3): 663-670.

Karampinos, D. C., K. F. King, B. P. Sutton and J. G. Georgiadis (2009). Myofiber ellipticity as an explanation for transverse asymmetry of skeletal muscle diffusion MRI in vivo signal. *Ann Biomed Eng* 37(12): 2532-2546.

Kasahara, K., K. Hashimoto, M. Abo and A. Senoo (2012). Voxel- and atlas-based analysis of diffusion tensor imaging may reveal focal axonal injuries in mild traumatic brain injury -- comparison with diffuse axonal injury. *Magn Reson Imaging* 30(4): 496-505.

Kiesel KB, Butler RJ, Duckworth A, Halaby T, Lannan K, Phifer C, DeLeal C, Underwood FB. (2012). Experimentally induced pain alters the EMG activity of the lumbar multifidus in asymptomatic subjects. *Man Ther.* Jun;17(3):236-240.

Kim, W. H., S. H. Lee and D. Y. Lee (2011). Changes in the cross-sectional area of multifidus and psoas in unilateral sciatica caused by lumbar disc herniation. *J Korean Neurosurg Soc* 50(3): 201-204.

Kjaer, P., T. Bendix, J. S. Sorensen, L. Korsholm and C. Leboeuf-Yde (2007). Are MRI-defined fat infiltrations in the multifidus muscles associated with low back pain? *BMC Med* 5: 2.

Kolich, M., S. M. Taboun and A. I. Mohamed (2000). Low back muscle activity in an automobile seat with a lumbar massage system. *Int J Occup Saf Ergon* 6(1): 113-128.

- Kulig, K., A. R. Scheid, R. Beauregard, J. M. Popovich, Jr., G. J. Beneck and P. M. Colletti (2009). Multifidus morphology in persons scheduled for single-level lumbar microdiscectomy: qualitative and quantitative assessment with anatomical correlates. *Am J Phys Med Rehabil* 88(5): 355-361.
- Lange, R. T., G. L. Iverson, J. R. Brubacher, B. Madler and M. K. Heran (2012). Diffusion tensor imaging findings are not strongly associated with postconcussional disorder 2 months following mild traumatic brain injury. *J Head Trauma Rehabil* 27(3): 188-198.
- Last, A. R. and K. Hulbert (2009). Chronic low back pain: evaluation and management. *Am Fam Physician* 79(12): 1067-1074.
- Le Bihan, D., J. F. Mangin, C. Poupon, C. A. Clark, S. Pappata, N. Molko and H. Chabriat (2001). Diffusion tensor imaging: concepts and applications. *J Magn Reson Imaging* 13(4): 534-546.
- Lee, H. I., J. Song, H. S. Lee, J. Y. Kang, M. Kim and J. S. Ryu (2011). Association between Cross-sectional Areas of Lumbar Muscles on Magnetic Resonance Imaging and Chronicity of Low Back Pain. *Ann Rehabil Med* 35(6): 852-859.
- Lee, S. W., C. K. Chan, T. S. Lam, C. Lam, N. C. Lau, R. W. Lau and S. T. Chan (2006). Relationship between low back pain and lumbar multifidus size at different postures. *Spine (Phila Pa 1976)* 31(19): 2258-2262.
- Lipscomb, J., M. Drummond, D. Fryback, M. Gold and D. Revicki (2009). Retaining, and enhancing, the QALY. *Value Health* 12 Suppl 1: S18-26.
- Lüdemann L, Förchler A, Grieger W, Zimmer C. (2006). BOLD signal in the motor cortex shows a correlation with the blood volume of brain tumors. *J Magn Reson Imaging*. 23(4):435-443.
- Macintosh, J. E. and N. Bogduk (1991). The attachments of the lumbar erector spinae. *Spine (Phila Pa 1976)* 16(7): 783-792.

McPherson ML, Canaday BR, Heit HA, Rospond RM. A Pharmacist's Guide to the Clinical Assessment and Management of Pain. Washington, DC: American Pharmacists Association; 2004.

Madden, D. J., I. J. Bennett, A. Burzynska, G. G. Potter, N. K. Chen and A. W. Song (2012). Diffusion tensor imaging of cerebral white matter integrity in cognitive aging. *Biochim Biophys Acta* 1822(3): 386-400.

Madden, D. J., I. J. Bennett and A. W. Song (2009). Cerebral white matter integrity and cognitive aging: contributions from diffusion tensor imaging. *Neuropsychol Rev* 19(4): 415-435.

Main, C. J., N. Foster and R. Buchbinder (2010). How important are back pain beliefs and expectations for satisfactory recovery from back pain? *Best Pract Res Clin Rheumatol* 24(2): 205-217.

Malanga, G. and E. Wolff (2008). Evidence-informed management of chronic low back pain with nonsteroidal anti-inflammatory drugs, muscle relaxants, and simple analgesics. *Spine J* 8(1): 173-184.

Mannion, A. F., M. Muntener, S. Taimela and J. Dvorak (2001). Comparison of three active therapies for chronic low back pain: results of a randomized clinical trial with one-year follow-up. *Rheumatology (Oxford)* 40(7): 772-778.

McCullough LE, Eng SM, Bradshaw PT, Cleveland RJ, Teitelbaum SL, Neugut AI, Gammon MD. (2012). Fat or fit: The joint effects of physical activity, weight gain, and body size on breast cancer risk. *Cancer*. 25. doi: 10.1002/cncr.27433. [Epub ahead of print]

McGill, S. (2002). *Low back disorders: evidence based prevention and rehabilitation*. Champaign, IL, Human Kinetics Publishers Inc.

McGill, S. M. (2004). Linking latest knowledge of injury mechanisms and spine function to the prevention of low back disorders. *J Electromyogr Kinesiol* 14(1): 43-47.

McMillan, A. B., D. Shi, S. J. Pratt and R. M. Lovering (2011). Diffusion tensor MRI to assess damage in healthy and dystrophic skeletal muscle after lengthening contractions. *J Biomed Biotechnol* 2011: 970726.

Mengiardi, B., M. R. Schmid, N. Boos, C. W. Pfirrmann, F. Brunner, A. Elfering and J. Hodler (2006). Fat content of lumbar paraspinal muscles in patients with chronic low back pain and in asymptomatic volunteers: quantification with MR spectroscopy. *Radiology* 240(3): 786-792.

Mohamed, F. B., L. N. Hunter, *et al.* (2011). Diffusion tensor imaging of the pediatric spinal cord at 1.5T: preliminary results. *AJNR Am J Neuroradiol* 32(2): 339-345.

Monsees GM, Kraft P, Hankinson SE, Hunter DJ, Schernhammer ES. (2012). Circadian genes and breast cancer susceptibility in rotating shift workers. *Int J Cancer*. Apr 2. doi: 10.1002/ijc.27564. [Epub ahead of print]

Mulcahey, M. J., A. Samdani, J. Gaughan, N. Barakat, S. Faro, R. R. Betz, J. Finsterbusch and F. B. Mohamed (2012). Diffusion tensor imaging in pediatric spinal cord injury: preliminary examination of reliability and clinical correlation. *Spine (Phila Pa 1976)* 37(13): E797-803.

Niemelainen, R., M. M. Briand and M. C. Battie (2011). Substantial asymmetry in paraspinal muscle cross-sectional area in healthy adults questions its value as a marker of low back pain and pathology. *Spine (Phila Pa 1976)* 36(25): 2152-2157.

Noorhassim I, Rampal KG. (1998). Multiplicative effect of smoking and age on hearing impairment. *Am J Otolaryngol*. 19(4):240-3.

Noseworthy, M. D., A. D. Davis and A. H. Elzibak (2010). Advanced MR imaging techniques for skeletal muscle evaluation. *Semin Musculoskelet Radiol* 14(2): 257-268.

O'Donnell, L. J. and C. F. Westin (2011). An introduction to diffusion tensor image analysis. *Neurosurg Clin N Am* 22(2): 185-196, viii.

O'Sullivan, P. B., G. D. Phyty, L. T. Twomey and G. T. Allison (1997). Evaluation of specific stabilizing exercise in the treatment of chronic low back pain with radiologic diagnosis of spondylolysis or spondylolisthesis. *Spine (Phila Pa 1976)* 22(24): 2959-2967.

Ogawa S, T.M.Lee, A.R. Kay, D.W. Tank. (1990). Brain magnetic resonance imaging with contrast dependent on blood oxygenation. *Proc Natl Acad Sci U S A.* 87(24):9868-72.

Panjabi, M. M. (1992a). The stabilizing system of the spine. Part I. Function, dysfunction, adaptation, and enhancement. *J Spinal Disord* 5(4): 383-389; discussion 397.

Panjabi, M. M. (1992b). The stabilizing system of the spine. Part II. Neutral zone and instability hypothesis. *J Spinal Disord* 5(4): 390-396; discussion 397.

Pease, A. and R. Miller (2011). The use of diffusion tensor imaging to evaluate the spinal cord in normal and abnormal dogs. *Vet Radiol Ultrasound* 52(5): 492-497.

Price, S. J. (2007). The role of advanced MR imaging in understanding brain tumour pathology. *Br J Neurosurg* 21(6): 562-575.

Padhani A.R., Krohn KA, Lewis JS, Alber M. (2007) Imaging oxygenation of human tumours. *Eur Radiol.* 17(4):861-72.

Ramprasad M, Shenoy DS, Sandhu JS, Sankara N. (2011). The influence of kinesiophobia on trunk muscle voluntary responses with pre-programmed reactions during perturbation in patients with chronic low back pain. *J Bodyw Mov Ther.*15(4):485-95.

Roelofs, P. D., R. A. Deyo, B. W. Koes, R. J. Scholten and M. W. van Tulder (2008a). Non-steroidal anti-inflammatory drugs for low back pain. *Cochrane Database Syst Rev*(1): CD000396.

Roelofs, P. D., R. A. Deyo, B. W. Koes, R. J. Scholten and M. W. van Tulder (2008b). Nonsteroidal anti-inflammatory drugs for low back pain: an updated Cochrane review. *Spine (Phila Pa 1976)* 33(16): 1766-1774.

- Roy, J. E. and K. E. Cullen (2002). Vestibuloocular reflex signal modulation during voluntary and passive head movements. *J Neurophysiol* 87(5): 2337-2357.
- Rubin, D. I. (2007). Epidemiology and risk factors for spine pain. *Neurol Clin* 25(2): 353-371.
- Scott, N. A., C. Moga and C. Harstall (2010). Managing low back pain in the primary care setting: the know-do gap. *Pain Res Manag* 15(6): 392-400.
- Shafaq, N., A. Suzuki, A. Matsumura, H. Terai, H. Toyoda, H. Yasuda, M. Ibrahim and H. Nakamura (2012). Asymmetric Degeneration of Paravertebral Muscles in Patients with Degenerative Lumbar Scoliosis. *Spine (Phila Pa 1976)*.
- Sihvonen, T., K. A. Lindgren, O. Airaksinen and H. Manninen (1997). Movement disturbances of the lumbar spine and abnormal back muscle electromyographic findings in recurrent low back pain. *Spine (Phila Pa 1976)* 22(3): 289-295.
- Smeets, R. J., D. Wade, A. Hidding, P. J. Van Leeuwen, J. W. Vlaeyen and J. A. Knottnerus (2006). The association of physical deconditioning and chronic low back pain: a hypothesis-oriented systematic review. *Disabil Rehabil* 28(11): 673-693.
- Soares, M. O. (2012). Is the QALY blind, deaf and dumb to equity? NICE's considerations over equity. *Br Med Bull* 101: 17-31.
- Sosnovik, D. E., R. Wang, G. Dai, T. Wang, E. Aikawa, M. Novikov, A. Rosenzweig, R. J. Gilbert and V. J. Wedeen (2009). Diffusion spectrum MRI tractography reveals the presence of a complex network of residual myofibers in infarcted myocardium. *Circ Cardiovasc Imaging* 2(3): 206-212.
- Standaert, C. J., S. M. Weinstein and J. Rumpeltes (2008). Evidence-informed management of chronic low back pain with lumbar stabilization exercises. *Spine J* 8(1): 114-120.
- Stejskal EO, Tanner JE (1965) Spin diffusion measurements: Spin echoes in the presence of a time-dependent field gradient. *J. Chem Phys.* 42:288-292.

- Storheim, K. (2012). Targeted physiotherapy treatment for low back pain based on clinical risk can improve clinical and economic outcomes when compared with current best practice. *J Physiother* 58(1): 57.
- Stout, A. (2010). Epidural steroid injections for low back pain. *Phys Med Rehabil Clin N Am* 21(4): 825-834.
- Tanaka, T. H., G. Leisman, H. Mori and K. Nishijo (2002). The effect of massage on localized lumbar muscle fatigue. *BMC Complement Altern Med* 2: 9.
- Vadakkumpadan, F., H. Arevalo, A. J. Prassl, J. Chen, F. Kicking, P. Kohl, G. Plank and N. Trayanova (2010). Image-based models of cardiac structure in health and disease. *Wiley Interdiscip Rev Syst Biol Med* 2(4): 489-506.
- Wallwork, T. L., W. R. Stanton, M. Freke and J. A. Hides (2009). The effect of chronic low back pain on size and contraction of the lumbar multifidus muscle. *Man Ther* 14(5): 496-500.
- Ward, S. R., A. Tomiya, G. J. Regev, B. E. Thacker, R. C. Benzl, C. W. Kim and R. L. Lieber (2009). Passive mechanical properties of the lumbar multifidus muscle support its role as a stabilizer. *J Biomech* 42(10): 1384-1389.
- Wardlaw G, Wong R, Noseworthy MD. (2008). Identification of intratumour low frequency microvascular components via BOLD signal fractal dimension mapping. *Phys Med.* 24(2):87-91.
- Waseem, Z., C. Boulias, A. Gordon, F. Ismail, G. Sheean and A. D. Furlan (2011). Botulinum toxin injections for low-back pain and sciatica. *Cochrane Database Syst Rev*(1): CD008257.
- Weinstein, M. C., G. Torrance and A. McGuire (2009). QALYs: the basics. *Value Health* 12 Suppl 1: S5-9.
- Whitehurst, D. G., S. Bryan, M. Lewis, J. Hill and E. M. Hay (2012). Exploring the cost-utility of stratified primary care management for low back pain compared with current best practice within risk-defined subgroups. *Ann Rheum Dis.* in press.

- WHO. (1995). "Physical status: The use and interpretation of anthropometry. ." from http://apps.who.int/bmi/index.jsp?introPage=intro_3.html.
- Wilke, H. J., S. Wolf, L. E. Claes, M. Arand and A. Wiesend (1995). Stability increase of the lumbar spine with different muscle groups. A biomechanical in vitro study. *Spine (Phila Pa 1976)* 20(2): 192-198.
- Williams, N. H., M. Hendry, R. Lewis, I. Russell, A. Westmoreland and C. Wilkinson (2007). Psychological response in spinal manipulation (PRISM): a systematic review of psychological outcomes in randomised controlled trials. *Complement Ther Med* 15(4): 271-283.
- Wong, D. A., and Trasfeldt, E. *MacNab's Backache*, 4th ed. New York, NY. 2007.
- Yoshihara, K., Y. Nakayama, N. Fujii, T. Aoki and H. Ito (2003). Atrophy of the multifidus muscle in patients with lumbar disk herniation: histochemical and electromyographic study. *Orthopedics* 26(5): 493-495.
- Yoshihara, K., Y. Shirai, Y. Nakayama and S. Uesaka (2001). Histochemical changes in the multifidus muscle in patients with lumbar intervertebral disc herniation. *Spine (Phila Pa 1976)* 26(6): 622-626.
- Zappala, G., M. Thiebaut de Schotten and P. J. Eslinger (2012). Traumatic brain injury and the frontal lobes: what can we gain with diffusion tensor imaging? *Cortex* 48(2): 156-165.
- Zaraiskaya T, Kumbhare D, Noseworthy MD (2006). Diffusion tensor imaging in evaluation of human skeletal muscle injury. *J Magn Reson Imaging*. 24(2):402-8.
- Zhang, Z., Q. Chan, M. P. Anthony, D. Samartzis, K. M. Cheung, P. L. Khong and M. Kim (2012). Age-related diffusion patterns in human lumbar intervertebral discs: a pilot study in asymptomatic subjects. *Magn Reson Imaging* 30(2): 181-188.

Appendix 1 Clinical Context

DTI and CSA results have shown to be correlated with the ODI and VAS questionnaires, but only if certain constraints are met: BMI of the subject must be under 35, and, DTI's SNR must be greater than 20.

There are at least three uses. The first is as an objective measure of the subject's pain. Typically the 'gold standards' consist of several questionnaires, which may include the ODI or R-M, and modified VAS results, and clinical observation, which may include tests such as the (Laségue) straight leg raise test. These all require input from the patient, and this subjective information may be skewed to the more severe end if there is a monetary incentive.

Also, there are many aspects of care, which add inefficiencies and/or inaccuracies to the treatment process. Recovery from the symptoms of LBP is highly variable. It has even been shown that a person's beliefs about their control over their situation can influence alleviation of symptoms (Foster *et al.* 2010; Henschke *et al.* 2010; Main *et al.* 2010). Some primary care physicians have knowledge gaps, which Scott coined 'know-do gap' in reading 'red flags', diagnostic imaging, and providing sick leave and financial assistance (Scott *et al.* 2010). The scans and analyses submitted here require very little interpretation, when developed fully, and may circumvent the 'know-do' gap, decreasing the economic burden and increasing accuracy of diagnosis. Further, the JNK index correlates with symptoms of LBP and may not require analysis of the relationship between a person's beliefs and the underlying cause. As described in this paragraph, the

underlying symptoms may have many contributors: true physiology, psychological factors, and/or financial motivations. While objective measures like the ODI and VAS questionnaires may be contaminated by financial motivations, the results from the DTI and T2W scans are only influenced by the first two.

The costs to treat the symptoms of CLBP can be reduced if a stratified primary care management strategy is undertaken (Whitehurst *et al.* 2012), as described in detail in Appendix 1.2. The results of these scans may be applied to putting the subject in the correct stream. The benefits of stratified care are increased quality adjusted life years (QALY) for a slightly reduced cost, compared to standard practices.

As described in Appendix 1.1 below, the QALY is a limited measure for evaluation of LBP symptoms. The JNK index and LBP-specific questionnaires such as the ODI and VAS may provide more utility in assessing the quality of patient care. Although ideal, there may be cost limitations, and, unless subjects are already required to have undergone an MRI, may not be applied to a whole target population.

Appendix 1.1 Quality Adjusted Life Years (QALYs)

A QALY is a measure of the patient's life expectancy and how well they are living at that moment. QALYs are used to guide healthcare allocations decisions (Herdman *et al.* 2011). QALY is the product of a person's life expectancy and a utility rating, so one year in complete health is given a value of one. As an example: a patient who has a lifespan of one year with a utility factor of 0.5, perhaps from LBP, will have a

QALY of 0.5, and a person who lives 6 months in perfect health will also have a QALY of 0.5 (Lipscomb *et al.* 2009).

QALYs can be used on populations and take into account the length and quality of a treatment or cost/benefit analysis. The measure is also versatile, since the utility factor can be calculated based on a custom questionnaire or measure that can focus on an aspect of quality of life for the disease/treatment in question. QALYs are not an ideal measure, since lower back abnormalities are seldom fatal. For LBP symptoms, the first part of the product isn't needed. However, QALYs are necessary since they are the outcome measure of LBP treatment in many population-based studies such as those by Whitehurst *et al.* (2012). Another limitation is that QALYs are primarily made for population-based care decisions, but are applied to individual patients on occasion, and the optimal decisions for the community are sometimes at odds with the best outcome for the individual (Weinstein *et al.* 2009).

The QALY must address several issues (Drummond *et al.* 2009), such as:

- What is the value being assessed?
- Who is asking, the individual, physician, or health care decision maker?
- How are the healthcare outcomes defined?
- What is the ideal outcome or what outcome will produce a value of 1.0 for the utility factor?

The results from a questionnaire must address answer all of these questions based on the application of the QALY measure. For these multiple purposes, there are several different

QALYs. This overview will only discuss ‘conventional’ QALYs for the interest of simplicity, since conventional QALYs are used to assess stratified care by Whitehurst *et al.* (2012). The QALY utility factor can be assessed by many indices such as the 7-item Health Utilities Index, the 8- item Health Utilities Index, the 6- item SF-6D Scale, the 4 item Quality of Well-Being Scale, the 5-item Assessment of Quality Scale, or the EuroQual 5 item scale (EQ-5D). To calculate QALY utility factor in the assessment of stratified care by Whitehurst *et al.* (2012), the EQ-5D is used. It measures mobility, self care, performance of usual activities, pain/discomfort, and anxiety/depression (Weinstein *et al.* 2009). The questionnaire consists of two pages of questions and a one page VAS with the endpoints labeled the ‘best worst you can imagine’ and ‘the best health you can imagine’. Respondents are asked to apply answers to their status today. The scale is linear, such that an improvement from 0.1 to 0.3 is an equivalent improvement from 0.5-0.7. The use of QALYs has been approved by the US Panel on Cost-Effectiveness in Health and Medicine (Gold *et al.* 1996) and the National Institute of Health and Clinical Excellence (NICE) in Britain (Soares 2012). However, Weinstein *et al.* (2009) believes the differing focus, extent, and categories are the limitations of the various questionnaires. Even if these limitations are accounted for, Weinstein *et al.* (2009) believes the results may be population-specific; the same level of disability may result in a different utility factor in Maritime Canada and Southern Ontario. The JNK index does not have these limitations. If both were administered, each would reduce the limitations of the other as a measure of LBP severity.

Appendix 1.2 Stratified Primary Care

Whitehurst et al (2012) slotted patients into either stratified care or standard care for LBP symptoms at a physiotherapy clinic in the UK. Under stratified care patients are slotted into one of three groups based on their estimated risk level and severity; low-risk, medium risk or high-risk groups. Their control group received care “in line with standard physiotherapy” (Whitehurst *et al.* 2012).

The outcome was measured as conventional QALYs based on the EQ-5D questionnaire. The results are shown in figure 10.1 (Reproduced from “Exploring the cost-utility of stratified primary care management for low back pain compared with current best practice within risk-defined subgroups”, Whitehurst et al, 2012 in press, with permission from BMJ publishing group ltd.) The ratio of stratified/standard QALY is on the x-axis and stratified/standard cost is on the y-axis. The ideal treatment will be in the lower right quadrant (improved outcome for lower cost). Data that cluster in the lower area and straddle the y axis are (same outcome for lower cost) also positive results for stratified care, and perhaps so are data which cluster in the upper right quadrant (increased benefit for increased cost), depending on the importance of improvement. The low risk group is cheaper but doesn't result in improved QALY, the medium risk group shows that stratified care is cheaper and has improved QALY, and the high risk group shows improved outcomes, but at a greater monetary cost.

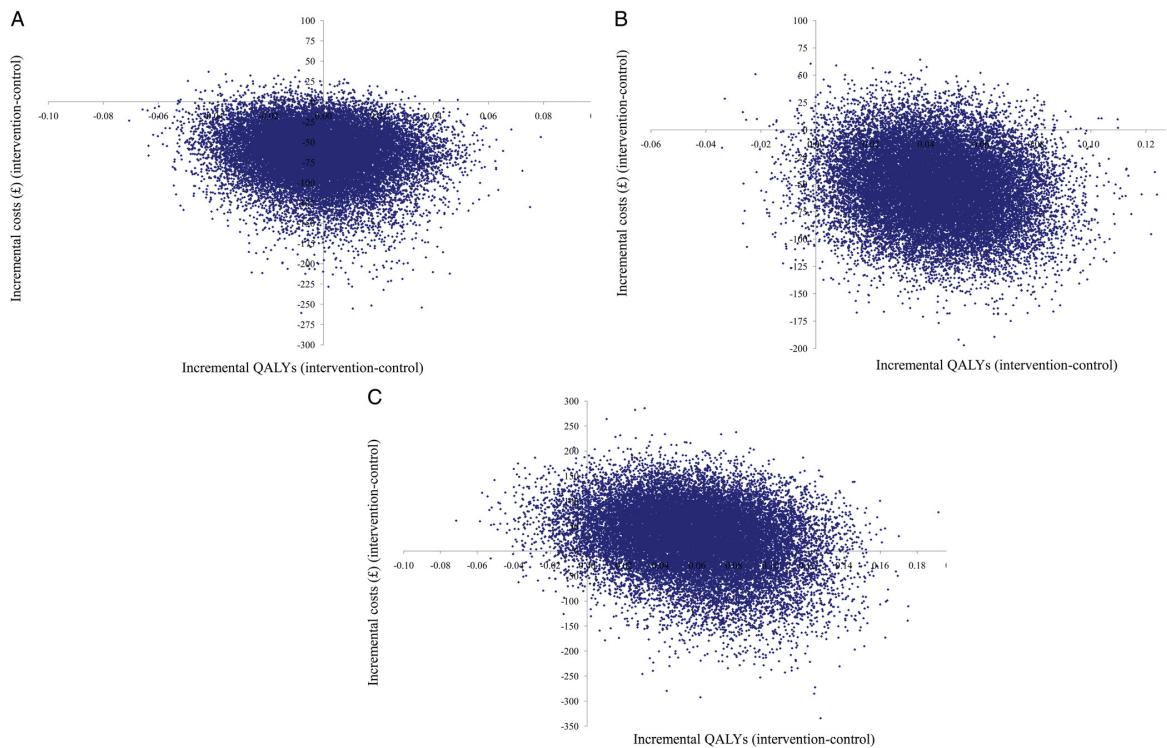


Figure 0.1 Cost-utility curve for the (A) low risk, (B) medium risk, and (C) high risk stratified categories. ‘Intervention’ refers to stratified care, ‘control’ is standard care. Reproduced from Exploring the cost-utility of stratified primary care management for low back pain compared with current best practice within risk-defined subgroups, Whitehurst et al, 2012 in press, with permission from BMJ publishing group ltd.)

Other studies have also shown that non-standard and stratified care is more beneficial than standard practice (Hill *et al.* 2011; Chou 2012; Storheim 2012). It is possible that the JNK index may increase utility. Also it may allow stratified care to be scalable (applied quickly to a great number of primary care or physiotherapy centers with minimal delay and only incremental cost). Whitehurst *et al* (2012) states: “*Training physiotherapists to use the prognostic screening tool and deliver the systematic targeted treatments incur costs due to the time commitments of trainers, trainees and mentors.*” Since there is no training of clinicians with the DTI and T2W scans, there are no incurred costs.

Whitehurst *et al* (2012) also states “*Capacity constraints are also relevant, particularly with regard to the numbers of physiotherapists with the training and expertise to deliver the high-risk treatment package.*” The MRI and JNK index respond to the needs described by Whitehurst, since they are scalable (described above, able to accept increased volume with negligible impact on contribution margin), and can be applied immediately across any physiotherapy clinic with access to a MRI with DTI sequences.